Report MCR-72-91

SYSTEMS-LEVEL STUDY OF A NONSURVIVABLE JUPITER TURBOPAUSE PROBE

Volume I - Summary

R. S. Wiltshire, Program Manager
Martin Marietta Corporation
Denver Division
Post Office Box 179
Denver, Colorado 80201

June 1972

Final Report

Prepared for

GODDARD SPACE FLIGHT CENTER

Greenbelt, Maryland 20771

STANDARD TITLE PAGE

1. Report No. MCR-72-91	2. Government Accession No.	3. Recipient's Catalog No.
4. Title and Subtitle Systems-Level Study of a Nonsurvivable Jupiter Turbopause Probe. Vol I Summary, Vol II Supporting Technical Studies, Vol III Appendixes		5. Report Date June 1972
		6. Performing Organization Code
7. Author(s) R. S. Wiltshire, Program Manager		8. Performing Organization Report No. MCR-72-91
9. Performing Organization Name and Address Martin Marietta Corporation Denver Division P.O. Box 179 Denver, Colorado 80201		10. Work Unit No.
		11. Contract or Grant No. NAS5-11445
12. Sponsoring Agency Name and Address National Aeronautics and Space Administration Goddard Space Flight Center Greenbelt Road Greenbelt, Maryland 20771		13. Type of Report and Period Covered Study Report June 4, 1971 thru March 4, 1972
		14. Sponsoring Agency Code
15. Supplementary Notes		

16. Abstract

This nine-month study of a probe to explore the Jovian atmosphere and environment included five major tasks: definition of science requirements, mission evaluation, definition of the probe system, definition of spacecraft support requirements, and nonequilibrium flow-field analysis for communications blackout evaluation.

This report emphasizes the overall mission and system design and describes the integration of the various technology efforts into complete mission designs. Included are the study constraints, science and mission objectives, mission selection rationale, and design summaries describing required engineering implementation. Critical technical problems and major trade study results are discussed.

Results showed that a nonsurvivable turbopause probe mission to Jupiter, with adequate data return to meet the science objectives, is feasible and practical within the 1975 state of the art. Many probe mission options are practical using the Pioneer or MOPS spacecraft with the 5-segment solids Titan IIID/Centaur/Burner II launch vehicle.

17. Key Words (Selected by Author(s))	18. Distribution Statement
1. Nonsurvivable Turbopause Probe 2. Jupiter Atmosphere 3. Mission and System Design 4. Outer-Planet Missions	

19. Security Classif. (of this report)	20. Security Classif. (of this page)	21. No. of Pages	22. Price
UNCLASSIFIED	UNCLASSIFIED		6.75

STANDARD TITLE PAGE

1. Report No. MCR-72-91	2. Government Accession No.	3. Recipient's Catalog No.
4. Title and Subtitle Systems-Level Study of a Nonsurvivable Jupiter Turbopause Probe. Vol I Summary, Vol II Supporting Technical Studies, Vol III Appendixes		5. Report Date June 1972
		6. Performing Organization Code
7. Author(s) R. S. Wiltshire, Program Manager		8. Performing Organization Report No. MCR-72-91
9. Performing Organization Name and Address Martin Marietta Corporation Denver Division P.O. Box 179 Denver, Colorado 80201		10. Work Unit No.
		11. Contract or Grant No. NAS5-11445
12. Sponsoring Agency Name and Address National Aeronautics and Space Administration Goddard Space Flight Center Greenbelt Road Greenbelt, Maryland 20771		13. Type of Report and Period Covered Study Report June 4, 1971 thru March 4, 1972
		14. Sponsoring Agency Code
15. Supplementary Notes		

16. Abstract

This nine-month study of a probe to explore the Jovian atmosphere and environment included five major tasks: definition of science requirements, mission evaluation, definition of the probe system, definition of spacecraft support requirements, and nonequilibrium flow-field analysis for communications blackout evaluation.

This report emphasizes the overall mission and system design and describes the integration of the various technology efforts into complete mission designs. Included are the study constraints, science and mission objectives, mission selection rationale, and design summaries describing required engineering implementation. Critical technical problems and major trade study results are discussed.

Results showed that a nonsurvivable turbopause probe mission to Jupiter, with adequate data return to meet the science objectives, is feasible and practical within the 1975 state of the art. Many probe mission options are practical using the Pioneer or MOPS spacecraft with the 5-segment solids Titan IIID/Centaur/Burner II launch vehicle.

17. Key Words (Selected by Author(s))	18. Distribution Statement
1. Nonsurvivable Turbopause Probe 2. Jupiter Atmosphere 3. Mission and System Design 4. Outer-Planet Missions	

19. Security Classif. (of this report)	20. Security Classif. (of this page)	21. No. of Pages	22. Price
UNCLASSIFIED	UNCLASSIFIED		

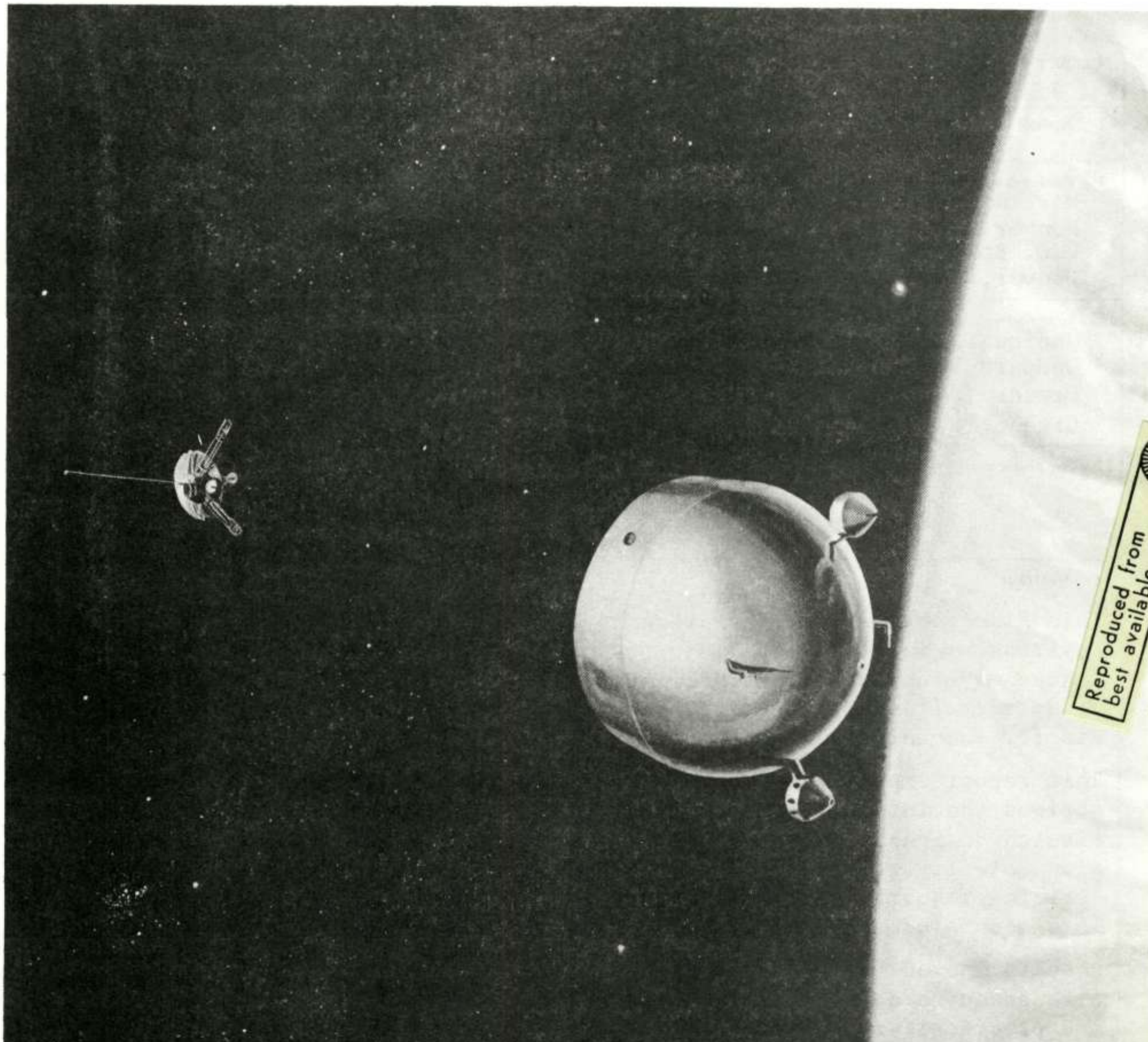

Nonsurvivable Jupiter Turbopause Probe

FOREWORD

This final report has been prepared in accordance with requirements of Contract NAS5-11445 to present data and conclusions from a nine-month study for Goddard Space Flight Center by the Martin Marietta Corporation, Denver Division. The work was done under the management of the NASA Project Manager, Mr. George M. Levin, Advanced Plans Staff, NASA-Goddard Space Flight Center. The report is divided into the following volumes:

I - SUMMARY

II - SUPPORTING TECHNICAL STUDIES

III - APPENDIXES

ACKNOWLEDGEMENTS

The following Martin Marietta Corporation, Denver Division, personnel participated in this study, and their efforts are greatly appreciated:

R. S. Wiltshire	Study Leader, Program Manager
Leonard R. Anderson	Mission Analysis
Eugene A. Berkery	Telecommunications, Data Handling, Power, and ACS, Lead
Leo R. Bonorden	Mechanical Design
Ronald D. Bryant	Nonequilibrium Flow-Field Analysis, Lead
Jack O. Bunting	Science Instruments
Dennis V. Byrnes	Navigation
Patrick C. Carroll	Systems, Lead
Revis E. Compton, Jr.	Telecommunications
Robert G. Cook	Mechanical Design
C. Thomas Edquist	Aerophysics
Robert B. Fischer	Mission Analysis
John W. Hungate	Systems
Carl L. Jensen	Thermal Analysis
Melvin W. Kuethe	Mechanical/Structural/Probe Integration, Lead
Kenneth W. Ledbetter	Science, Lead
James M. Lefferdo	Aerophysics, Lead
Wayne D. Meitzler	Mission Analysis
Jack D. Pettus	Data Link Analysis
Robert J. Richardson	Receiver Systems
Arlen I. Reichert	Propulsion
Peter C. Steel	Aeroheating
John G. Vega	Data Handling
E. Doyle Vogt	Mission Analysis, Lead
Donald E. Wainwright	Systems
Clifford M. Webb	Thermal Analysis
Charles E. Wilkerson	Data Handling

CONTENTS

Figure

I. INTRODUCTION

The material in this report summarizes the results of a nine-month system level study of a nonsurvivable turbopause probe mission to explore the atmosphere and environment of Jupiter. Included are the study constraints, science and mission objectives, mission selection, and design summaries describing required engineering implementation, discussions of critical technical problems and trade studies, and conclusions and recommendations.

Basic study objectives were to assess the technical feasibility of a nonsurvivable turbopause probe to Jupiter during the 1978 to 1980 launch opportunity and define the gross mission and technology requirements.

The study included five major tasks--definition of science requirements, mission evaluation, probe system definition, spacecraft support-requirements definition, and nonequilibrium flow-field analysis for communications blackout evaluation. Definition of science requirements included establishment of science measuremer characteristics necessary to meet science objectives. Mission analyses included definition of interplanetary, approach, and entry trajectories; deflection maneuver analysis, and trajectory dispersion analysis. Definitions of probe systems included evaluation of entry heating and heat protection with survival depth, communications system design with depth, as well as probe hardware integration and configuration design. Definitions of spacecraft support requirements included identification of interfaces, and definition of structural, power, functional, and operational requirements. Figure I-1 presents the study flow logic for the overall effort. A major study subtask was evaluation of electron density in the probe wake, which determines the point of communications blackout and mission termination. This evaluation was made by performing a detailed nonequilibrium thermochemical analysis of the hypersonic flow field surrounding the entry vehicle.

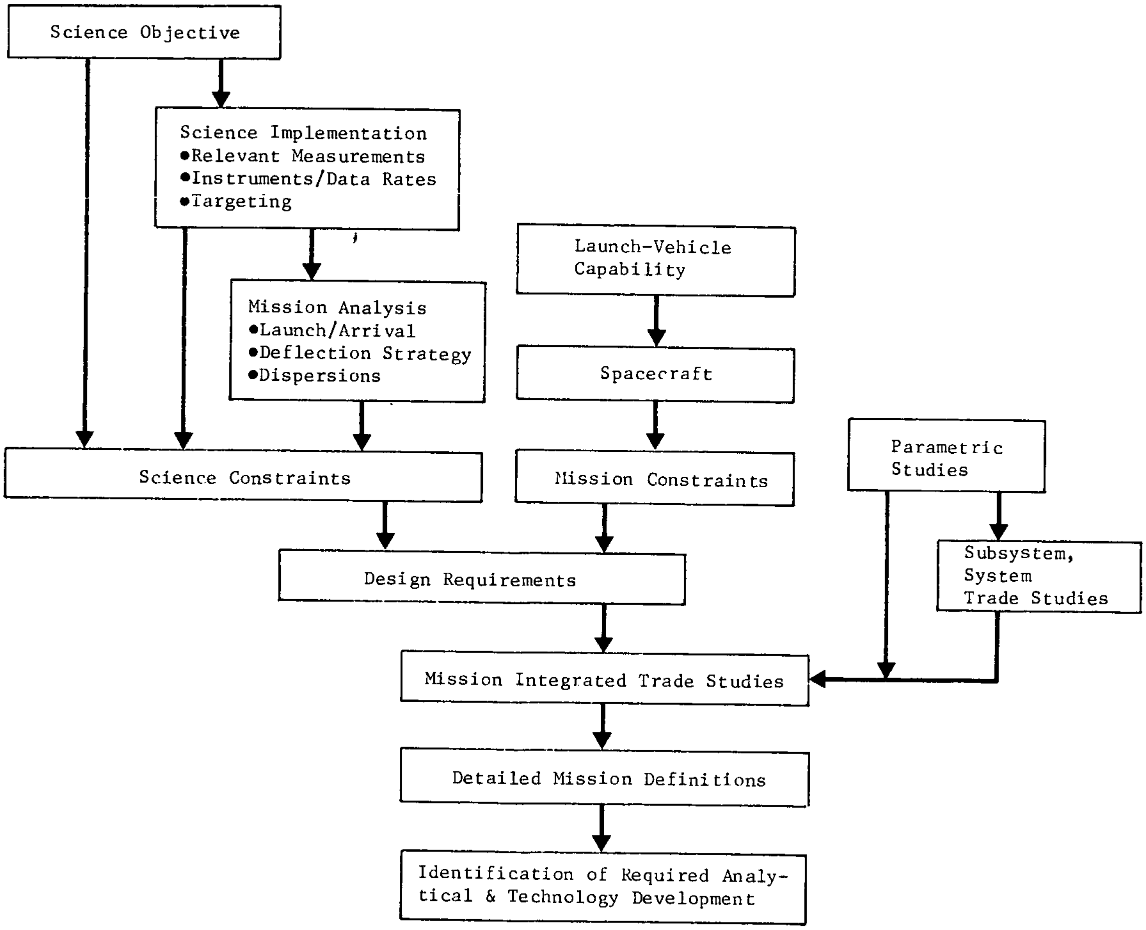

Fig. I-1 Study Flow Logic

The study was conducted in three major phases:

1) Criteria;
2) Mission trades;
3) Mission definitions.

The criteria phase emphasized defining the science and mission constraints based on the science objectives and preliminary evaluation of mission trajectory and targeting. Design requirements were established and a reference mission defined to investigate system-level integration problems. In addition, basic subsystem and mission parametric studies were begun.

During the mission trade phase, the results of the parametric studies were used to perform integrated mission trades, investigate various mission options, and establish criteria for the final mission definitions. The third and final phase consolidated the results of all final analyses and provided a detailed definition of the mission options of primary interest.

To ensure that study results would be as objective as possible, many outside contacts were made with interested scientists and engineering firms. Martin Marietta has retained a group of consultant scientists for assistance in the planetary program studies, and they provided many helpful suggestions and advice for this study. These include Dr. D. M. Hunten (Kitt Peak National Observatory), Dr. R. Goody (Harvard University), Dr. W. B. Hanson (University of Texas), and Dr. R. Vogt (California Institute of Technology). In addition, valuable assistance in definition of scientific instruments was obtained from Dr. Siegfried Bauer (GSFC), Dr. Eugene Maier (GSFC), Ballard Troy (GSFC), Dr. Hasso Niemann (GSFC), Dr. Lawrence Brace (GSFC), Dr. Donald Heath (GSFC), and Dr. Daniel Harpold (GSFC). Mr. Harvey Allen consulted with us on the technical approach and attendant technical problems.

In addition, outside engineering consultation was obtained for beryllium materials technology, thermal-control insulation, propulsion, advanced telecommunications (K-band), and space power systems; and this information was integrated into the study.

II. SUMMARY

The objective of this study was to investigate the feasibility of a Jovian atmospheric mission with probe survival to a few tens of kilometers below the turbopause. The probe is carried as a passenger and separated from a spacecraft designed to fly by Jupiter. The probe descends through the Jovian atmosphere, performing a series of scientific investigations primarily related to determining the structure, composition, ionization, and photochemistry of the upper atmosphere and the bulk composition of the lower atmosphere. During this science measurement period, the probe transmits the results to the spacecraft, which in turn stores or relays the data to Earth. The probe is exposed to greater and greater aerodynamic heating until, at some point in its trajectory, it is destroyed. The terminal trajectory is shown in Fig. II-1.

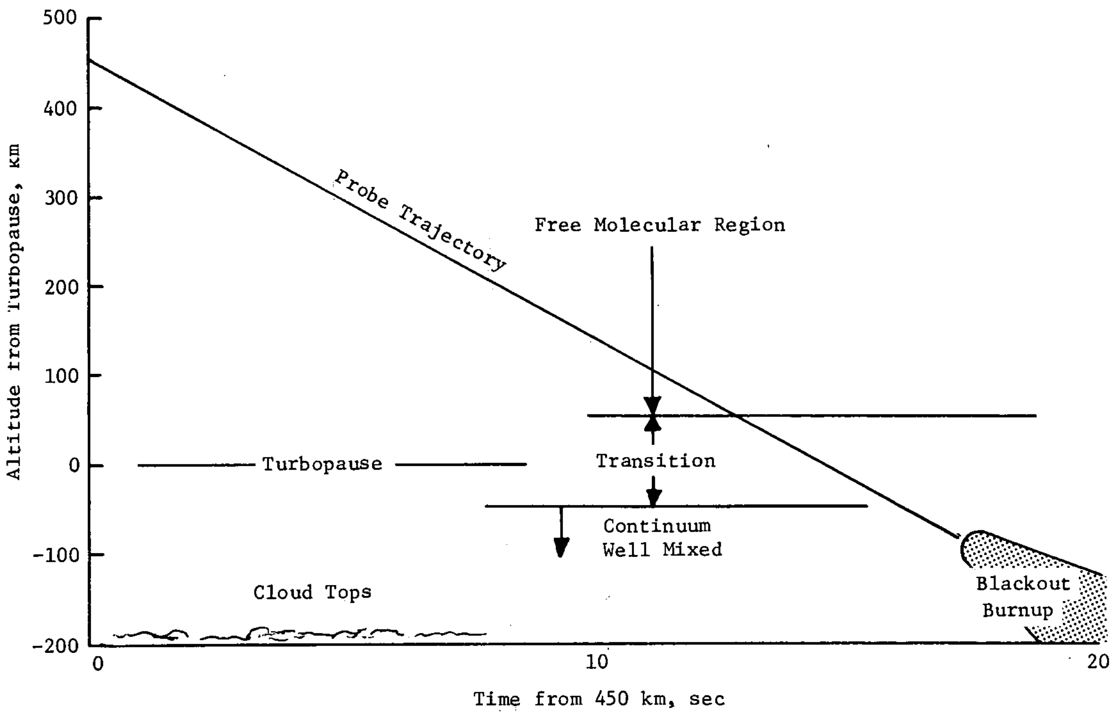

Fig. II-1 Jupiter Turbopause Probe Terminal Trajectory

The Titan IIID-Centaur-Burner II family of launch vehicles was used in this study with launch payload capability to 1090 kg (2400 lb). Launch opportunities were from 1978 to 1980, with both Pioneer and Thermoelectric Outer-Planet Spacecraft (TOPS) to be used as representative carrier vehicles. Under GSFC redirection during the latter portion of the study, a 1977 Jupiter-Saturn (JS 77) launch opportunity was investigated using the Modified Outer-Planet Spacecraft (MOPS). The MOPS configuration was based on a concurrent Martin Marietta study.

A broad range of spacecraft flyby mission options was investigated and many proved adaptable to the nonsurvivable turbopause probe concept. Table II-1 lists typical missions that provide excellent opportunities to fly a probe into Jupiter's atmosphere, with system weights and spacecraft support requirements within the capability of the spacecraft and launch vehicle specified.

Table II-1 Typical Jupiter Turbopause Probe Missions

	Probe/ Science Optimized	Radiation-Compatible Spacecraft	Grand Tour 1978	Grand Tour 1979	Solar Apex	Jupiter-Saturn 1977
Launch Vehicle, Titan IIID-Centaur-Burner II	5-seg	5-seg	7-seg	7-seg	5-seg	5-seg
Spacecraft	Pioneer	Pioneer	TOPS	TOPS	Pioneer	MOPS
Launch Date	10/21/78	10/13/78	10/3/78	11/11/79	10/9/78	9/5/77
Flyby Periapsis Radius, R_J	1.1	4.0	1.9	6.6	1.8	4.8
Science Data Rate, bps	1300	914	958	914	958	914
Probe Weight, kg (lb) (+15% Margin)	59.6 (132)	59.3 (131)	88.2 (194)	88.2 (194)	88.2 (194)	81.2 (179)

Note that all presently considered missions can be launched by the 5-segment solid version of the Titan IIID-Centaur-Burner II. The missions designed for the cancelled TOPS did require 7-segment solids on the launch vehicle.

All probes fall into two basic categories--the simple probe weighing about 59 kg (130 lb) and the more complex weighing about 81 kg (179 lb). The simple probe can be used on any mission in which the spacecraft is initially targeted to the entry point and, after releasing the probe, deflects itself onto the appropriate flyby trajectory. For spacecraft missions with postencounter objectives, such as flying on to a second planet, it may be desirable from the spacecraft mission viewpoint to leave the spacecraft trajectory undisturbed, and to require that the probe provide the deflection maneuver and necessary reorientation for zero angle of attack at entry. This requires the addition of a ΔV propulsion solid rocket and an attitude-control system on the probe. These subsystems, plus the increased power, structural size, and support, result in the weight increase of 22 kg (49 lb).

The major uncertainty affecting the engineering feasibility of the nonsurvivable turbopause probe mission is the radiation belt hazard. Although a thorough analysis of radiation environment effects on the probe was beyond the scope of the study, a preliminary evaluation indicated that probe survival of the most severe estimated environment was feasible if appropriate material and component selection is made and local shielding provided. The effect of possible residual reradiation on the science instrument background noise has not been evaluated. However, appropriate design approaches to both instrument electronics and local materials selection appear to provide a solution to this problem with some penalty.

Critical studies of science instrument implementation, mission survival, and data return showed that all engineering subsystems required for this mission are feasible, and the technology is within the 1975 state of the art. For science instruments, the neutral-particle retarding potential analyzer (NRPA) and the neutral mass spectrometer both require some research and development.

The NRPA has never been flown; however, it is an offshoot of the IRPA, and no serious problems are anticipated in its development. For the mass spectrometer, the inlet sampling system portion of the instrument must be developed and tested, while the quadrupole analyzer section is current state of the art and has been flown many times with a conventional inlet system. For the very low measurement pressure and rapid response required on this mission, a molecular-beam sampling system has been proposed instead of the conventional molecular-leak type. Technology for this system is available, but the specific design must be proved.

The study showed that probe survival is feasible far enough below the turbopause to meet all science objectives. It also showed that probe burnup altitude is significantly below or after communications blackout altitude, and therefore, heating is not the critical factor in terminating the mission. Because both heating and blackout are directly related to atmospheric density, burnup will always follow blackout altitude, even though atmospheric uncertainties may shift the actual location of these occurrences. The probe heat protection system is less than 10% of probe weight for survival to required depths, and the data-link communications frequency of X-band (10 GHz) provides sufficient penetration below the turbopause to meet the science criteria before communications blackout.

Results of this study show that a variety of mission options for a nonsurvivable turbopause probe to Jupiter are feasible and practical within the 1975 state of the art.

III. MISSION DEFINITION

This chapter provides an overview of the turbopause probe concept, science objectives, and mission description. Science objectives are general for any type of probe mission to Jupiter's upper and lower atmosphere, and a probe that can survive a brief distance below the turbopause can satisfactorily meet the science objectives. Science instruments required to obtain relevant measurements are identified, and brief descriptions of the mission and required hardware implementation are given.

A. TURBOPAUSE CONCEPT

In past years, much emphasis has been placed on exploration of the outer planets. Of these, Jupiter is the largest and of singular importance to planetary studies. It is the most accessible, of almost stellar mass, probably has a significant internal heat source; its composition is close to that of the Sun; and it represents a different stage in planetary evolution from that of the terrestrial planets.* The scientific objective for a Jupiter probe is to determine major characteristics of the upper and lower atmosphere, such as composition, structure, and ionization. The upper atmosphere is the region of diffusive gravitational separation of light and heavy gases, with its base at the turbopause. In the atmosphere below the turbopause, the constituents become mixed so that the composition is nearly constant and heavier gases become appreciable.

---

*R. M. Goody and G. M. Levin: *The Jovian Turbopause Probe*, Part I and II, GSFC Report X-110-70-442 and 443, Dec 1970.

Exploration of the Jovian atmosphere by remote means has proved difficult, and indeed, unsatisfactory. The only reliable procedure to obtain measurements related to abundances and physical variables is by means of *in situ* probe-carried experiments. Both survivable and nonsurvivable probe concepts have been considered. The survivable probe concept is highly desirable because it will provide a relatively long measurement period in the lower atmosphere. However, the Jovian entry environment is harsh because of its large gravitational attraction, which results in entry velocities from 50 to 75 km/sec. Therefore, heat-shield development must be undertaken for the survivable probe. The nonsurvivable probe concept provides a means of obtaining a significant portion of the scientific data at an early date and at less cost. Calculations of trajectory, heating, communications link, and measurement capability of the nonsurvivable probe indicate that the mission will survive below the Jupiter turbopause, allowing measurements in the mixed region of the atmosphere before the probe is finally destroyed by the increasing aerodynamic heating. Thus, the nonsurvivable probe can measure the upper atmosphere of Jupiter as well as obtain information on the bulk composition in the region of mixed atmosphere.

B. SCIENCE OBJECTIVES AND RELEVANT MEASUREMENTS

In this section, science objectives are discussed and relevant measurements required to meet these objectives are identified. Science objectives for a nonsurvivable probe to Jupiter were first reported in a document published by GSFC.* The required science instruments specified by GSFC as necessary to obtain the measurements are briefly identified here and more detailed descriptions are in Chapter IV Subsection A1.

---

*R. M. Goody and G. M. Levin: *The Jovian Turbopause Probe*, Part I & II, GSFC Report X-110-70-442 and 443, Dec 1970.

1. Objectives

The science objectives of a Jovian turbopause probe mission resulting from prior studies are twofold:

1) To directly determine the bulk composition of the mixed atmosphere;
2) To investigate the properties of the upper atmosphere and ionosphere.

An important requirement imposed by the first objective is that the probe must penetrate far enough below the turbopause to determine bulk composition. This requires a time sufficient to make measurements with a mass spectrometer.

An investigation of the upper atmosphere and ionosphere, specifically their structure, composition, ionization, and photochemistry, is equally important. Measurements in these regions should determine temperature, composition, particle separation, positive ion density, and electron density, permitting thorough understanding of both regions.

2. Relevant Measurements and Performance Criteria

To satisfy science requirements and objectives a list was made of measurements related to objectives. These are shown in Table III-1 with corresponding performance criteria and the instruments that acquire each measurement.

Although each measurement provides information important to understanding the Jovian atmosphere, one of the more significant is the neutral hydrogen/helium (H/He) ratio in the mixed lower atmosphere which is measured by three instruments (NMS, NRPA, PH/SP). The H/He measurements obtained above the turbopause will not accurately represent the bulk composition below. Therefore, penetration below the turbopause to obtain hydrogen and helium abundance data with the mass spectrometer and NRPA is necessary to fulfill the science criteria of this mission.

Table III-1 Science Implementation Summary

Science Objectives	Relevant Measurements	Altitude, km (0 = turbopause)	Sampling Requirements	Instrument[1]
A. Determine Bulk Composition of Atmosphere	1. H/He Ratio	0 to -60	2 below 0 km	NMS PH/SP
	2. Relative Abundances of Isotopes[2]	100 to -60	2 below 30 km	NMS
	3. Relative Abundances Atmospheric Constituents[3]	100 to -60	2 below 30 km	NMS/NRPA
B. Investigate Upper Atmosphere & Ionosphere	4. Neutral-Particle Concentration Profiles	1,000 to 0	1 measurement per scale height for each constituent	NRPA
	5. Ion-Concentration Profiles	50,000 to 0		IRPA
	6. Electron Density & Temperature Profiles	50,000 to 0		ETP
	7. Neutral-Particle Temperature Profiles	1,000 to 0		NRPA
	8. Ion-Temperature Profiles	50,000 to 0		IRPA
	9. Lyman α Dayglow Profiles of H & He	1,000 to 20		PH/SP

[1]NMS - neutral mass spectrometer; PH/SP - photometer/spectrometer; NRPA - neutral-particle retarding potential analyzer; IRPA - ion-retarding potential analyzer; ETP - electron temperature probe

[2]Isotopes of interest are H^1, D^2, He^3, He^4, C^{12}, C^{13}, N^{14}, Ne^{20}, Ne^{22}, A^{36}, A^{38}

[3]Minor constituents include CH_4, CH_3, CH_2, NH_3

In determining the bulk composition of the atmosphere, relative abundance measurements are taken for a set of 11 isotopes. The heavier isotopes of the set are not expected to appear until near the turbopause. The H/He ratio is actually determined by combining readings from four isotopes, i.e., $(H^1 + H^2)/(He^3 + He^4)$. Relative abundances of such minor constituents as CH_4, CH_3, NH_3, and others may also be measured in the vicinity of the turbopause with the NRPA, if they exist in sufficient quantities to be within the range of the instrument.

Number density concentration profiles for neutral particles that exist in the upper atmosphere and ions that constitute the ionosphere will be established by the IRPA and NRPA. The ionosphere may begin at a very high altitude; thus to account for uncertainties, the search for positive ions should begin at an altitude of about

50,000 km. The range of the IRPA is from 1 to 5 amu to account for H_1^+, H_2^+, H_3^+, He^+, and HeH^+. There are not a measurable number of neutral particles above 1000 km altitude; thus measurements beginning here should collect all available information. However, this measurement is specified to begin at 5000 km to provide the same conservatism used for ionic measurements. The mass range of the NRPA is from 1 to 20 amu. The primary neutrals detected will undoubtedly be H, H_2, and He, but, as the probe nears the turbopause, it may also pick up minor constituents.

Electron number density concentration profiles are to be established from where the ETP first picks them up according to its sensitivity, probably less than 50,000 km, down to the turbopause. In addition, rate of change of electron current caused by varying the voltage should be read accurately enough to yield an onboard-calculated electron temperature profile as the probe decends.

The purpose of the dayglow instruments is to establish dayglow profiles of two particular wavelengths of H and He ultraviolet re-emitted radiation as the probe descends. In particular, the wavelengths of interest are the H Lyman α line at 1216 Å, and He 584-Å line. In addition to information about resonance light scattering, this measurement gives a redundant, independent check of the H/He ratio. Measurements begin as soon as the photometric instruments are pointed toward Jupiter.

Science instruments required to make the measurements are listed in the right-hand column of Table III-1, and sketches of them with their locations on the entry probe are shown in Fig. III-1. Discussions of science-instrument operation and performance are in Chapter IV, Section A.

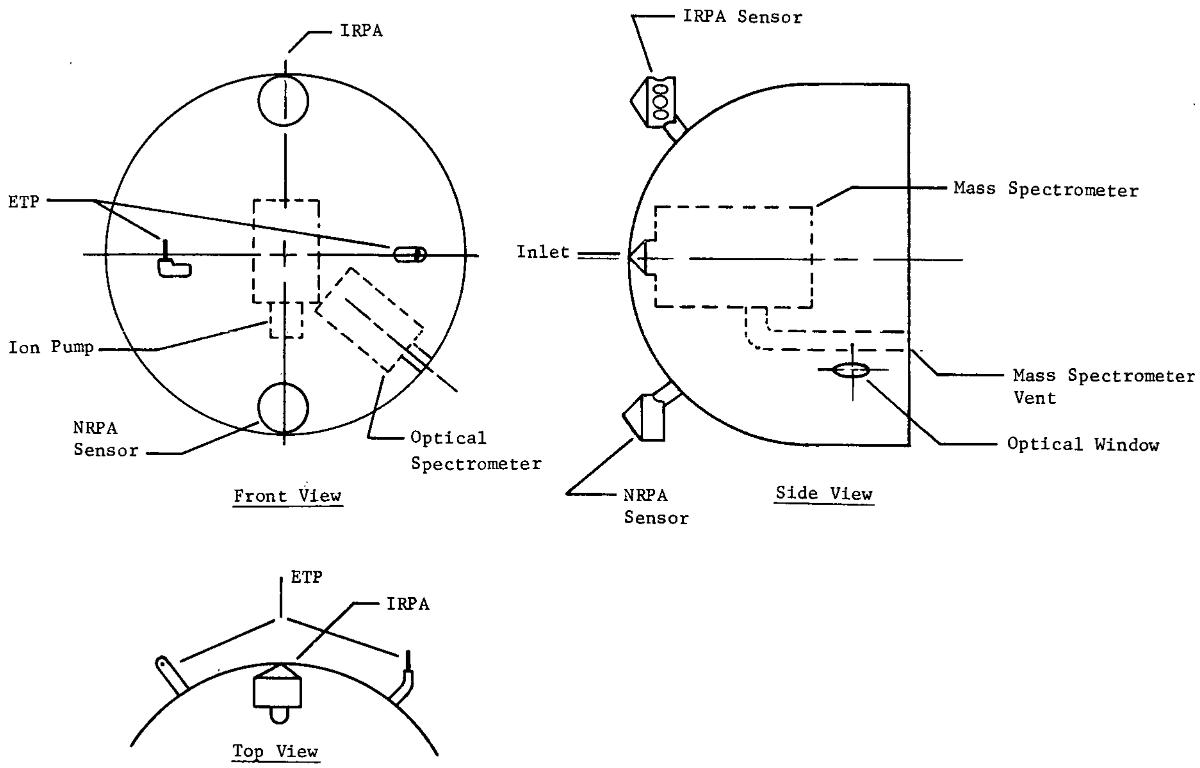

Fig. III-1 Science Instruments on Probe

C. MISSION SUMMARY

A brief overview of the turbopause mission is provided in this section. The mission profile is described first, then alternative configurations for the probe and spacecraft are presented.

1. <u>Mission Profile</u>

a. Launch Phase - The actual mission begins with the launch of the spacecraft from the Eastern Test Range into a 185-km (100 n-mi) parking orbit. After a short coast, the spacecraft is injected onto the required interplanetary trajectory. The launch phase must be consistent with the specific launch-vehicle performance and standard launch constraints like range safety and parking-orbit coast time.

b. Interplanetary Phase - The interplanetary phase of the missions considered covers a period of 1.5 to 2.0 years. During this transfer from Earth to Jupiter, the probe temperature is controlled by internal insulation and heaters powered by the spacecraft. Protection from meteoroid damage is provided by an environmental enclosure that also contributes to probe thermal control.

Two midcourse maneuvers are performed during transfer. The first, approximately 10 days after launch, is used to reduce injection error. The velocity increment required for this maneuver typically has a mean value of 15 m/sec and a standard deviation of 10 m/sec, resulting in a required midcourse capability of 45 m/sec. A second midcourse maneuver is used to target the spacecraft trajectory for the deflection maneuver. Performed 13 days before deflection, this maneuver has a required velocity increment capability of about 10 m/sec (3σ).

c. Deflection Maneuver - At a range of 10 to 50 million km (or 10 to 70 days) from arrival at Jupiter, the deflection maneuver is performed. This must satisfy three objectives:

1) Separate the probe from the spacecraft on a trajectory impacting the desired entry site;
2) Orient the probe in the attitude required for zero angle of attack at entry;
3) Establish communications geometry for the probe/spacecraft communications link.

For the deflection maneuver, three operational sequences have been identified and analyzed during the study (Fig. III-2). Detailed descriptions of these modes are provided in Section IV.D.

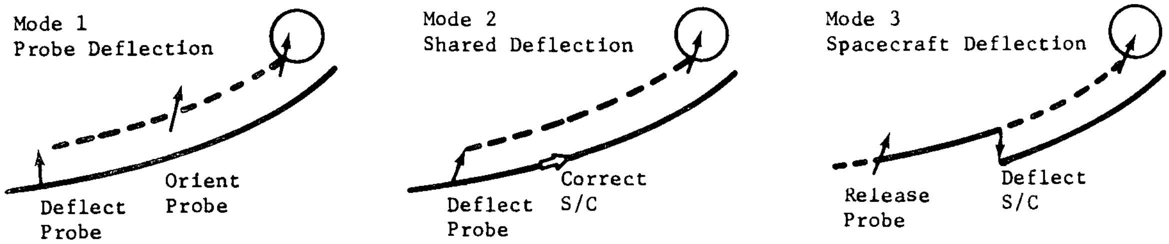

Fig. III-2 Comparison of Deflection Modes

Required entry conditions are illustrated in Fig. III-3. Posigrade low-inclination trajectories with low-latitude entry sites are preferred because they result in decreased relative entry velocity. Entry-site longitude is constrained by a science requirement to enter at least 20° from the evening terminator. This both ensures that entry occurs in the ionized environment and enhances the day-glow measurements. Conversely, science performance (i.e., number of measurements) is improved by lower entry angles, which result in entry sites nearer to or past the terminator. Thus, the entry longitude selected is 20° from the terminator. Finally, thermal considerations and instrument sampling constraints require that relative angle of attack at entry be nominally zero ±10°.

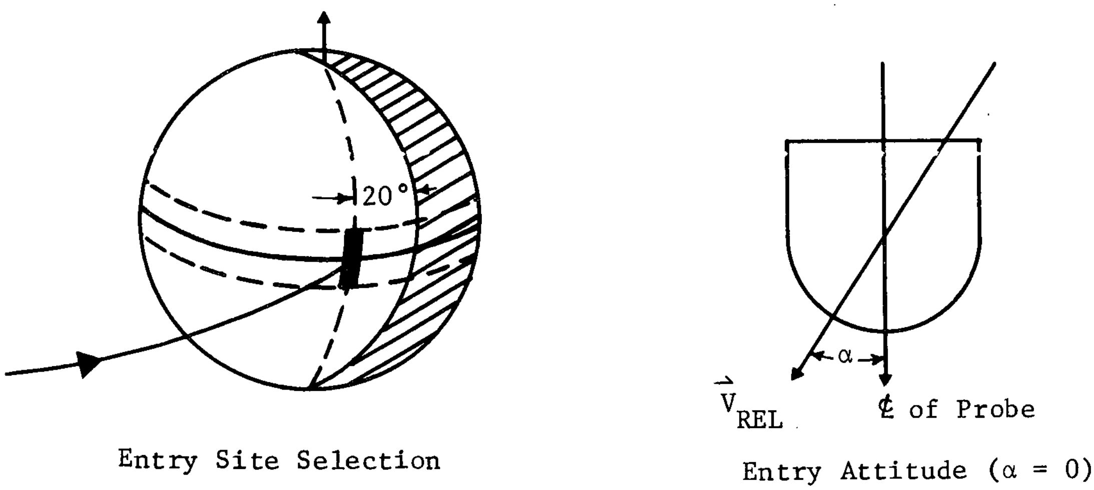

Fig. III-3 Entry Conditions

Two types of probe/spacecraft communications geometry at entry have been considered (Fig. III-4). In the tail geometry, the spacecraft is on the extension of the probe longitudinal axis at entry. In the side geometry, the spacecraft is at the point on its trajectory nearest the entry site at the time of probe entry. During the course of the study, tail geometry was shown to be the superior (See Chapter IV Subsection C2.) of the two approaches because the space-loss reduction did not compensate for the reduction in probe antenna gain for the side case.

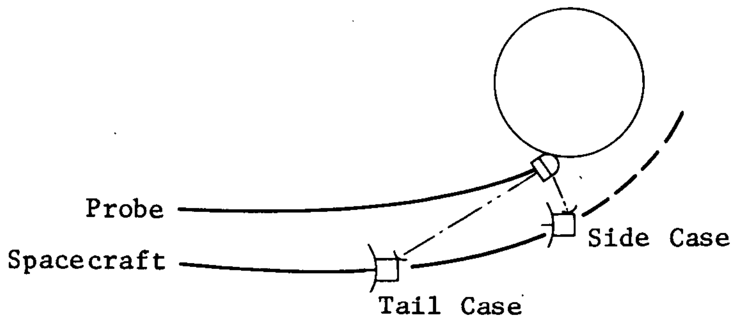

Fig. III-4 Communications Geometry

Figure III-5 shows the sequence of events from probe separation to entry for a typical probe deflection mission like that envisioned for a 1977 Jupiter/Saturn flyby in which the spacecraft is not required to provide the deflection maneuver.

d. Acquisition and Communications Link - After deflection, the probe and spacecraft coast along their separate trajectories for 10 to 70 days (depending on deflection radius.) At approximately 3/4 hour before entry, the spacecraft acquires the probe RF signal. The acquisition activity must be designed to ensure to an acceptable level that the spacecraft will find the probe during its programmed search in both position and frequency. Therefore, the extent of this search is determined by analysis of dispersions associated with the deflection maneuver.

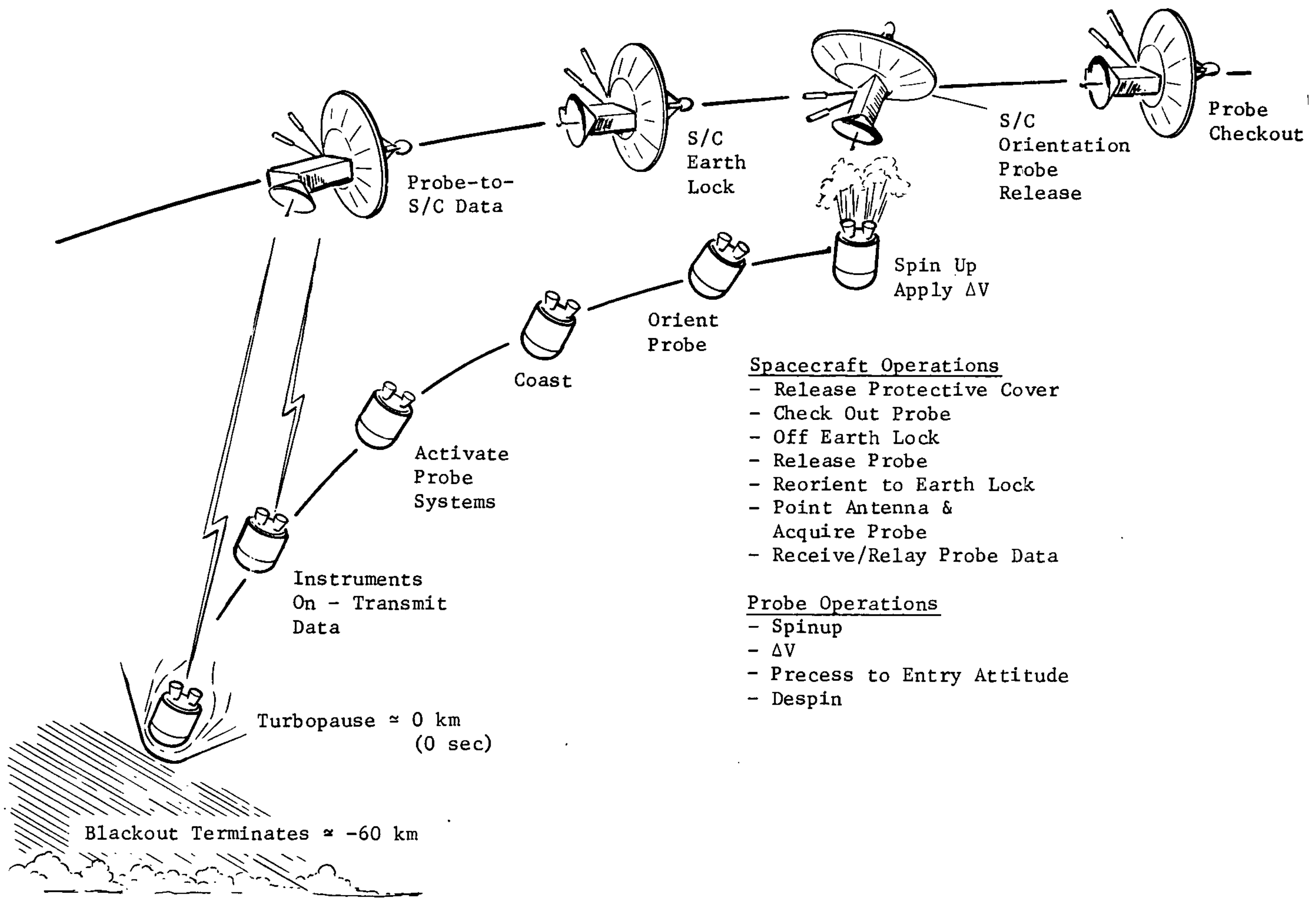

Fig. III-5 Probe Release/Entry Sequence - Probe Deflection

Following acquisition, the communications link must be maintained throughout the mission. In certain missions, this may be accomplished while using a fixed antenna on the spacecraft. In other missions, it is possible to move the spacecraft antenna according to a predetermined program to follow the relative movement of the probe. In either case, spacecraft antenna beamwidth must be great enough to accommodate dispersions in spacecraft-probe relative geometry. Fluctuations in doppler rate must also be considered.

e. *Measurement Performance* - Immediately after acquisition, transmission is started from the probe to the spacecraft. Engineering data on the status of probe subsystems are first telemetered to the spacecraft. Then data from the upper atmosphere instruments (Langmuir probe, IRPA, and optical instrument) are taken and transmitted. (Acquisition time is selected to ensure that these measurements are taken by the time an altitude of at least 50,000 km above the turbopause is reached.) The NRPA and mass spectrometer are operating and transmitting data by the time an altitude of at least 5000 km is attained. Data are taken, processed, transmitted to, and stored on the spacecraft for delayed relay to Earth. Measurement performance time for the mission is approximately 30 min from 50,000 km to the turbopause and 2 sec below the turbopause (for an entry angle of -25°).

f. *Mission Termination* - The turbopause mission terminates approximately 60 km below the turbopause. Just below this point, communications blackout occurs for the 10-GHz communication frequency used in the mission. The heat sink on the probe permits the structure to survive down to about 0.5 sec past blackout for an entry angle of -25°.

2. Probe/Spacecraft Configurations

The general configuration of the turbopause probe is shown in Fig. III-6. The level of complexity for the probe is a function of

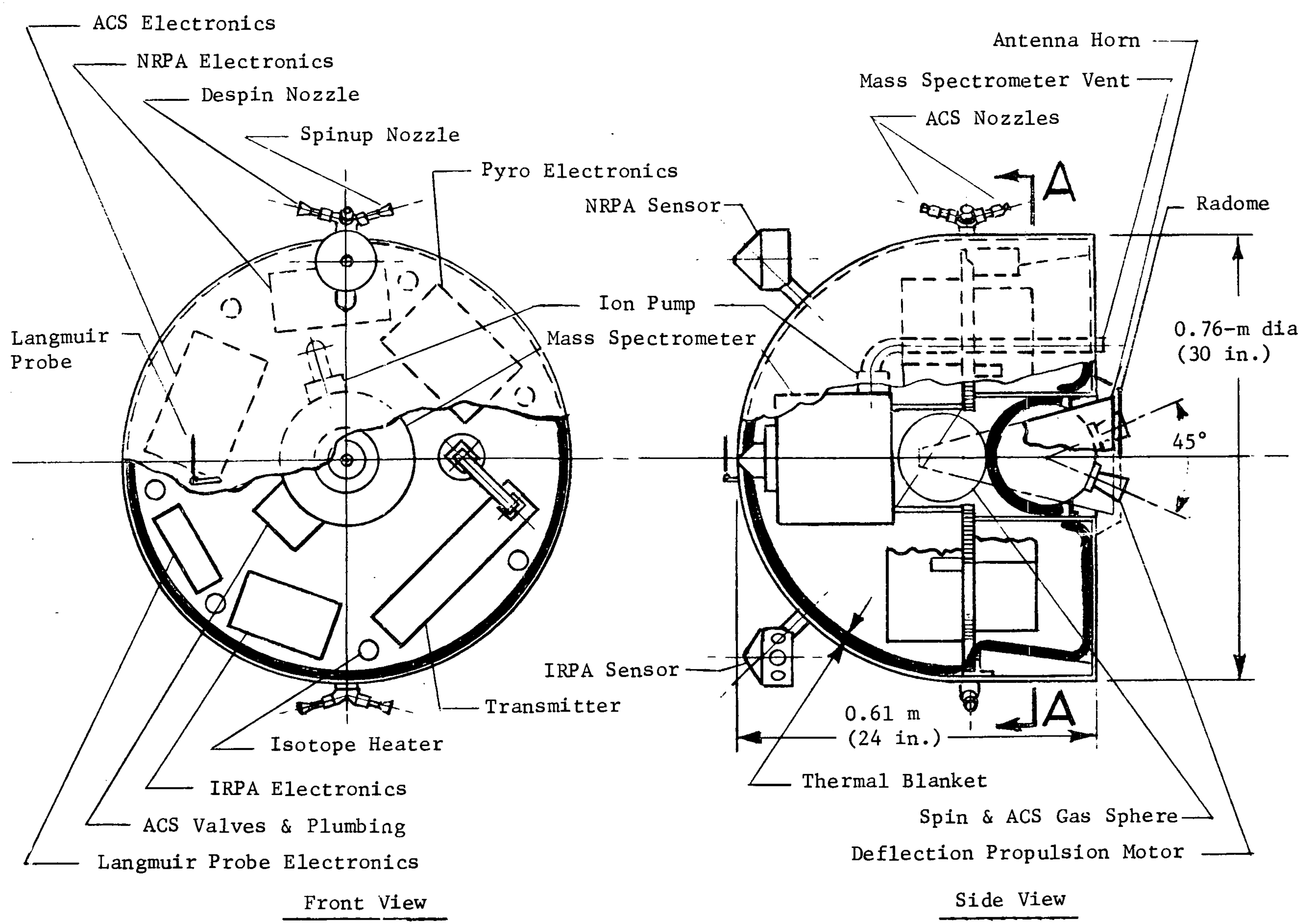

Fig. III-6 Probe Configuration

the deflection mode used in the mission (Chapter IV, Section D). The more complex probe is expanded from the simple probe by the addition of a deflection propulsion solid rocket and an attitude-control system, as shown in the figure. The probe consists of a hemisphere that has a short cylindrical skirt with a diameter of between 71 cm (28 in.) for the simple probe and 76 cm (30 in.) for the slightly larger, more complex version. Weights vary from 59 kg (130 lb) to 86 kg (190 lb). Typical weights are shown in Table III-2.

Table III-2 Probe Weights

	Simple Probe, kg (lb)	Complex Probe, kg (lb)
Science	14.4 (31.7)	14.4 (31.7)
Structure & Heat Sink	12.2 (26.9)	12.6 (27.7)
Telecommunication	10.7 (23.5)	10.7 (23.5)
Propulsion & ACS	1.2 (2.7)	14.7 (32.5)
Electrical	7.0 (15.4)	9.9 (21.8)
Other	6.5 (14.7)	8.9 (19.8)
Contingency (15%)	7.8 (17.3)	10.1 (22.0)
Total	59.6 (131.6)	81.2 (179.0)

Detailed designs for the probe for three alternative turbopause missions are in Chapter V of this volume.

Initially, the study was to consider the Pioneer F and G and TOPS for the design missions. At GSFC's direction, the MOPS was added to the study. The Pioneer spacecraft is an operational spin-stabilized vehicle with a design life of two to five years. TOPS and MOPS are more complex three-axis stabilized vehicles. TOPS was designed for a life of up to 12 years; MOPS has a design life of 3.5 years, which provides sufficient endurance for a Jupiter-Saturn mission. Weight summaries of these three vehicles are shown in Table III-3 and configurations in Fig. III-7.

Table III-3 Spacecraft Weight Summary

	Pioneer	TOPS	MOPS
Spacecraft, kg (lb)	248.3 (547.0)	658.0 (1450.0)	665.9 (1468.0)
Modifications, kg (lb)	31.5 (69.4)	33.6 (74.0)	25.2 (55.6)
Total, kg (lb)	279.8 (616.4)	691.6 (1524.0)	691.1 (1523.6)

In general, probe missions using either Pioneer or MOPS can be launched by the Titan IIID/5-segment-Centaur-Burner II. Missions using TOPS require the 7-segment version of the launch vehicle. Performance data for these vehicles are in the appendix to this volume.

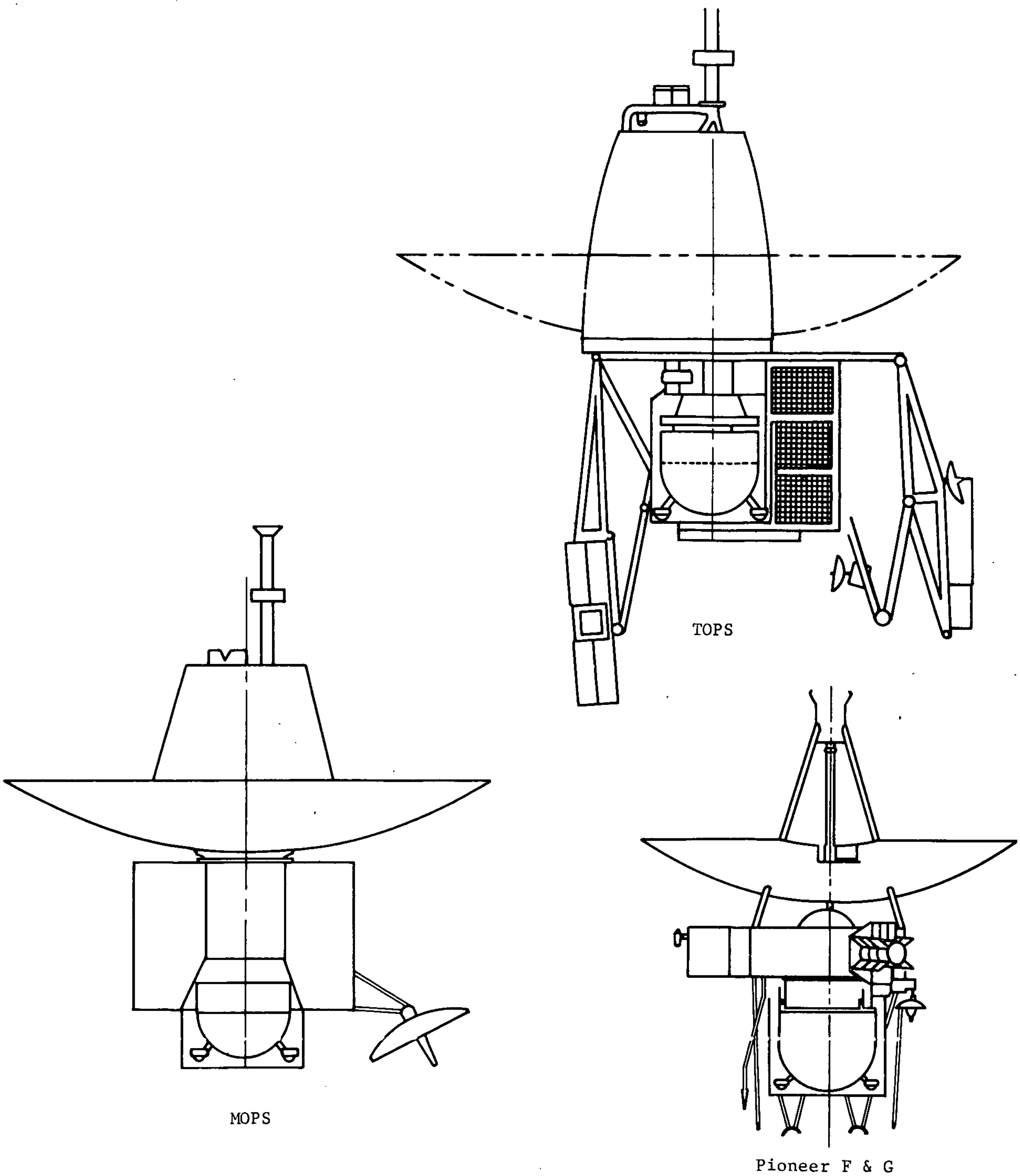

Fig. III-7 Comparison of Candidate Spacecraft

IV. CRITICAL MISSION STUDIES

The studies summarized in this chapter cover the technical areas considered most critical to the success of the turbopause probe mission. The previous chapter established the mission and science objectives; this chapter deals with the implementation required to meet those objectives. Science instrument implementation and measurement performance is discussed, followed by mission survival and data return. Mission survival to the required depth into the atmosphere depends on appropriate design for communications blackout, probe thermal protection from aerodynamic heating, and hardening against radiation damage. Data return depends first on probe acquisition by the spacecraft, in which trajectory dispersions establish the requirements for the spacecraft probe tracking antenna and receiver system, and second on the communications link capability.

In addition, this chapter includes a brief description of the deflection maneuver analysis. The deflection strategy greatly affects both probe design and the spacecraft support role. In some missions, the spacecraft provides the deflection ΔV, and a very simple probe can be designed. In other missions, the probe must carry both propulsion for deflection and an attitude-control system for reorientation before entry.

A. SCIENCE RETURN

This section discusses the science instrument implementation required to obtain relevant measurements and the measurement performance obtained for typical probe entry trajectories. Performance is measured against the minimum criterion of number of measurements required to meet the science objectives, discussed in Chapter III Section B.

1. Science Instrumentation

Baseline instruments proposed for a turbopause probe mission are shown below:

1) Mass Spectrometer
2) Ion retarding potential analyzer
3) Neutral particle retarding potential analyzer
4) Langmuir probes
5) Ultraviolet dayglow photometers or spectrometer.

These five instruments are adequate for satisfying the science objectives given in Chapter III Section B.

a. Neutral Mass Spectrometer (NMS) - The NMS measures isotopic relative abundances enabling determination of the important ratio of total hydrogen to total helium. It has a nominal range of 1 to 38 amu and operates near and below the turbopause until communications blackout. The eleven isotopes to be measured are H^1, D^2, He^3, He^4, C^{12}, C^{13}, N^{14}, Ne^{20}, Ne^{22}, A^{36}, and A^{38}. The instrument is a molecular beam sampler, with the inlet system designed to allow operation at a suitable pressure level (Fig. IV-1). It is placed inside the probe body with the aperture at the stagnation point and consists of an ionizer, a quadrupole analyzer section, and a secondary electron multiplier. The analyzer field is successively readjusted for the 11 isotopes under consideration so that only particles of that specific mass/charge will have a stable enough trajectory to be collected and measured.

To reduce the possibility of beryllium sputtering, the forward area of the probe heat sink is plated with a material such as platinum or rhodium. The high atomic weight of the plating material reduces sputtering caused by impact of the atmospheric particles.

b. Positive Ion Retarding Potential Analyzer (IRPA) - The primary function of the IRPA is to establish the positive-ion number density concentration profiles through the ionosphere as the probe descends.

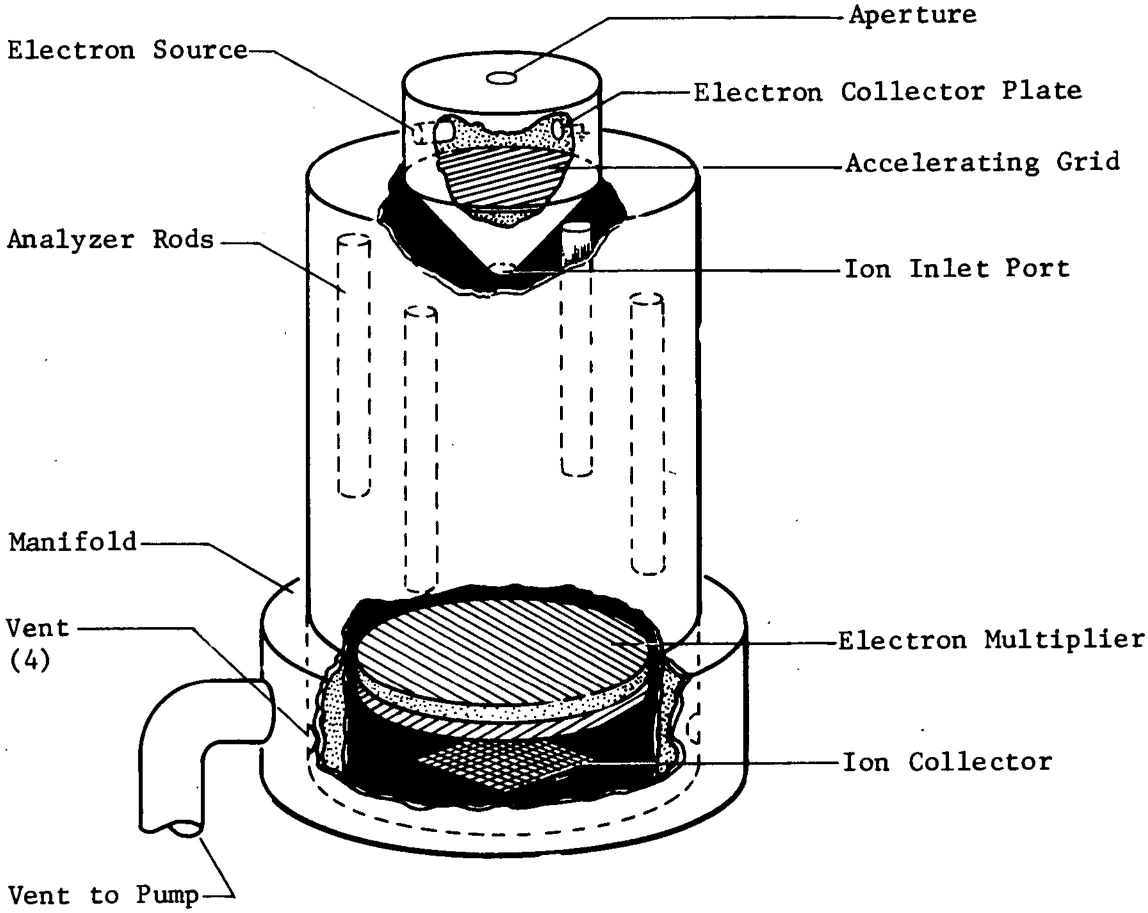

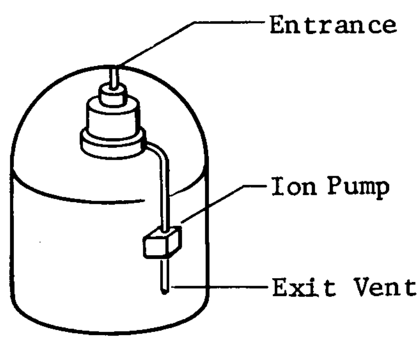

Spectrometer Location

Fig. IV-1 Neutral Mass Spectrometer, Configuration and Location

A secondary purpose is to establish ion temperatures in conjunction with the concentrations. The instrument has a range of 1 to 5 amu that encompasses H_1^+, H_2^+, H_3^+, He^+, HeH^+. It will begin operation at an altitude of about 50,000 km and take data for about 25 minutes before the grid wires burn up near the turbopause. Ions enter the aperture and are retarded by a set of grids successively varied over a range of voltages. After being collected, the ion current at each voltage is telemetered back to be used to establish a current-voltage curve from which density and temperature can be derived. Ion temperatures can be obtained by sampling a large number of points and using onboard processing before sending back the data.

The configuration of the IRPA and its location on the probe are shown in Fig. IV-2. The conical entrance and IRPA location off the probe body are to reduce particle interference both for the IRPA and other instruments.

c. Neutral Particle Retarding Potential Analyzer (NRPA) - The NRPA establishes the neutral-particle number density concentration profiles through the upper atmosphere as the probe flow field goes from free molecular into the transitional region. A secondary purpose is to establish neutral-particle temperature in conjunction with the concentrations. The instrument has a dual range covering 1 to 20 amu, looking primarily for H, H_2, and He, but with a wide enough range to detect other compounds. It will begin operation at an altitude of about 5000 km above the turbopause and take data down through the turbopause.

Operation of the NRPA is similar to that of the IRPA. It has oppositely charged grids to repel all charged particles and allow only neutral particles to enter. An electron gun then ionizes the neutral particles. The resulting ion current at each voltage is

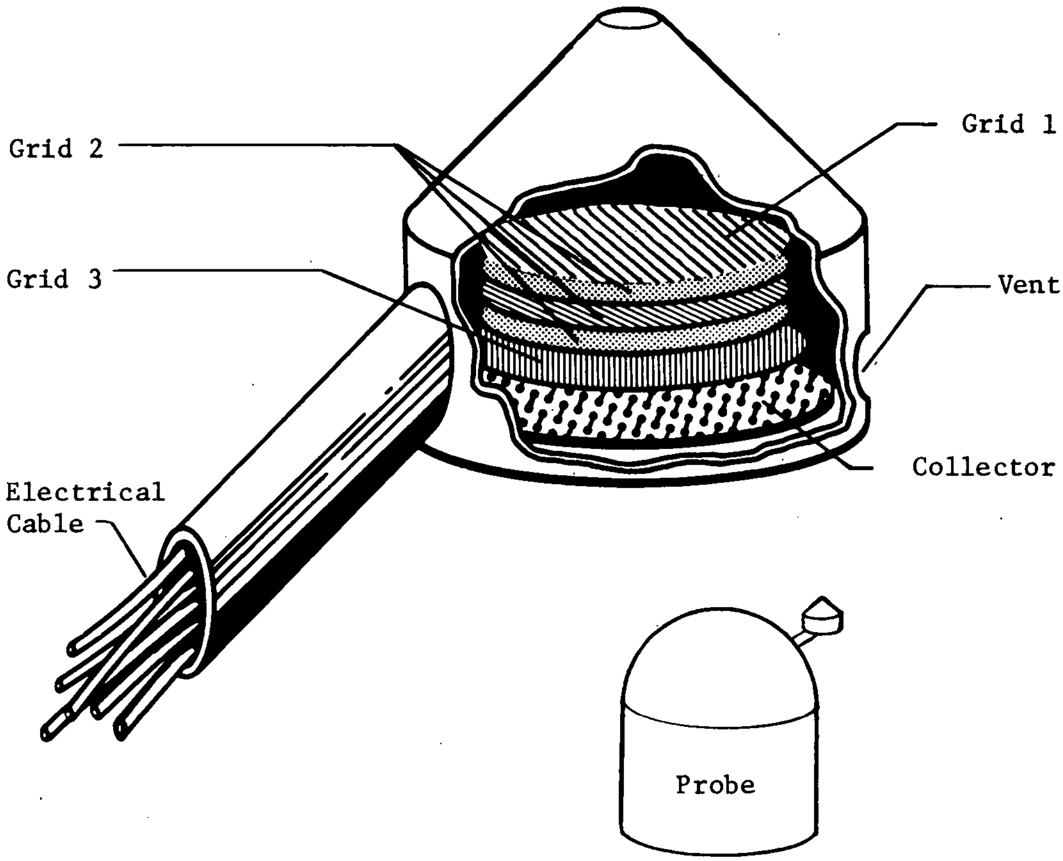

Analyzer Location

RPA Element	Potential Relative to Probe Ground
Grid 1	0 V
Grid 2	Variable retarding voltage (-3 to 63 V in 5.5-V steps)
Grid 3	-20 V to exclude electron collection & suppress emission of secondary electrons from collector
Collector	- 5 V

Fig. IV-2 Ion Retarding Potential Analyzer (IRPA), Configuration and Location used to establish the current-voltage curve from which the density and temperature can be determined. Onboard processing is required to obtain the neutral-particle temperatures.

The configuration of the NRPA is shown in Fig. IV-3. It is located symmetrically across the probe centerline from the IRPA, with its aperture even with the stagnation point.

d. *Langmuir Probe (Electron Temperature Probe - ETP)* - The ETP establishes electron number density concentration profiles and electron temperature profiles as the vehicle descends through the ionosphere in free molecular flow. It will begin searching for electrons at 50,000 km and will continuously take data down to the turbopause.

Two ETPs are used. One is perpendicular to the flight velocity vector, has a constant voltage applied, and measures the electron current as it varies with descent altitude. These measurements are processed on board to yield the electron number density. The other ETP is fixed so that the sensor is parallel to the flight velocity vector and has variable voltage applied. When this variable voltage is high and negative, the ETP measures the ion current, which is processed on board to result in the ion number density. As the voltage is swept from negative to positive, current readings are taken to obtain the shape of the current-voltage curve. Through the use of further onboard processing, electron temperature is obtained.

The configuration and location of the two instruments are shown in Fig. IV-4. The guards protrude from the vehicle nose, roughly 90° from the RPA struts. The sensor is a 7.6-cm-long hollow tube 1.6 mm in outside diameter. Electrical heaters are included in the hollow ETP and heated before use to remove any contaminant particles that may have been collected on the sensor.

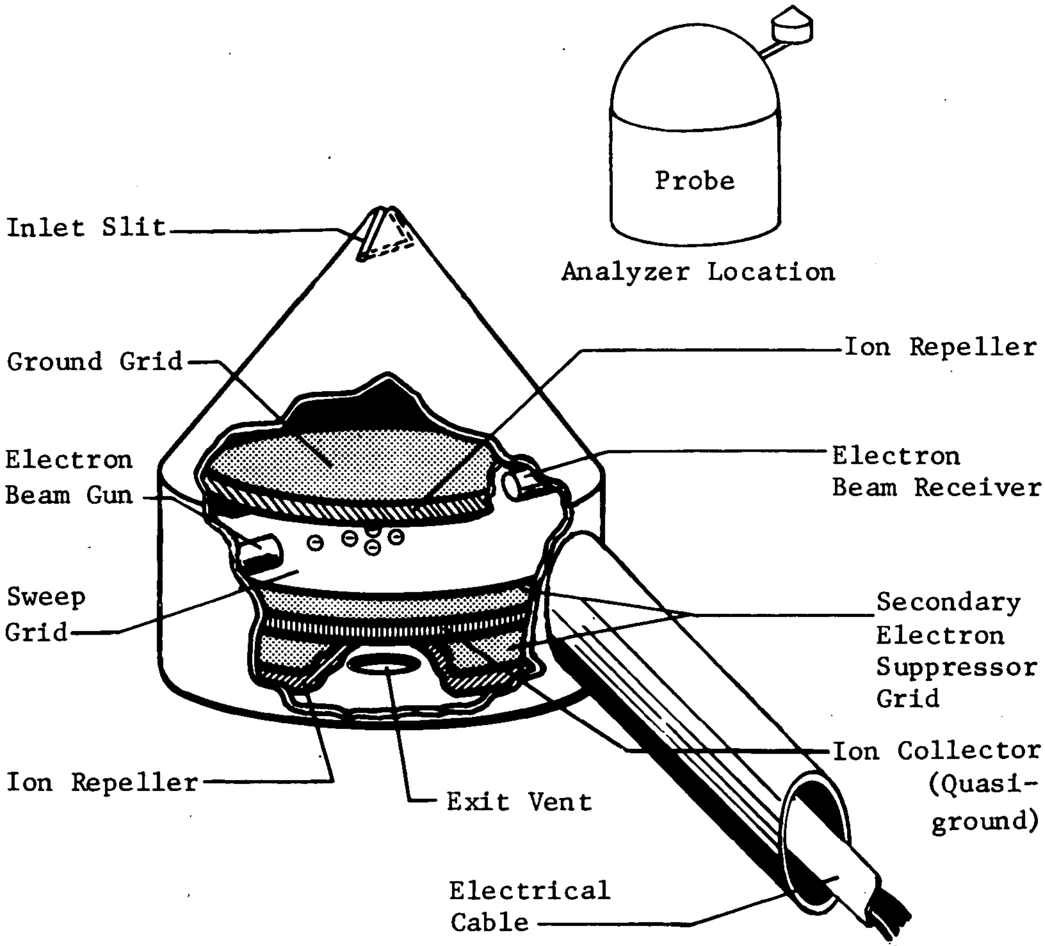

RPA Element	Potential Relative to Ground
Ion repeller	+300 V
Beam receiver anode	0 V
Sweep grid	0 to 280 V
Secondary electron suppressor grid	-300V

Fig. IV-3 Neutral Particle Retarding Potential Analyzer, Configuration and Location

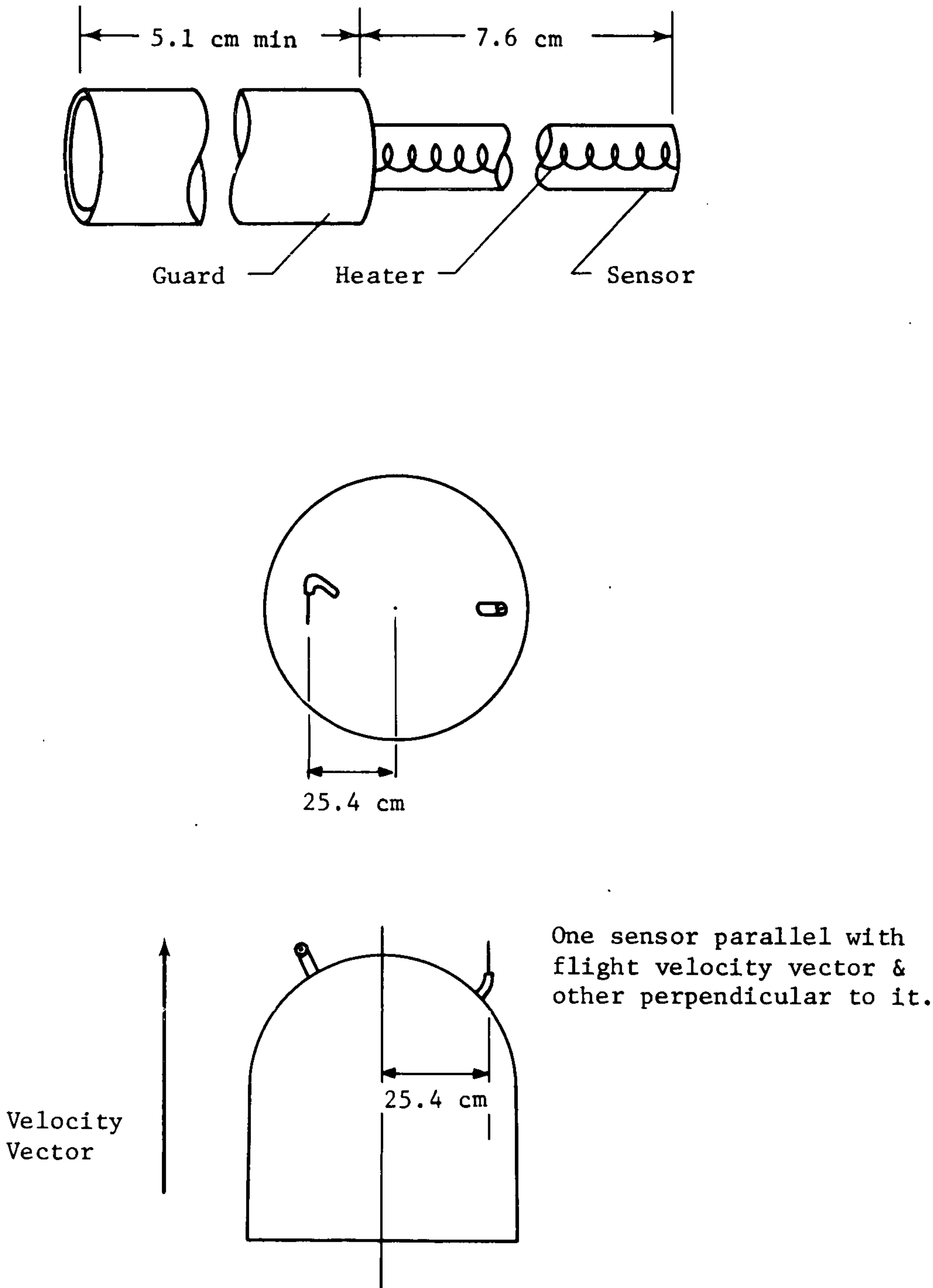

Fig. IV-4 Langmuir Probe (Electron Temperature Probe)

e. *Ultraviolet Dayglow (Photometers or Spectrometer)* - The ultraviolet dayglow instrument measures the intensity of the hydrogen Lyman alpha dayglow at a wavelength of 1216 Å. Hydrogen dayglow comes primarily from resonance scattering of atomic hydrogen, but a small amount may be from dissociative flourescence of diatomic hydrogen. Because these are the dominant particles in the upper atmosphere, the results will bear directly on the structure of the region. Three prime candidate sensors have been identified for this instrument:

1) An ultraviolet photomultiplier photometer is satisfactory only for the hydrogen measurement. The photometer optics (window and filter) have a lower cutoff point at about 900 Å minimum and will not transmit the helium dayglow at 584 Å. It is a two-detector photomultiplier photometer, patterned after the Mariner 5 instrument. One typical detector unit is shown in Fig. IV-5. Each detector has a UV filter, in one case composed of magnesium fluoride and the other of calcium fluoride. Light of the appropriate wavelength is passed and strikes the photocathode causing electron cascades which are subsequently multiplied and collected as current by the anode. The current reading is proportional to the intensity of the light.
2) The reflection grating spectrometer shown in Fig. IV-6 is satisfactory for both hydrogen and helium dayglow measurements. It is a body-fixed objective-grating spectrometer with no moving parts. A mechanical collimator defines the field of view and a fixed concave grating disperses and images the spectrum. Fixed slits and channel multiplier detectors are placed at the wavelengths of interest in the image plane. Photon counting techniques are used, and random pulses are counted. Detectors used would be channeltrons placed at 1216 Å, 584 Å, and at a background wavelength. Thus, this one instrument would make all necessary dayglow measurements. The field of view is rectangular, about 2 x 20°.

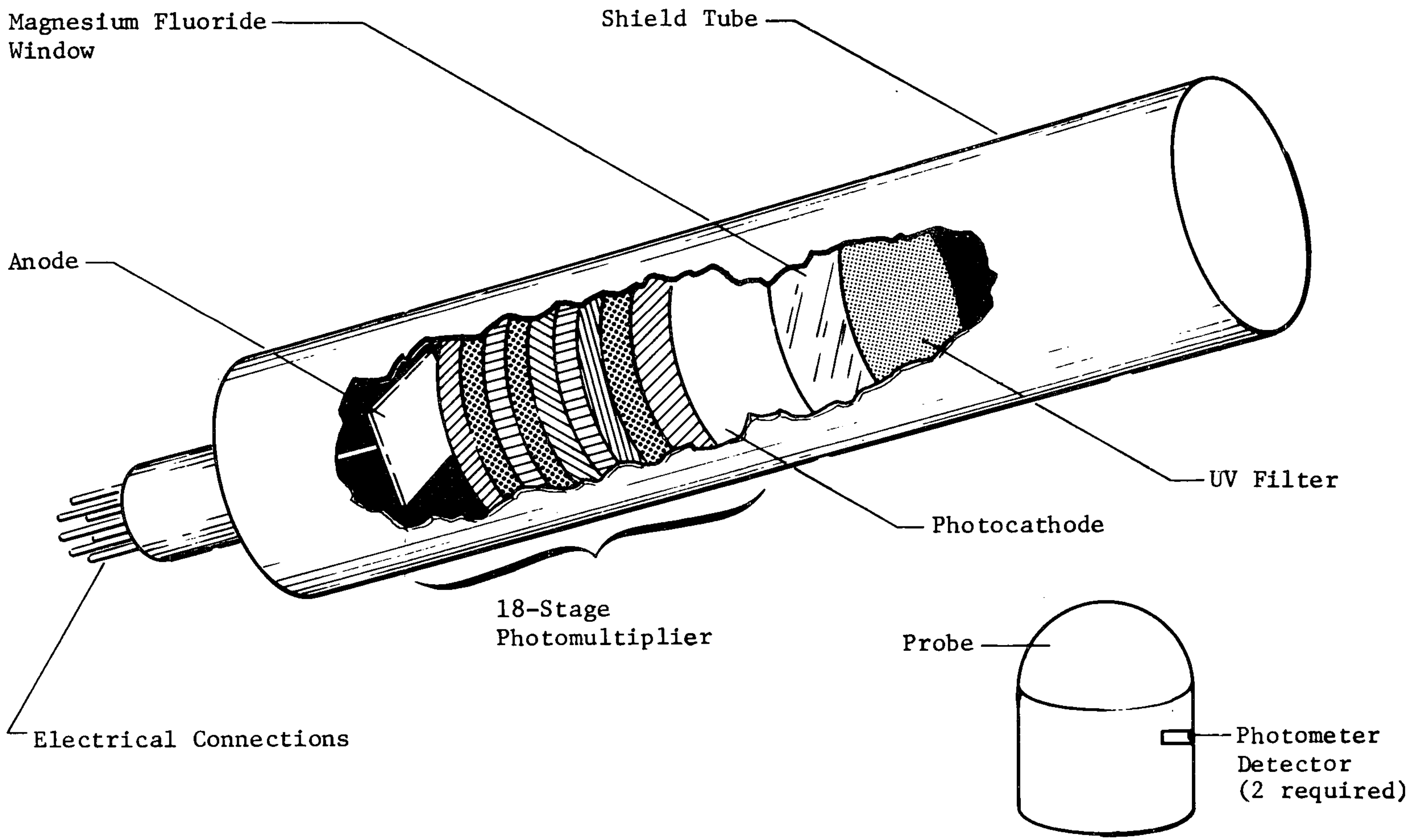

Fig. IV-5 Hydrogen Photomultiplier Photometer, Configuration and Location

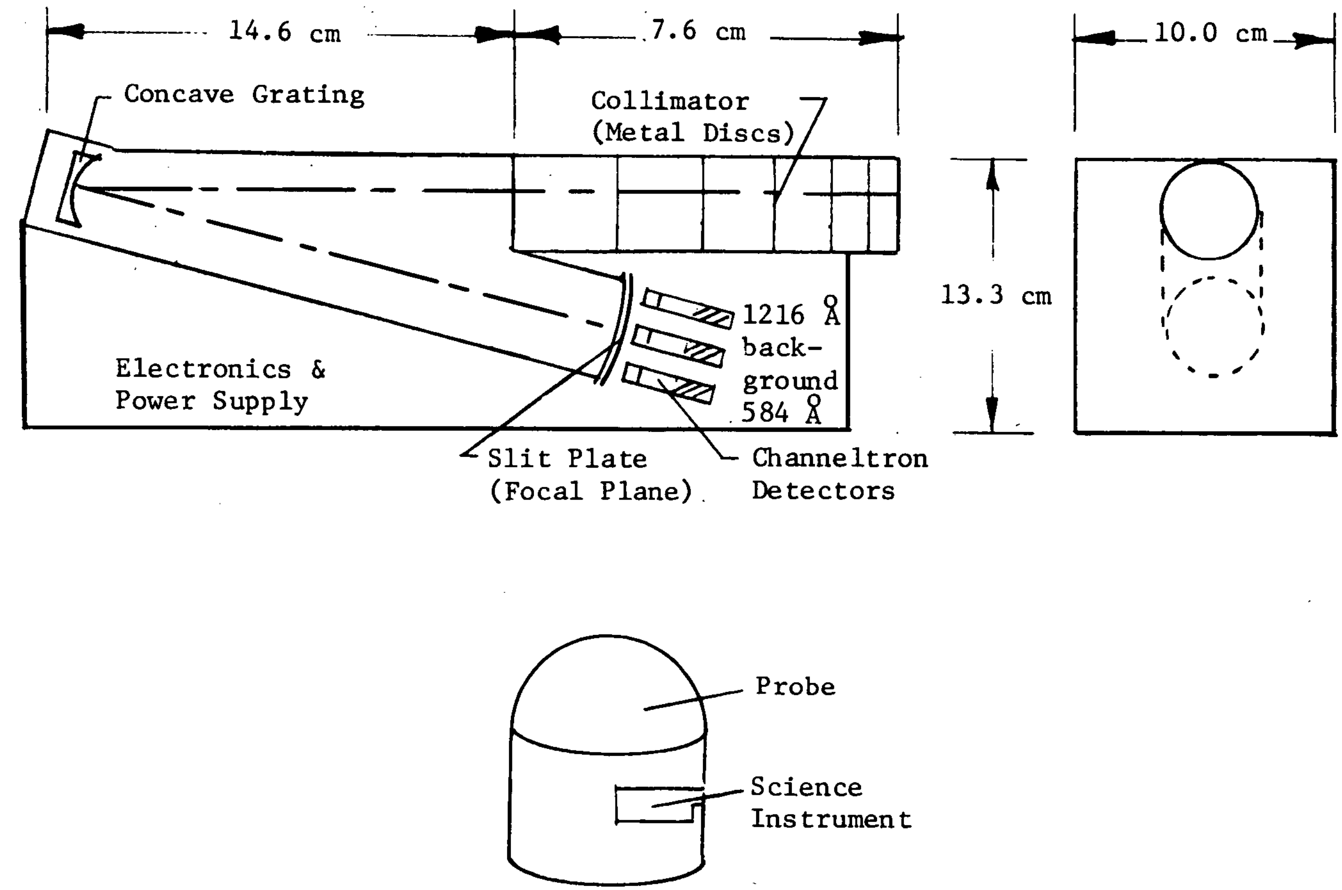

Fig. IV-6 Ultraviolet Reflection Grating Spectrometer, Configuration and Location

3) The thin-filter channeltron photometer shown in Fig. IV-7 is sufficient for both hydrogen and helium dayglow, but is not the most efficient for hydrogen at its wavelength. To collect the light from the 584-Å helium dayglow, a channeltron detector is required because the light at this wavelength cannot pass through any glass optics. The light passes through a very thin, 1690-Å thickness, tin filter supported by wire mesh, and strikes the side of the tube, which is coated with a photosensitive semiconductor coating. A high voltage is applied along the tube and a gradient thus established. Incidence of photons on this surface causes a current to flow that is proportional to intensity.

2. Science Measurement Time

The number of measurements made is a function of the instrument measurement interval and rate of probe descent. The instrument hardware design constrains the time it requires to obtain a measurement, but descent velocity is a function only of entry angle. The probe ballistic coefficient has negligible effect on the trajectory.

Figure IV-8 shows the effect of entry angle on descent velocity and measurement time. The upper graph shows that, while inertial velocity is almost independent, relative velocity increases significantly with increasing flight path angle and radial velocity increases drastically.

This change in radial velocity directly affects the time between any two altitudes, as shown by the lower curve in Fig. IV-8. It shows the time from entry to turbopause and from turbopause to blackout as a function of entry angle. By comparing the two graphs, it can be seen that, as the radial velocity goes up, the time to make measurements decreases rapidly. This strongly indicates that the lower flight path angles are much more desirable because they extend the measurement time.

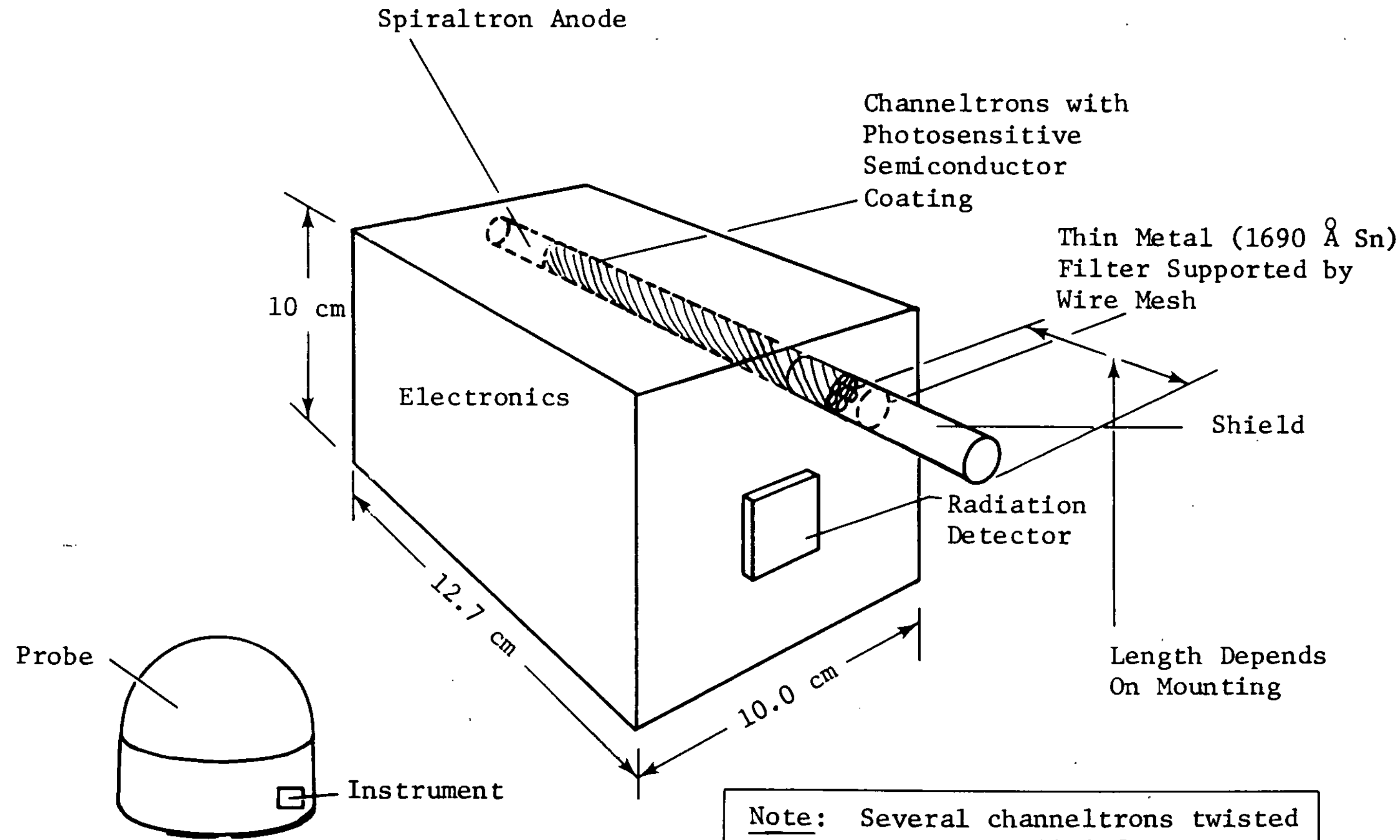

Note:	Several channeltrons twisted and in parallel form a spiraltron.

Fig. IV-7 Helium Channeltron Photometer, Configuration and Location

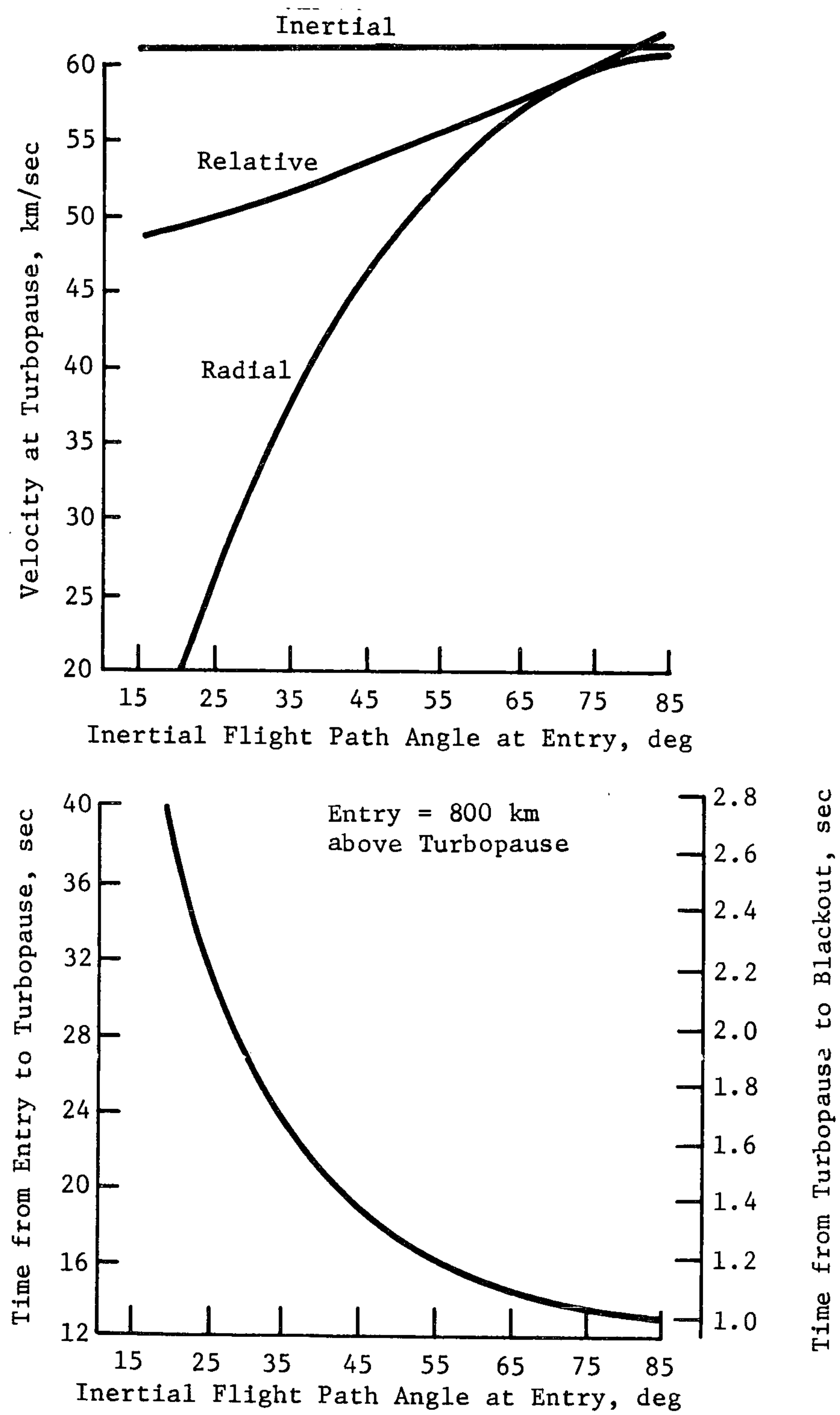

Fig. IV-8 Effect of Flight Path Angle on Entry Velocity and Time to Turbopause

Figure IV-9 shows the measurement per scale height for each of the ions and neutrals specified by the models as a function of entry flight path angle for 200 km above the turbopause. According to the models, there are a measurable number of all particles at this altitude. Again, evidence is strong that the lower the entry angle, the better the mission. An entry angle of about -26° is required to give 1.0 measurements per scale height for neutral helium. For entry angles up to about -35°, the difference from 1.0 is small. The mission with the greatest flight path angle under study, $\gamma_E = -34°$, shows a measurement performance for neutral helium of about 0.9 per scale height, which is acceptable.

The mass spectrometer must take a minimum of two measurements for each isotope below the turbopause. The effect of entry angle on this instrument's measurement performance is shown in Fig. IV-10. The top curve of this figure represents the mass spectrometer measurements for the reference location of the turbopause. The criterion of obtaining two measurements below the turbopause is satisfied for all flight path angles, but as before, the performance increases with lower values. Because of the uncertainty in the turbopause models being used, the study considered the effect of its location being in error as much as one order of magnitude in density. This results in lowering the altitude of the turbopause about 40 km. The lower curve in Fig. IV-10 represents the measurements obtainable by the mass spectrometer below the turbopause if it is displaced 40 km down in the atmosphere. From this, it can be seen that an entry angle of -25° or less is required to satisfy the criterion.

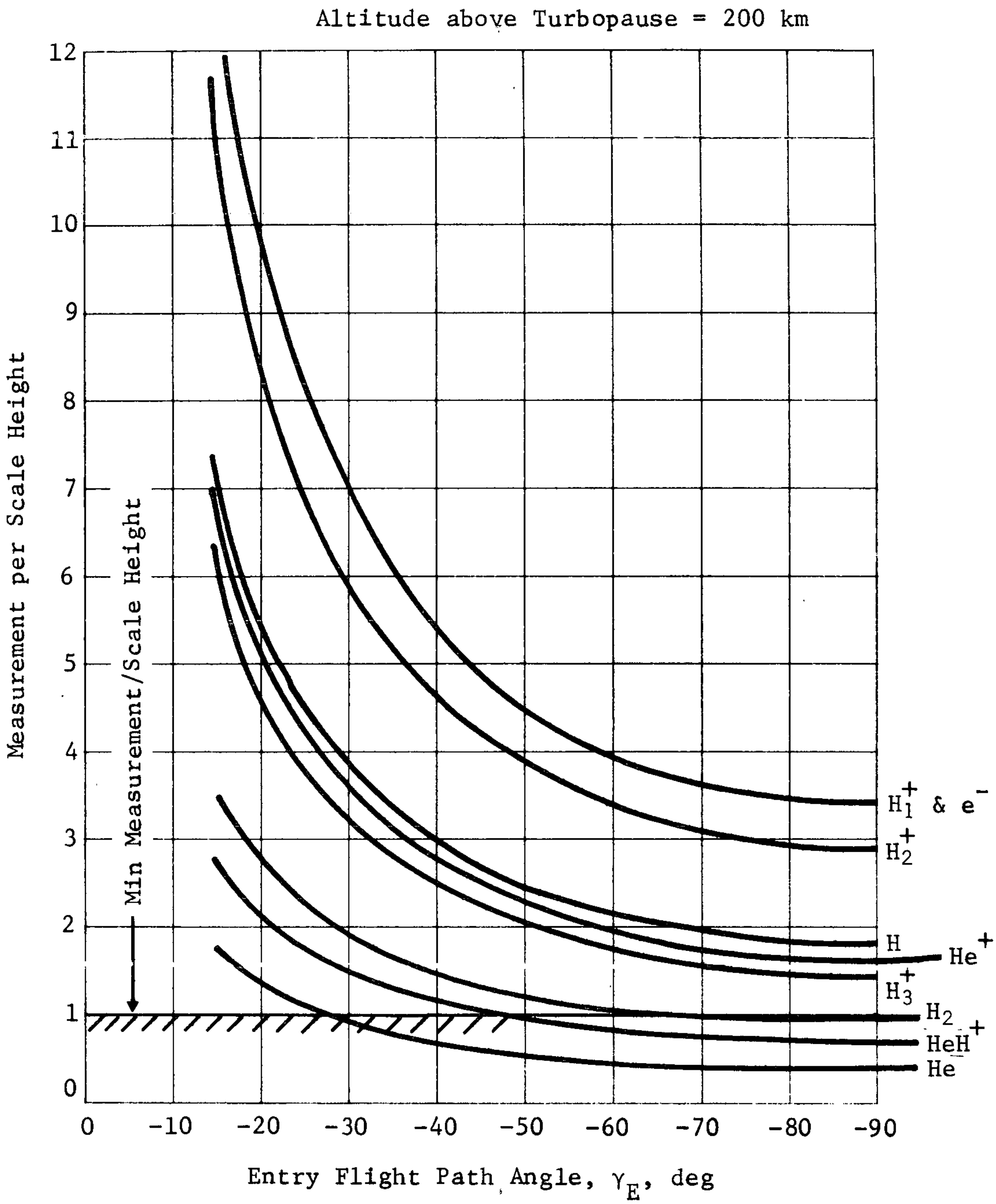

Fig. IV-9 Measurement Performance for Ions and Neutrals

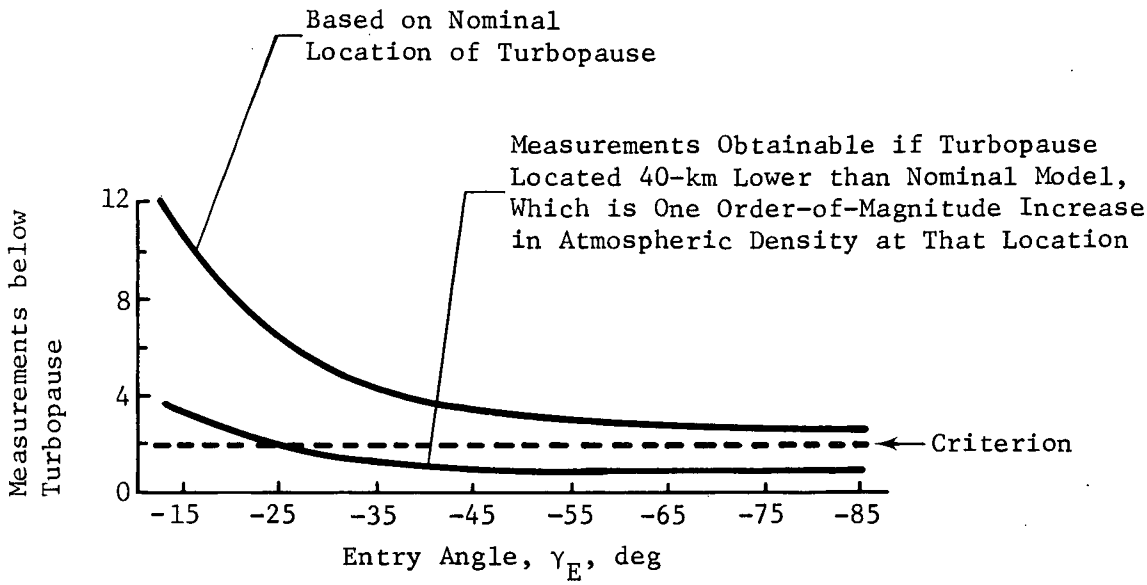

Fig. IV-10 Mass Spectrometer Measurement Performance

B. MISSION SURVIVAL

The critical areas in mission survival and thus successful science return, involve the communications blackout, probe entry burnup altitude, and probe and spacecraft survival in the radiation environment. Communications blackout altitude is a function of atmospheric density, number of electrons produced in the probe wake as it descends deeper into the atmosphere and communications radio frequency. Higher radio frequencies can penetrate greater wake electron densities and, therefore, greater depths into the atmosphere. However, practical hardware considerations limit the higher radio frequencies to an upper limit of about K-band (20 GHz).

Probe entry burnup altitude is a direct function of atmospheric density and the particular heat-sink design and is a relatively predictable phenomenon. Analyses have shown that the probe burnup altitude occurs significantly below or after communications blackout altitude, and therefore, heating is not the critical factor in terminating the mission. Because both heating and blackout are directly related to atmospheric density, burnup will always follow blackout altitude even though atmospheric uncertainties may shift the actual locations of these occurrences. It has been shown, then, that the mission is always terminated by the communications blackout.

Radiation belts affect the probe mission success in three basic ways. The first is direct radiation damage to the components with reduction of their operating efficiencies. The second is residual reradiation induced by initial exposure to maximum radiation. The third is the possibility of severe background noise in the science data measurements from both direct radiation at higher altitudes and residual radiation after passing through the belts. Analyses have shown that probe radiation survival is practical by selection of appropriate components and materials in conjunction with local shielding. At the mission measurement altitudes, the primary radiation-belt intensity can be expected to diminish below critical levels, and residual radiation can be minimized by careful material selection. This problem must be reevaluated after the Pioneer F and G flights provide more accurate radiation data.

1. Communications Blackout

Communications blackout is critical to mission success because science objectives and data return from the probe to the spacecraft must be completed before blackout. The science objective relating to investigation of the properties of the upper atmosphere and ionosphere is easily completed far above the anticipated blackout altitude. The science objective relating to direct determination of the bulk composition of the mixed lower atmosphere requires that the probe obtain two full measurements with the mass spectrometer below the turbopause, which is the boundary of the mixed lower region. The possible number of measurements below the turbopause (71,750-km radius) depends on the time of survival to blackout altitude and on the mass spectrometer measurement interval. Time to blackout from the turbopause may be increased somewhat by using a shallower entry flight path and a higher data transmission frequency, which allow deeper penetration. However, higher frequencies are constrained to a limit of about K-band (20 GHz) and equipment at this frequency would require further development for a probe mission. The relationship between the blackout altitude and data transmission frequency of the probe has been a key output of one of the major study tasks, and Fig. IV-11 presents the results. Depths between 60 and 75 km below the turbopause are possible before blackout occurs. These data are based on a complex nonequilibrium flow-field analysis using upper-limit or worst-case assumptions. Change in altitude is fairly insensitive to change in frequency, although a difference of 10 km in altitude when varying frequency from X-band (10 GHz) to K-band (20 GHz) has some effect in terms of increased science data.

Because the number of measurements to a given depth depend almost entirely on entry flight path angle and mass spectrometer measurement interval, performance can now be evaluated to the known survival blackout depth. Entry flight path angle is constrained to values of about -20 to -30° by specific mission trajectory constraints. For a practical mass spectrometer measurement interval of 0.4 sec, the number of measurements obtained from the turbopause to 60 km below varies between 4.5 to 7.3. Therefore, for all missions studied, attainable measurements at RF frequencies between X-band and K-band are more than twice those required to meet the science measurement criterion of two below the turbopause. Note that a single mass spectrometer measurement consists of a sweep through 11 separate isotopes. Because the science objectives can be met at any of the RF frequencies shown, it is advantageous to design the communications system for X-band (10 GHz) because space-proven hardware designs are state of the art and transmitter powers up to twice those required for the turbopause probe mission (20 W) are readily attainable.

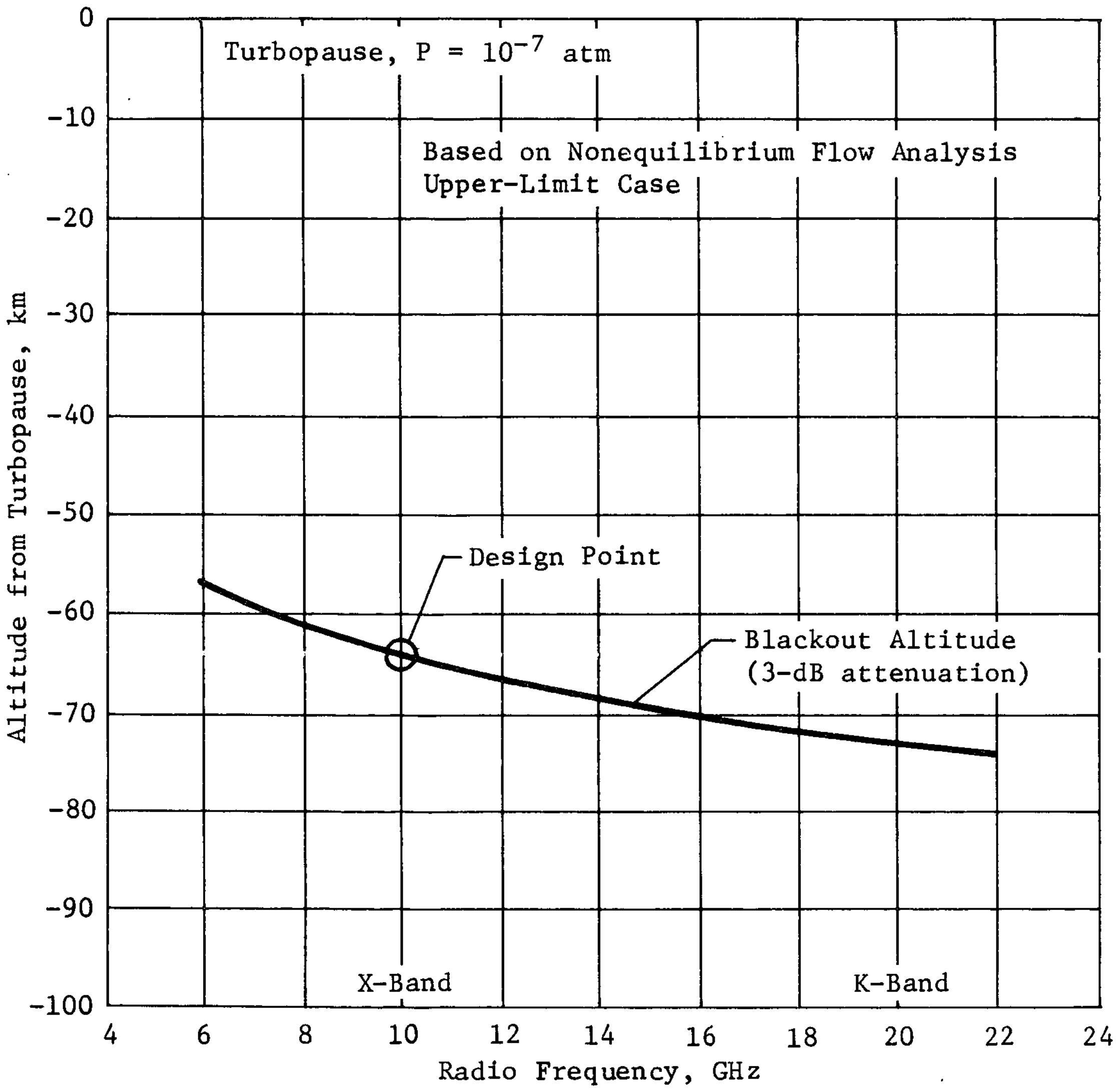

Fig. IV-11 Blackout Altitude vs RF Frequency *a. Aerophysics* - The communications blackout phenomenon results from RF signal attenuation when the signal passes through a plasma of electrons. Electrons are generated around the probe as it enters the atmosphere and are carried back into the probe wake. The probe antenna is mounted facing aft and must send the RF signals through the wake to the spacecraft. Therefore, calculation of the electron density and other parameters in the wake region is fundamental to blackout phenomenon estimates.

Electron density and electron collision frequency in the wake of the Jovian turbopause entry vehicle have been predicted by a detailed nonequilibrium thermochemical analysis of the hypersonic flow field surrounding the entry vehicle. Figure IV-12 is a schematic of the hypersonic flow field.

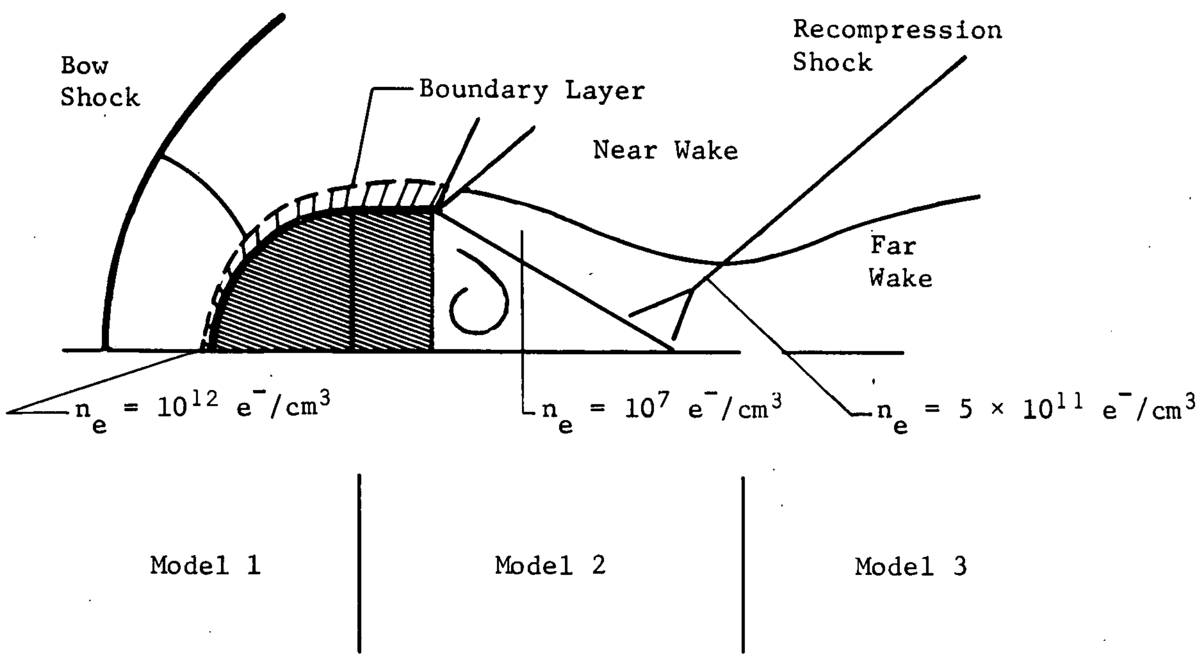

Fig. IV-12 Probe Hypersonic Flow Model

The inviscid hypersonic shock-layer calculations were made using techniques developed by Cornell Aeronautical Laboratory for both the subsonic and supersonic flow fields. These methods provide edge conditions for the vehicle boundary-layer analysis, which used Aerotherm Corporation equilibrium boundary-layer techniques. After completion of the boundary-layer analysis, the flow was expanded isentropically to a specified base pressure to start the near-wake analysis.

The near wake is defined as the viscous free shear layer aft of the entry vehicle and the recirculation region at the vehicle base. The free shear-layer analysis used is an adaptation of the techniques described in a GASL turbulent mixing method and the Korst-Chapman mixing theory. It is important to note that the free shear layer is a region of frozen chemistry and changes in the near-wake chemical-composition profiles are caused primarily by fluid mechanics and mixing effects.

As the near-wake flow field reattaches at some distance behind the entry vehicle, it is rapidly recompressed to a higher pressure, and a shock is formed at the neck of the far wake. This shock is strong enough to create significant nonequilibrium thermochemical effects in the far-wake flow field. Therefore, the far-wake analysis accounts for nonequilibrium thermochemistry.

This type of analysis provides that the initial and/or boundary conditions used in any region of the flow-field analysis are physically and mathematically consistent with development and structure of the flow field of any previous upstream regions. Final outputs are electron density and electron collision frequency distributions in the near and far wake. Figure IV-13 shows the data points calculated by this method 60 km below the turbopause, with extrapolations to other altitudes. These data serve as input to the RF signal-attenuation analysis described below.

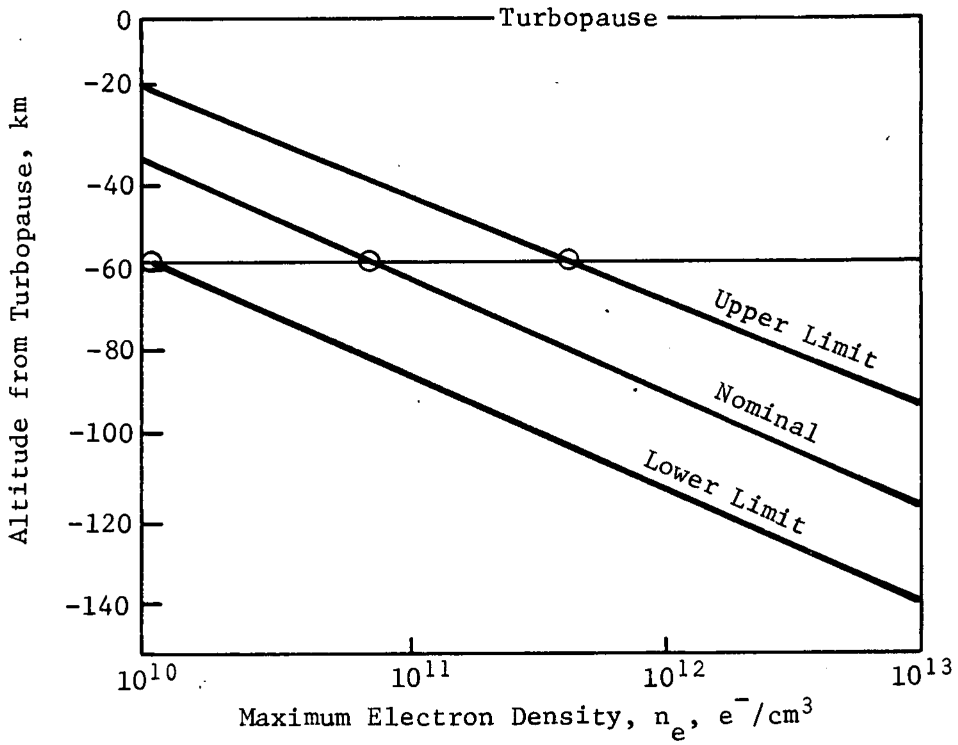

Fig. IV-13 Nonequilibrium Electron Density

b. Plasma Attenuation of RF Signals - From the nonequilibrium flow-field analysis described above, electron density and collision frequency contours were determined in the near and far wake where plasma/RF interaction occurs.

RF signals transmitted from the probe are affected by interaction of electromagnetic waves with plasma particles, primarily electrons. The interference is characterized by reflection, absorption, attenuation losses from collisions, phase shift, and refraction. Reflections are most pronounced at the plasma-atmosphere interfaces and in regions of rapidly varying electron density.

Transmission of RF signals through the plasma depends on the angle of transmission through the plasma, the frequency, transmitted power, antenna radiation characteristics, polarization of the wave, and location of the antenna on the probe. The plasma may also cause mismatch (i.e., alter the input impedance) and electrical breakdown of the antenna, with resultant distortion of the radiation pattern. As the probe descends further into the atmosphere, electron density increases to a point where plasma properties severely attenuate, reflect, or refract the transmitting signal. The RF link has been designed with enough RF power to operate with a plasma loss of 3 dB. Greater losses will result in data dropout, first at random and finally complete loss, with carrier dropout through the coherent RF link. Figure IV-14 shows the RF link cutoff frequency corresponding to the 3-dB RF-signal attenuation condition as a function of maximum electron density in the far wake. These data and those of Fig. IV-13 were used to construct the RF frequency-versus-altitude curve of Fig. IV-11.

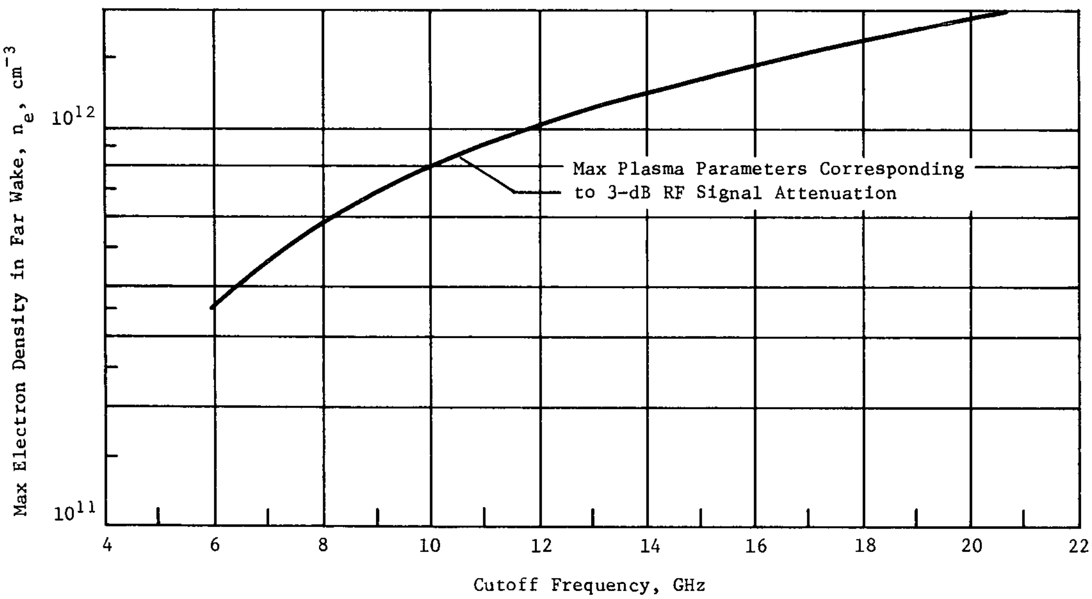

Fig. IV-14 Maximum Far-Wake Electron Density for RF Blackout

2. Probe Burnup

As discussed above, blackout occurs before severe heating, and thus terminates the mission. However, it is important to ensure that all probe systems are functioning at blackout so maximum science data are returned. Analyses have shown that a beryllium heat sink will provide the necessary thermal protection to the probe systems to a sufficient depth below blackout. Heat-sink-type protection can be provided for a reasonable weight and avoids the problem of possibly contaminating mass spectrometer samples, which would be likely with an ablative-type heat shield. Beryllium is uniquely qualified for heat-sink material because of its unusually high specific heat or capacity to absorb heat and its high strength-to-weight characteristics. Figure IV-15 shows the mission from turbopause to end of mission with a typical entry flight path angle of -25°. The heat sink is designed to provide a margin of survival of greater than 0.5 sec or about 15 to 20 km below initial blackout. Results of this analysis are presented in Fig. IV-16 in terms of heat-sink weight for a typical entry probe with a 76-cm (30-in.) diameter. Shallow entry angles generate greater total heat loads, and therefore higher heat-sink weights, than do steeper angles. However, the important point is that for a typical survival depth of 80 km, heat-sink weights are only 5.5 to 6.5 kg (12 to 14 lb) for a total probe weight of 77 kg (170 lb), or the heat sink is about 8.5% of the total probe weight.

a. Aeroheating and Heat Sink Design - The heat-sink design was based on the aeroheating inputs shown in Fig. IV-17. The effect of increasing heat load with shallow entry angle is evident here, as well as the fact that initial heating begins about 20 to 40 km below the turbopause and just before the onset of blackout. However, the beryllium heat sink is designed to absorb enough heat to ensure survival of the probe structure significantly beyond blackout altitude. Because both blackout and heating are directly related to atmospheric density, burnup will always follow blackout altitude, even though atmospheric uncertainties may shift the actual locations of these occurrences.

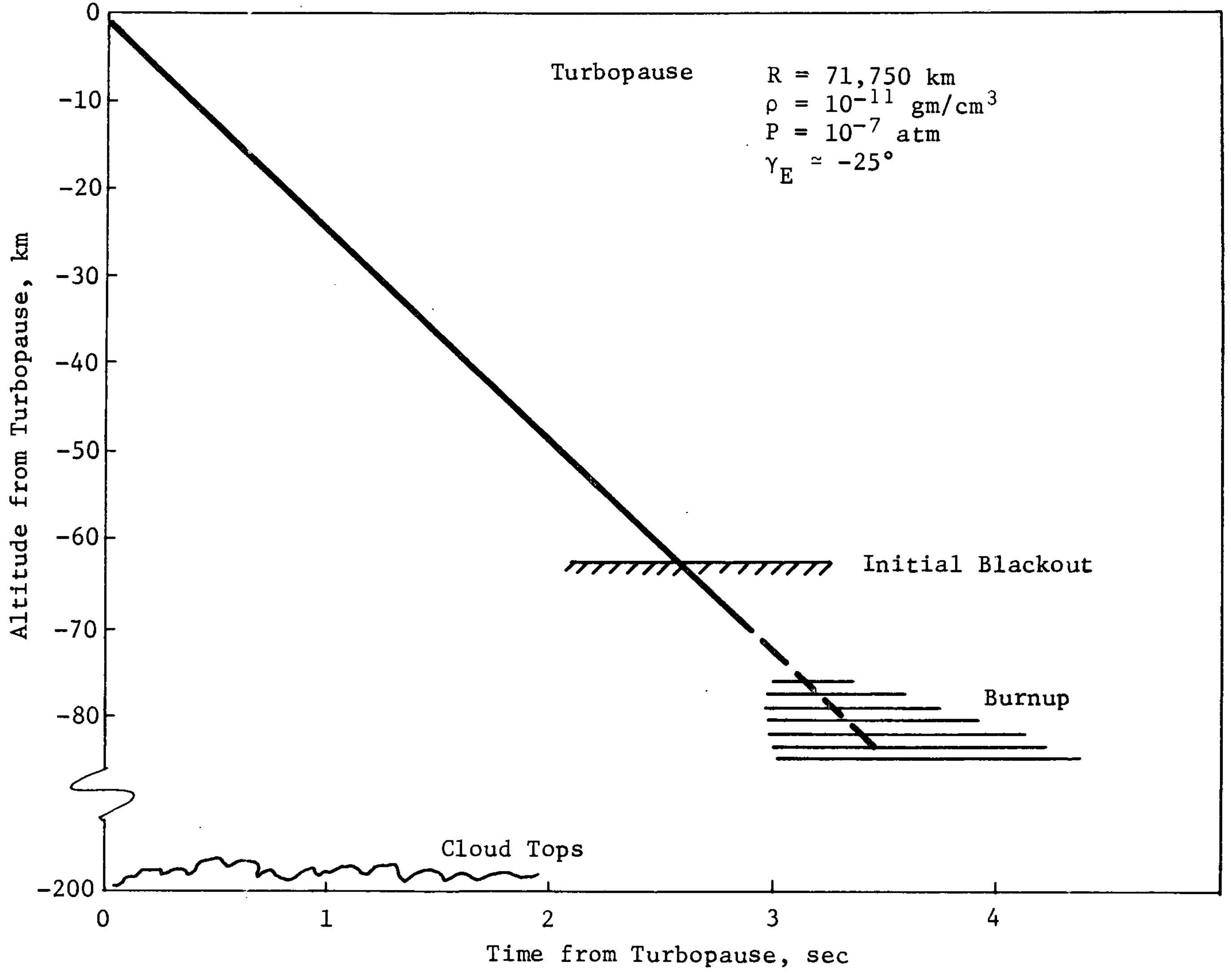

Fig. IV-15 Flight from Turbopause to End of Mission

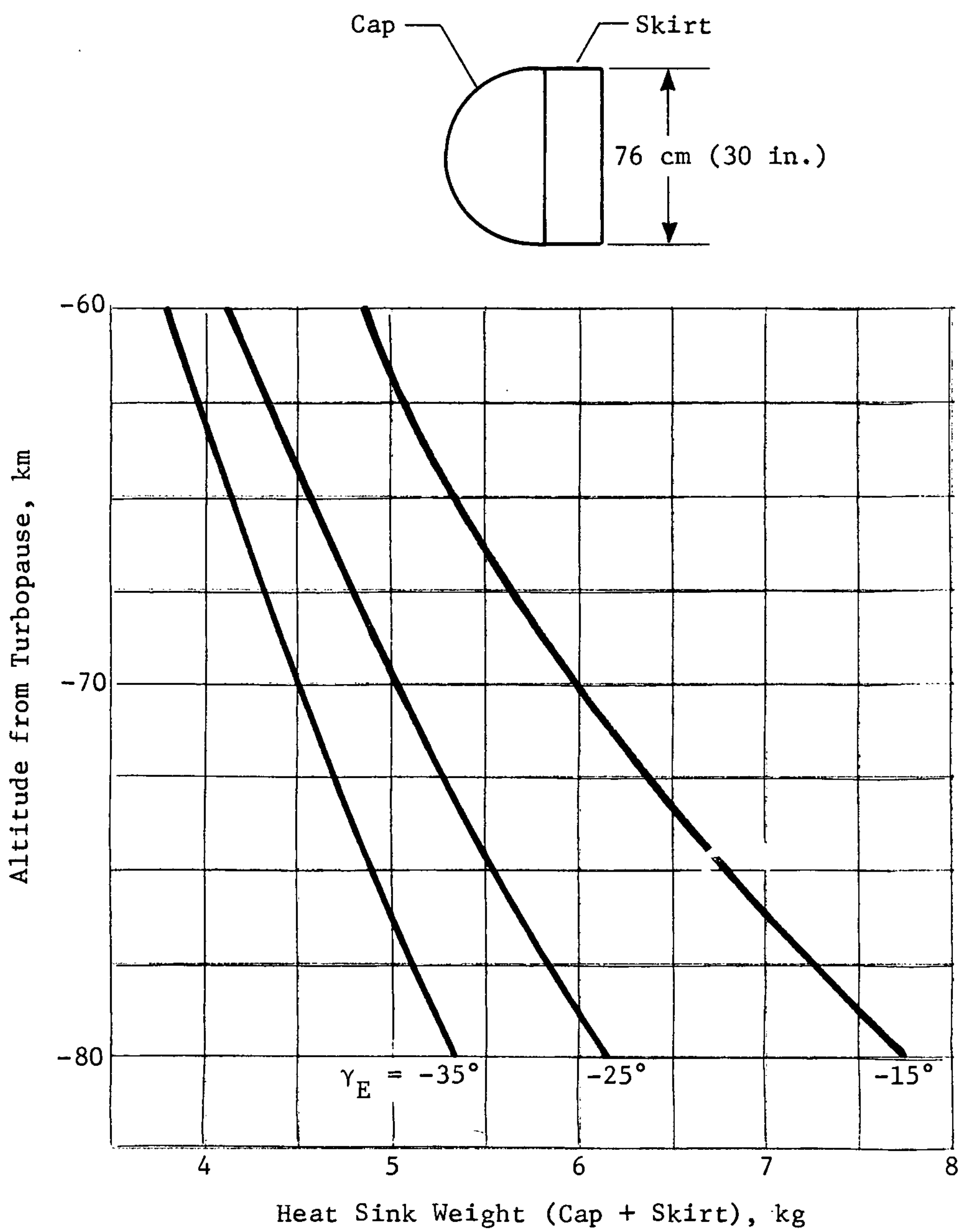

Fig. IV-16 Heat-Sink Weight vs Altitude

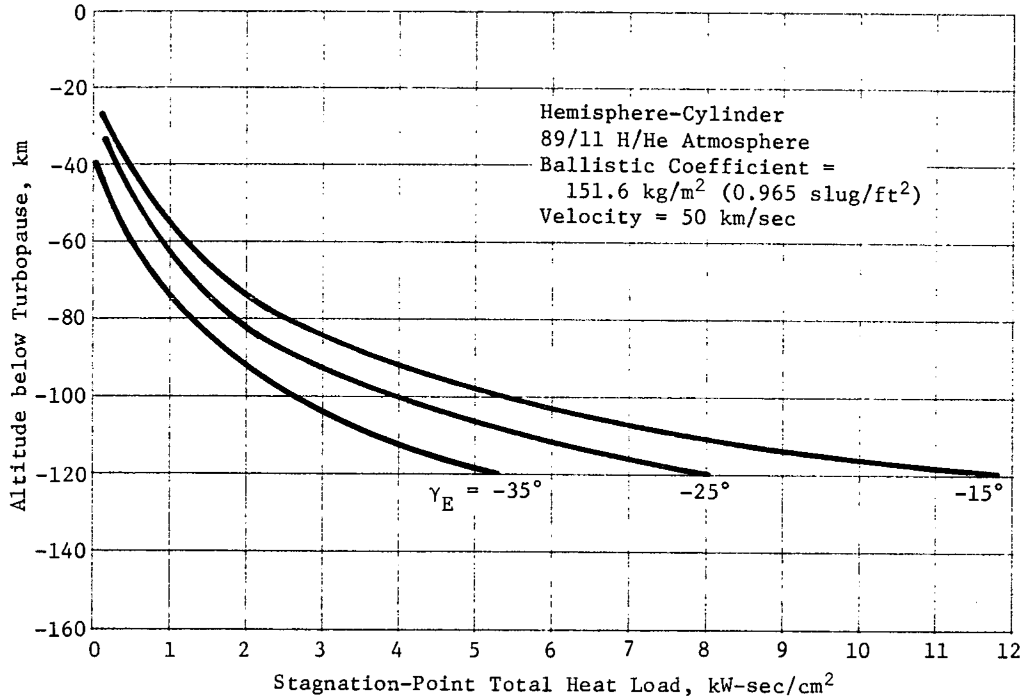

Fig. IV-17 Stagnation-Point Total Heat Load

The heat-sink design was based on thermal deformation criteria, front-face melting, back-face temperature limit, and strength considerations. Thermal stresses are important because of the extremely short temperature rise time. Typical heat-sink temperature rise time from onset to burnup is about 2.5 sec.

3. Radiation Hazard Survival

A potentially severe hardware constraint on any Jupiter probe system may be imposed by the radiation-belt hazard near Jupiter. In addition, the artifical radiation environment produced by the spacecraft RTGs and any isotope heaters in the probe must be included in estimates of total radiation fluence. Direct radiation damage, residual reradiation, and resultant background noise in the science measurements all pose a threat to mission success.

A preliminary analysis of major radiation effects indicated that practical design choices are available for hardening the probe design. Many spacecraft instruments currently proposed would probably suffer serious damage if the spacecraft were targeted to fly much within about 4 R_J of Jupiter. Hopefully, results from Pioneer F and G flights will reduce the present uncertainty in radiation-belt estimates, and therefore, possibly reduce the upper-limit model that must be used for design. The upper-limit Radiation Workshop model indicates that the probe will encounter a natural radiation-belt equivalent fluence of 10^{13} neutrons/cm^2, (10^{12} electrons/cm^2 + 10^{13} protons/cm^2) and the artificial environment from the RTGs and isotope heaters will produce 10^8 neutrons/cm^2 + 10^4 rad. Table IV-1 presents critical probe hardware-damage thresholds and recommendations for hardening.

Table IV-1 Probe Hardware Susceptibility to Radiation

Radiation-Sensitive Probe Elements	Sensitive Portion	Moderate to Severe Damage Threshold	Remedy*
Hydrogen Photometer	Photomultiplier Tube	$>10^{14}$ protons/cm^2	None required
	MgF_2 Filter	10^{14} electrons/cm^2	None required
Helium Photometer	Channeltrons	10^{11} protons/cm^2	High voltage off during high radiation
Optical Spectrometer	Channeltrons	10^{11} protons/cm^2	
Semiconductors	MOSFET	10^{13} neutrons/cm^2	Design for higher voltage turn-on
	SCRs	10^{13} neutrons/cm^2	Replace with power transistors & relays
Pyrotechnics	Squibs & chemical mixture	10^{13} neutrons/cm^2	Use pyros for functions before Jupiter encounter
Chemical Propulsion	Chemical mixture	10^{13} neutrons/cm^2	
Materials	Teflon, etc.	10^6 rad	Select materials

*Testing of all components and materials to expected levels. Reevaluate expected levels when Pioneer F & G data are available.

From the radiation-level data, it is evident that the artificial environment is a negligible threat to the system. However, natural radiation requires some very specific hardening changes, as indicated in the table. These changes are practical to implement, but the design penalties have not been evaluated in this study.

C. DATA RETURN

One of the key engineering functions of the mission is science data return. The sequence starts with data collection from the science instruments, followed by processing, probe acquisition by the spacecraft, transmission to the spacecraft, and storage and/or relay to Earth. The most critical function in this sequence is the probe RF-signal acquisition and lockon by the spacecraft probe tracking antenna and receiver system. This acquisition is made more difficult by the uncertainties in the relative positions of both spacecraft and probe, and by the narrow antenna beamwidth required on the spacecraft. For missions with large spacecraft flyby radii $\left(\text{greater than about } 4\ R_j\right)$, spacecraft antenna beamwidth must be narrowed to as low as 2.5° to increase antenna gain enough to overcome the large RF space loss. Because position uncertainties are also large at these flyby radii, an antenna position search pattern must be provided during the acquisition phase. However, at low flyby radii $\left(\text{i.e., } 1.1\ R_J\right)$ position uncertainties and space loss are so reduced that it is feasible to have a fixed broad-beam antenna on the spacecraft for probe acquisition and data retrieval. Data-link design, then, is a very strong function of specific mission characteristics.

C. 2

1. Probe Acquisition and Tracking

Analysis of the data link for various missions has resulted in selection of a practical concept for probe acquisition by the spacecraft before science data transmission and a procedure to ensure continued tracking of the probe to the end of the mission.

Critical design requirements for the probe acquisition system result from uncertainties of the position and change in position of the probe relative to the spacecraft. Uncertainty in position determines the required spacecraft antenna beamwidth, pointing angles, and possible position search pattern, while uncertainty in change of position affects frequency acquisition and lockon of the coherent communications link.

The key parameter influencing position uncertainty at acquisition is the coast time uncertainty--the 3-σ uncertainty in the nominal time interval from probe deflection to the end of the mission. It is caused by uncertainties and execution errors at deflection. The probe performance phase is initiated by a timer on the probe set to activate at a predetermined time after deflection. Enough margin must be allowed in this sequence so that science requirements are met whether the probe arrives early or late.

The probe performance phase, in which science data are being measured and transmitted, occurs from 50,000 km above turbopause down to blackout and lasts about 25 min. Coast-time uncertainty is a strong function of the mission and flyby radius. For low flyby radii, like 1.1 R_J in the probe-optimized mission, coast time uncertainty is 5 min, with small position dispersions. At 4.8 R_J, as in the JS 77 mission, coast-time uncertainty is 27 min and resulting position dispersions are large. However, at large radii, a given spacecraft antenna pointing angle covers a larger area in position than it does at low radii. Because of this compensating geometric relationship between range, angle, and coverage, all missions typically require a spacecraft antenna look-angle (cone-angle) spread of about 8° to cover down-range dispersions. Cross-range dispersions are much smaller.

Certain missions with large periapsis radii require a high spacecraft antenna gain, resulting in a beamwidth of 2 to 3° to hold the RF power to an acceptable value. Probe dispersions, and therefore spacecraft antenna look angles at acquisition and entry, are larger than the beamwidths, so a position search must also be performed to direct the spacecraft antenna at the probe. For this type of mission, the acquisition system consists of a simple spacecraft dish antenna with a single receiver and a preprogrammed down-range look-angle (cone-angle) search program with logic circuits attached to the receiver AGC voltage. Two such missions, which require a position search system, are shown in Fig. IV-18 for the JS 77 Mission (7) and the Radiation-Compatible Spacecraft Mission (2A). At acquisition, the probe will be somewhere in the dispersion ellipse. The spacecraft antenna is pointed to the first sector position and the logic circuit records the AGC voltage. The same steps are repeated for the other positions, and the antenna is returned to the position with the highest AGC voltage. Elevation (cross-cone) angle changes are very small, and position searches in that plane are unnecessary.

As discussed in Volume II, Chapter IV, Section F3, a probe in the left half of the ellipse at acquisition will end its mission in the left half and not move to some other random position in the ellipse. This fact is very helpful because the final position of the probe will be known at entry, based on probe location at acquisition. Antenna position logic will have different movement rates for the cone angle for different cone-angle positions.

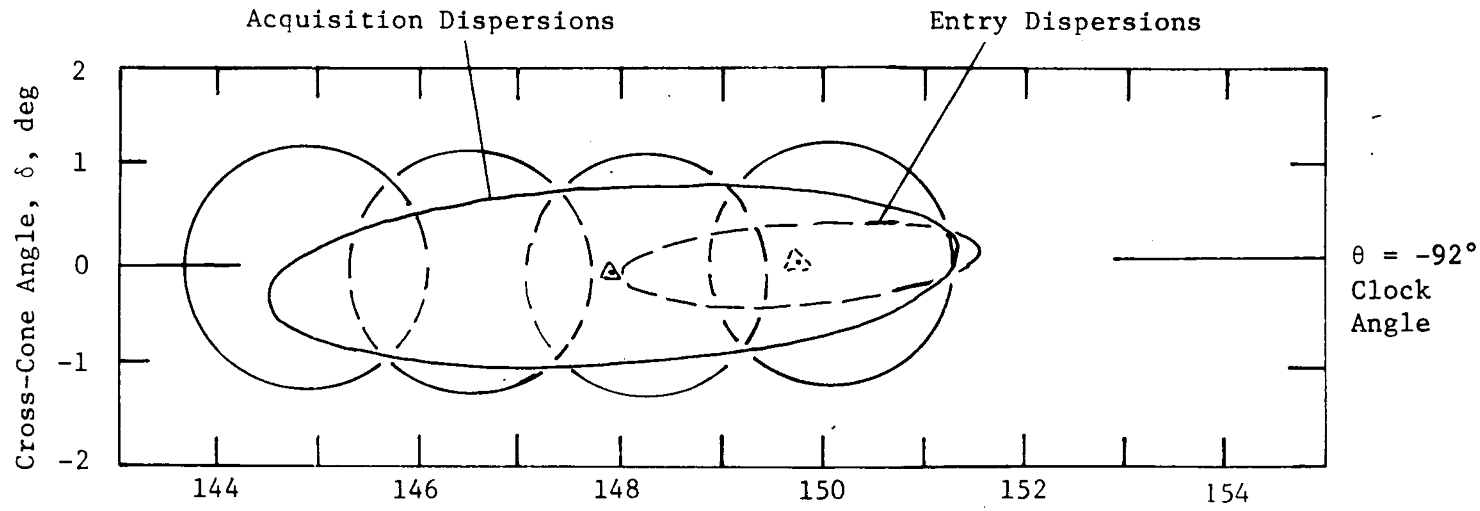

a. Mission 7 4-Position Search, 2.5° B/W

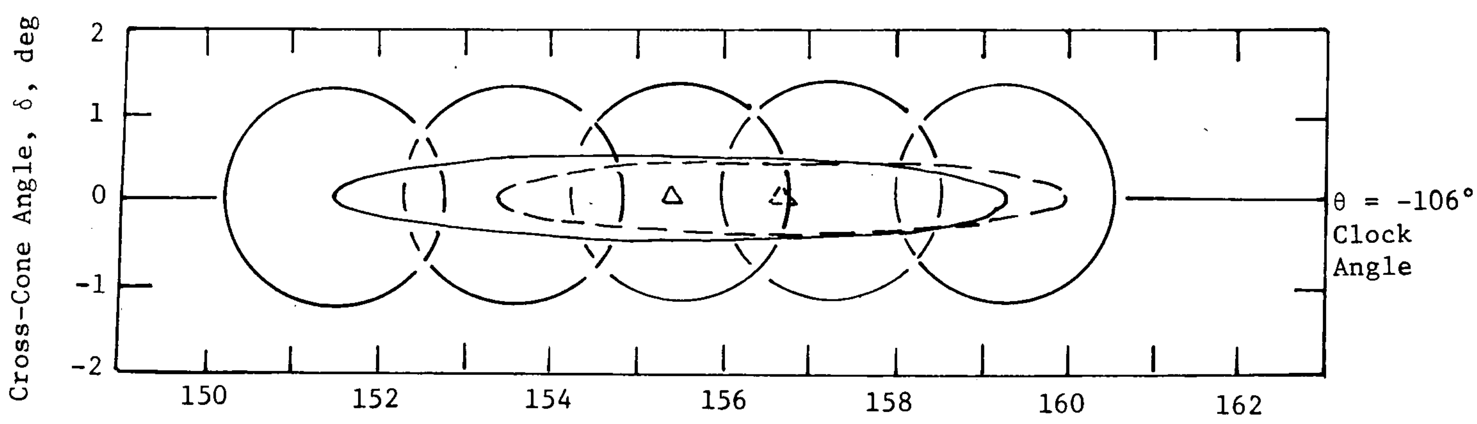

b. Mission 2A 5-Position Search, 2.5° B/W

Fig. IV-18 Spacecraft-Antenna Acquisition Requirements with Position Search

For instance, in Mission 7, a probe acquired in Position 1 will cause the antenna to move at a faster rate (cone-angle deg/min) than one acquired in Position 3. At each antenna position, a frequency search must also be performed. Frequency search time for Mission 7 is only 17 sec, therefore, a four-position sector search in frequency and position could be made in 2 min or less. This semiactive programmed tracking technique greatly simplifies spacecraft antenna and receiver subsystems and provides a reliable positioning system.

One case, the Probe-Optimized Mission (1A), allows a very simplified acquisition system with a fixed spacecraft antenna. Only frequency search is required. Because communications range and power requirements are very low with the flyby radius of 1.1 R_J, a wide-beam spacecraft antenna (16°) is possible, as shown in Fig. IV-19. Antenna spread completely encompasses both acquisition and entry dispersions, and therefore, the antenna can remain fixed in position during the entire mission.

2. Data Link

The basic data-link system includes subsystems necessary to collect, process, and transmit data to the spacecraft, which receives, processes, and stores or relays the data to Earth on the DSN link, depending on the data-handling capability of the spacecraft and mission schedules.

Probe data-link systems include data-handling, transmitter, and antenna subsystems. The RF link is designed to use phase-shift keying (PSK) to phase modulate (PM) the carrier with data that have been pulse-code modulated (PCM). To conserve the amount of RF power required, a coherent link was also chosen. The transmitter design was evaluated at both K-band (20 GHz) and X-band (10 GHz). However, results of the nonequilibrium electron-density wake study showed that X-band allowed sufficient atmospheric penetration to meet all science objectives, and X-band is therefore preferable to K-band because of availability of hardware. The probe antenna is a conical-horn design with a beam wide enough to cover the probe-to-spacecraft aspect angle caused by probe attitude errors and spacecraft/probe relative-position dispersion errors. Probe-antenna beamwidths of 8 to 10° proved adequate for all missions.

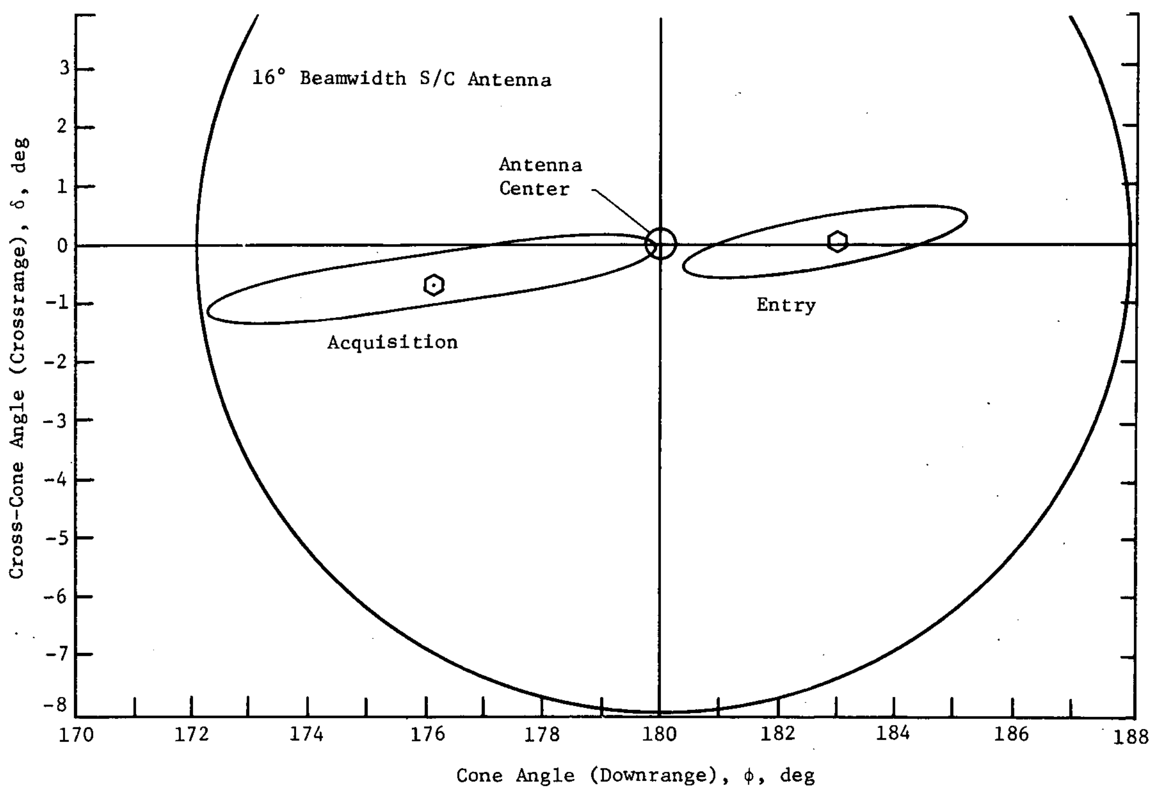

Fig. IV-19 Spacecraft-Antenna Acquisition Requirements without Position Search

Spacecraft data-link systems include receiver antenna, receiver, data handling (with storage capability), and Earth downlink equipment that is part of the basic spacecraft-to-Earth DSN design.

The spacecraft receiver antenna (probe tracking antenna) is a parabolic dish design with beamwidth set by the gain requirement in the link. Beamwidths vary from 16° down to 2.5°, depending on specific mission requirements.

a. Probe RF Transmitter - Transmission path loss is directly proportional to operating frequency. Therefore, required RF power increases as frequency increases to maintain a particular RF-link signal margin.

Preliminary analysis of the atmospheric-entry communications blackout problem indicated that frequencies in the K-band might be required to maintain a data link sufficiently below the turbopause to meet the science objectives without excessive (>3-dB) attenuation. Lower frequencies will be attenuated more because plasma attenuation is inversely proportional to frequency of operation. Therefore, a data-transmission system operating at K-band was initially chosen as an upper limit to consider for the design missions. Later, results of the communications blackout analysis (described in Subsection B1) showed that X-band (10 GHz) provides enough atmospheric depth of penetration to meet the science objectives. Detailed vendor and literature surveys were made to determine the projected 1975 state of the art for both X- and K-band and an upper limit on RF power for each. The best candidate for K-band power is a traveling-wave-tube amplifier. An upper limit is 25 W for space-qualified units by 1975. Solid-state devices may also meet the power requirements, but several development hurdles must first be overcome. In the future, if probe missions are designed for deeper penetration, higher frequencies like K-band will be required to overcome RF blackout to as great a depth as possible.

Figure IV-20 shows upper limits of TWTs and other devices and vendors who have space-qualified traveling wave tubes in the X-band. Projected power levels approach 100 W at 10 GHz, which well exceeds the 20-to-30-W range required for the design missions.

b. Coherent Versus Noncoherent Communications Link - For communications system designs in this study, a coherent receiver concept was chosen because it requires considerably lower probe transmitter power than a noncoherent system. The coherent receiver system does require a closely controlled reference oscillator and an initial frequency search and lockon of the phase-lock loop (PLL). Its major disadvantage is that the system must maintain frequency lockon to receive probe data. A prolonged disturbance of perhaps a few seconds is required to initiate loss of lock. Therefore, its occurrence is highly improbable. Probability of random equipment failure can presumably be made acceptably low and largely independent of the type of communications system used. Environmental effects are largely unknown, but lightning-like discharges, for example, would probably not occur above the cloud tops. Therefore, because coherent-system reliability is high, and its power requirements low, it was chosen for the data-link design.

A very cursory look at a noncoherent, nontracking communications system was made and, compared to the coherent system, probe transmitter power increased by a factor of 6. Because most mission designs require probe RF power of 20 W at 10 GHz, the noncoherent system would be prohibitively costly at 120 W. However, the Probe-Optimized Mission (1A), using the very low flyby radius of 1.1 R_J and thus low communications range, might use this type of system. This mission has a broad-beam (16°) spacecraft antenna that covers all position dispersion uncertainties from a fixed attitude. By narrowing the beam to about 7° and requiring a two-position movement, it would be possible to have a noncoherent system with a probe RF power of about 30 W at 10 GHz. This design possibility should be reevaluated in more detail in later studies.

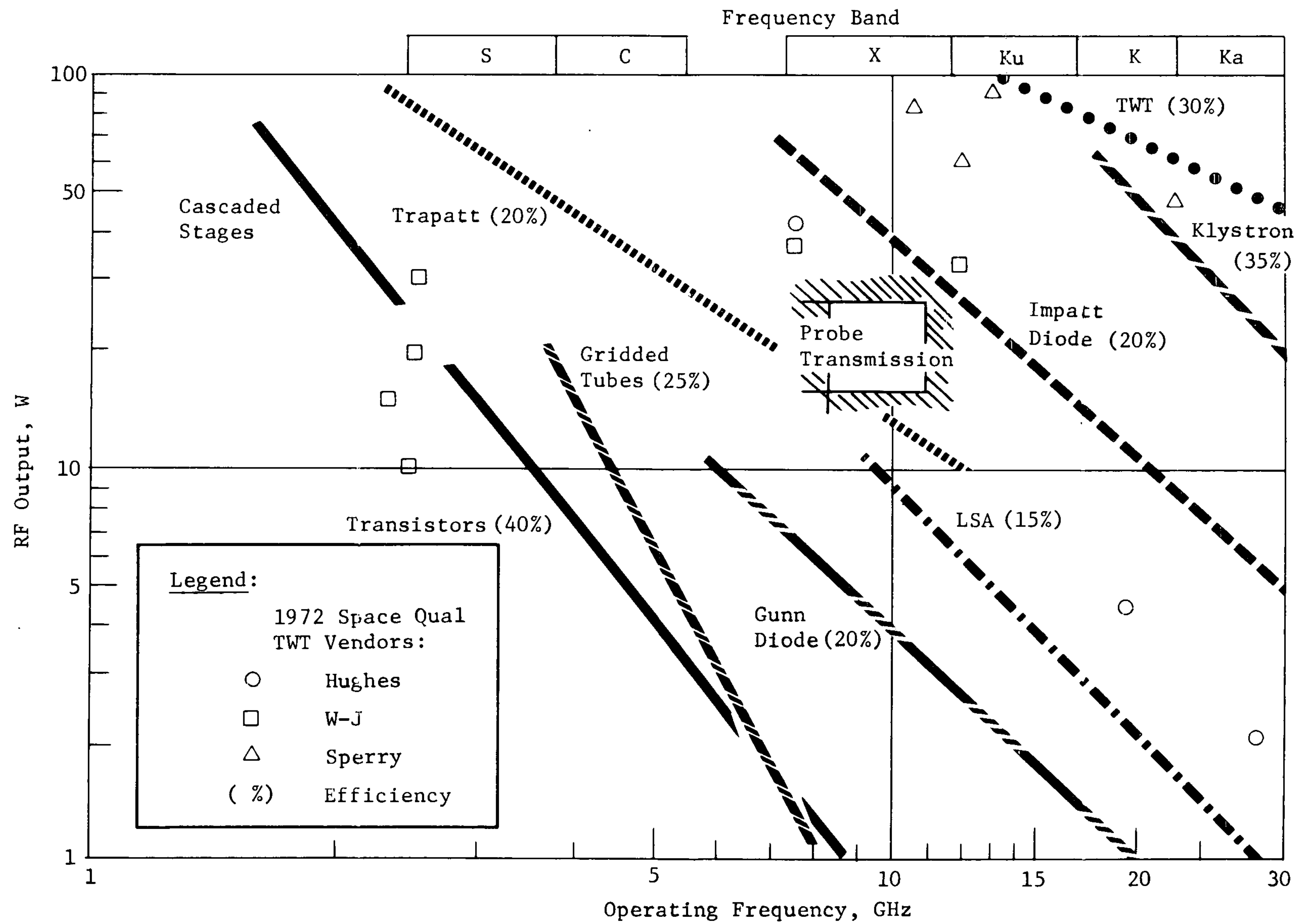

Fig. IV-20 Projected 1975 RF Power-Source Capability *c. Maximum-Range Mission* - An analysis was made to determine the maximum-range mission using practical constraints on the link design. It was assumed that a reasonable power limit of 40 W at X-band (10 GHz) would be attainable by 1975 state of the art. Also, based on results of design and integration efforts in this study, an 8° probe antenna, 2.5° spacecraft antenna, and a data rate of 1024 bps were assumed. The probe requires a parabolic dish for the 8° antenna design, which results in a 28-cm (11-in.) diameter. The antenna horn design used in all previous study missions was the preferred approach for wider beams of 10° or more because wider beams result in shorter, more compact antennas. However, at 8° and X-band, a horn antenna was too long for easy integration in the probe. The probe parabolic dish does appear practical; however, some detailed integration problems will have to be solved. The 2.5° S/C antenna beamwidth is about the narrowest highest-gain antenna design that will provide enough coverage to handle typical dispersions for the large flyby radii.

Figure IV-21 shows the results of this parametric analysis. For assumed conditions, maximum communications range is 5×10^5 km or 7 R_J. Note that the sample missions at corresponding flyby radii show somewhat higher required RF power because of the use of a 10° beamwidth horn-antenna design.

d. Relay Communication-Link Geometry Effect on RF Power - Transmitter power requirements are a strong function of the system antenna gains and communications range. However, when range is minimized, a very broad-beam low-gain probe antenna is required. Figure IV-22 shows the two link geometries that represent minimum range (side case) and maximum probe-antenna gain (tail case) that correspond to a small (nominally zero) aspect angle between probe and spacecraft. In the side case, probe-to-spacecraft aspect angle is nearly 90°, and the spinning probe requires an omnidirectional antenna pattern in the roll plane (toroidal), which results in an antenna gain of only 2.5 dB compared to about 18 dB for the tail case.

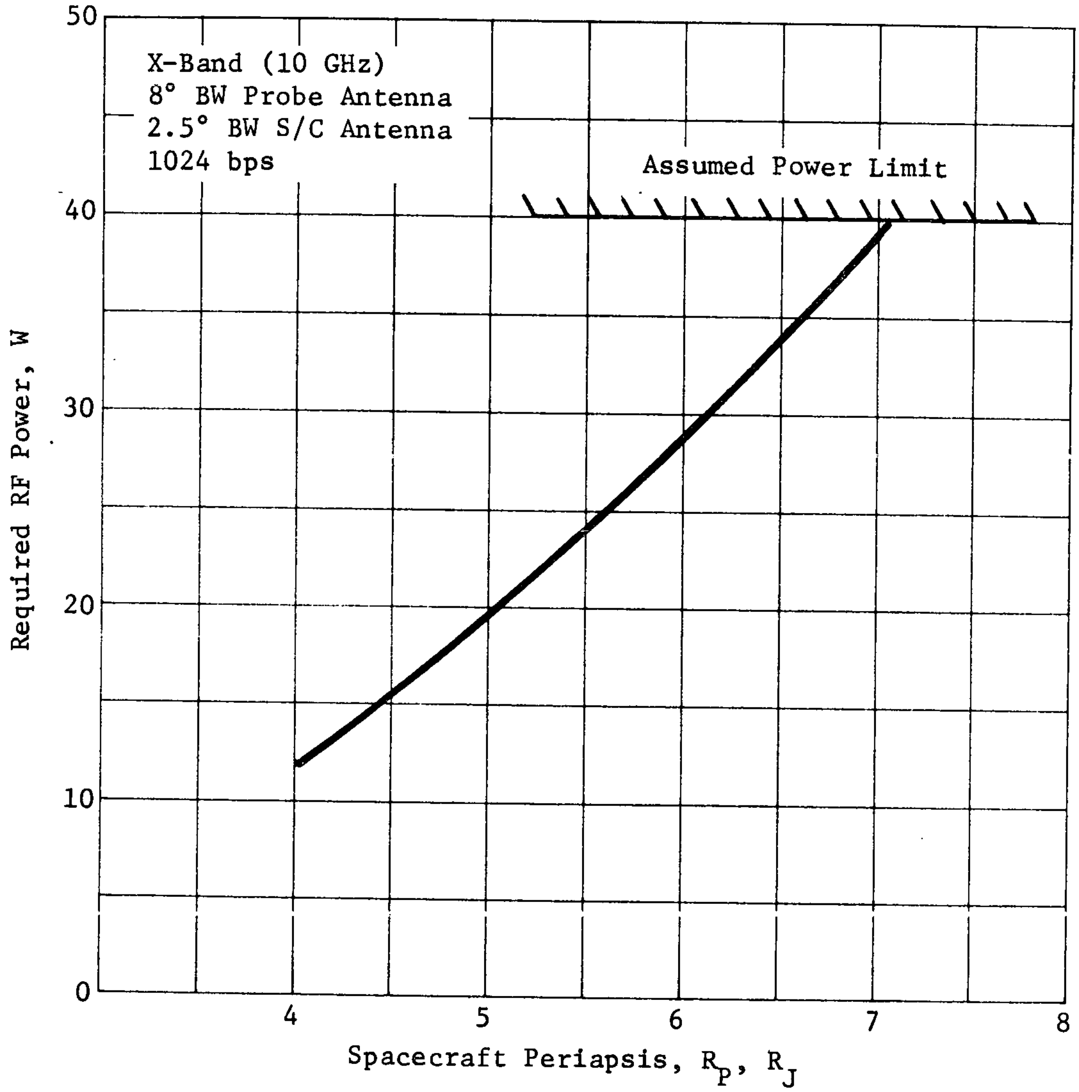

Fig. IV-21 RF Power Requirements with Range

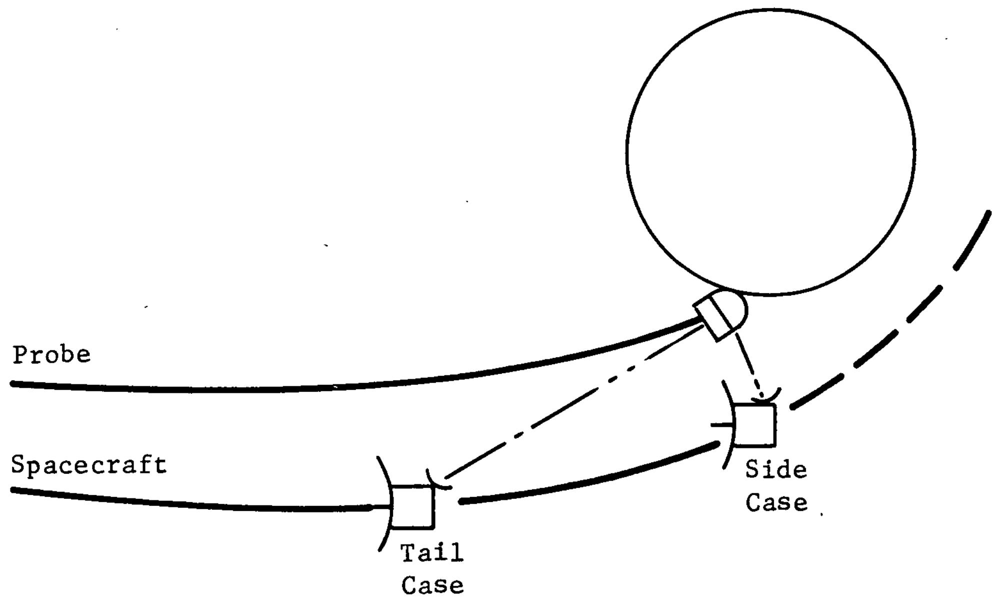

Fig. IV-22 Communications Link Geometry

The side case results in decreasing space (range) loss as the probe approaches entry, as seen in Fig. IV-22 and IV-23. Comparison of the range at entry for the side and tail cases is seen in Fig. IV-23. The side geometry minimizes the space-loss problem by reducing total range at entry. The decrease in space loss must be compared with the decrease in link gain resulting from a lower probe antenna gain. This comparison was made for three cases of R_P, with R_{EJ} = 10M km, γ_E = -35°, and at K-band. The relative required power is shown in Fig. IV-24. The power difference at entry is 5 dB for 1.1 R_J and increases with periapsis radius. Therefore, if 20 W were required at K-band for the tail case, the side case would require 3.16 × 20, or 63 W. The space-loss reduction did not compensate for the reduction in probe antenna gain for the side case.

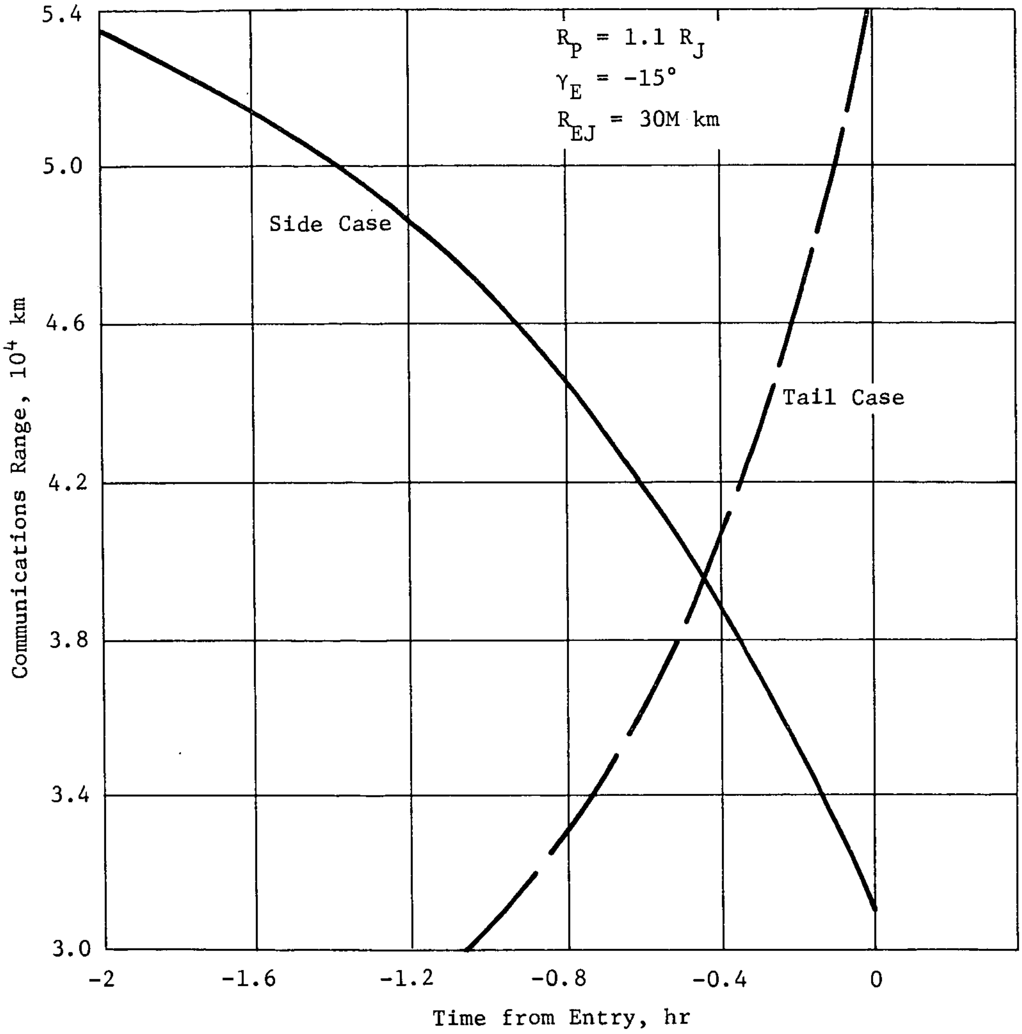

Fig. IV-23 Communications Range at Entry

Based on this trade study, the tail case results in the minimum probe power requirement at all flyby radii considered. Therefore, the mission designs of this study use the tail-geometry communications link.

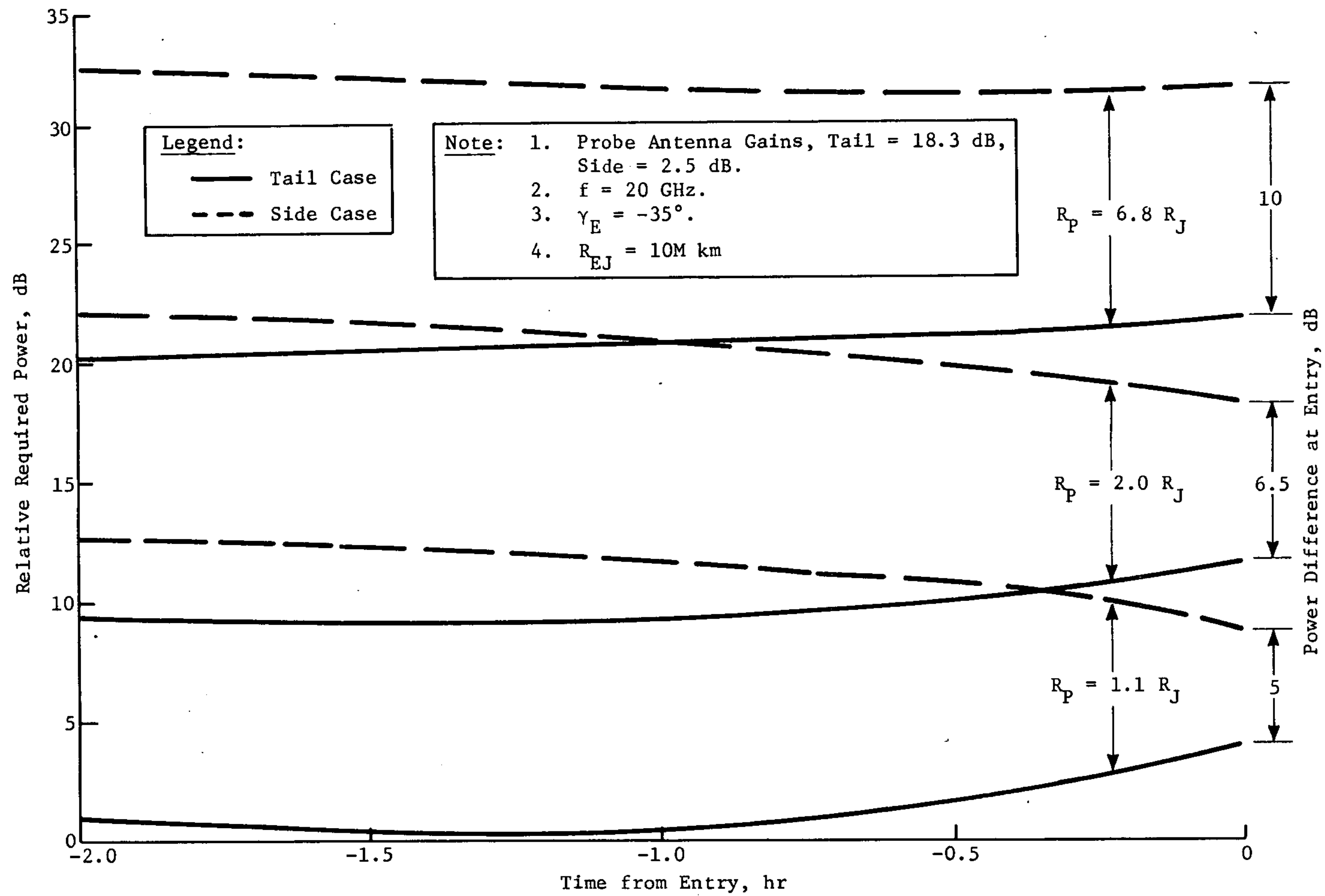

Fig. IV-24 Relative Communications Power Required for Side and Tail Geometries

D. DEFLECTION MANEUVER

The deflection maneuver is defined as the sequence of events required to--

1) separate the probe from the spacecraft and send it to the impact site;
2) align the probe for zero relative angle of attack at entry;
3) establish the relative geometry between probe and spacecraft for the communications link.

1. Selection of Deflection Modes

Three distinct modes or operational sequences identified to perform this deflection maneuver are shown in Fig. IV-25 and summarized below.

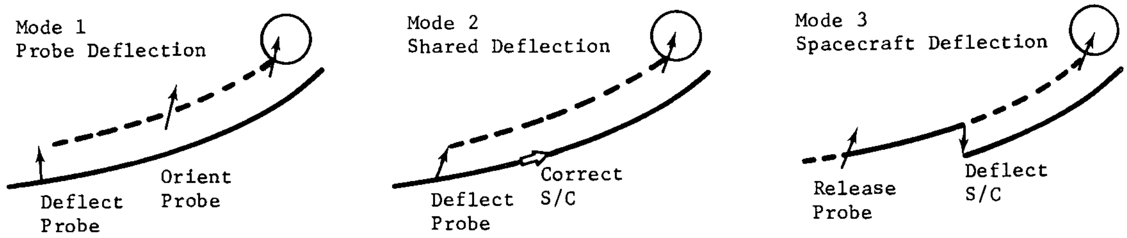

Fig. IV-25 Comparison of Deflection Modes

1) Mode 1 (Probe Deflection) - The spacecraft releases the probe in the attitude required for deflection ΔV, which puts it on the desired impact trajectory and establishes required communications geometry. After firing the ΔV, the probe then reorients itself to the attitude required for zero angle of attack at entry.
2) Mode 2 (Shared Deflection) - The spacecraft releases the probe in the proper attitude for zero angle of attack at entry. The probe fires a ΔV in that direction so it is deflected to the entry site. The spacecraft then accelerates to achieve required communications geometry at entry.

3) Mode 3 (Spacecraft Deflection) - The spacecraft trajectory is targeted to impact the entry site. The spacecraft releases the probe in the proper attitude for zero angle of attack. The spacecraft then orients itself and fires a ΔV to establish desired flyby trajectory and communications geometry.

Thus, the first mode requires the most complicated probe. It must be capable of providing the deflection ΔV as well as the precession and ACS maneuvers. The requirements for probe precession and ACS maneuvers are removed in the second mode. The third mode results in the simplest probe because all three requirements are removed and the full capability of the spacecraft is exploited.

A second consideration in the selection of the deflection mode is deflection-system weight penalty. The first mode has the minimal requirement because it uses deflection of the probe instead of the heavier spacecraft. Mode 3, which is a mirror image of Mode 1, has the same ΔV requirement as Mode 1. However, because the spacecraft is now being deflected, propellant weight is increased. This results in a propellant weight penalty approximately proportional to the difference in weight of the vehicle being deflected. Mode 2 was originally introduced with the hope that it might remove the precession and ACS maneuvers without generally increasing the weight penalty over Mode 1. However, because of the geometries involved, probe ΔV is consistently larger than for Mode 1 (or Mode 3) ΔV, while the spacecraft ΔV is only slightly smaller than the same value. This results in a total weight penalty of the same magnitude as Mode 3. These results are indicated in Fig. IV-26.

A final basis on which deflection modes can be compared is their resulting dispersions. Errors in the deflection maneuver result in dispersions that may complicate communication-link design or compromise science return. Mode 2 dispersions are worse than those of the other two modes because of the double contribution of execution errors on the probe and spacecraft ΔVs. Communication link dispersions (or equivalently, dispersions in relative geometry between probe and spacecraft) are approximately the same for the first and third modes. However, entry- or science-parameter dispersions are smaller for Mode 3 than for Mode 1 because of the decreased execution errors added to the probe at deflection in Mode 3. Typical results are shown in Fig. IV-26.

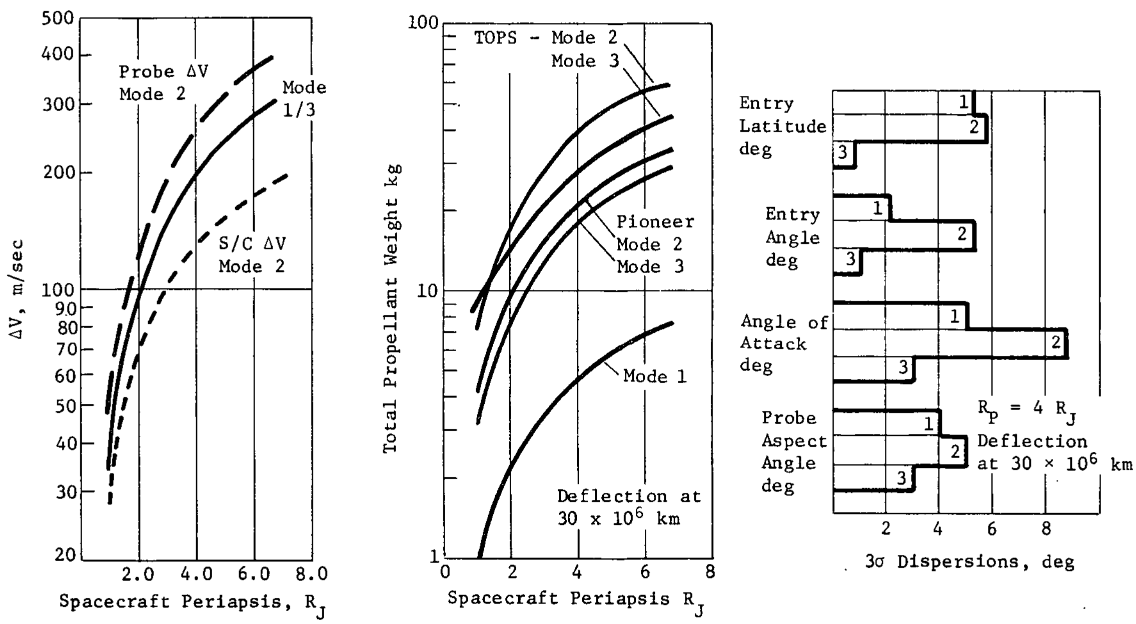

Fig. IV-26 Deflection Mode Selection

Thus, Mode 3 deflection is considered optimal for missions involving no post-Jupiter objectives, where the relatively light Pioneer spacecraft can be used. For missions involving post-Jupiter objectives and the heavier MOPS or TOPS spacecraft, Mode 1 deflection is generally superior because it does not change the spacecraft flyby trajectory and is not heavily penalized by a the propellant weight.

2. Selection of Deflection Radius

Once the deflection mode has been chosen for a given mission, the distance from Jupiter for the deflection maneuver must be selected. As indicated in Fig. IV-27, ΔV requirements are reduced significantly as deflection radius is increased. Note that the reduction in going from 10 to 30M km is much more pronounced than in going from 30 to 50M km. This decrease in ΔV magnitude results in a corresponding decrease in the effect of proportionality error of the actual ΔV delivered, and therefore, in ensuing dispersions.

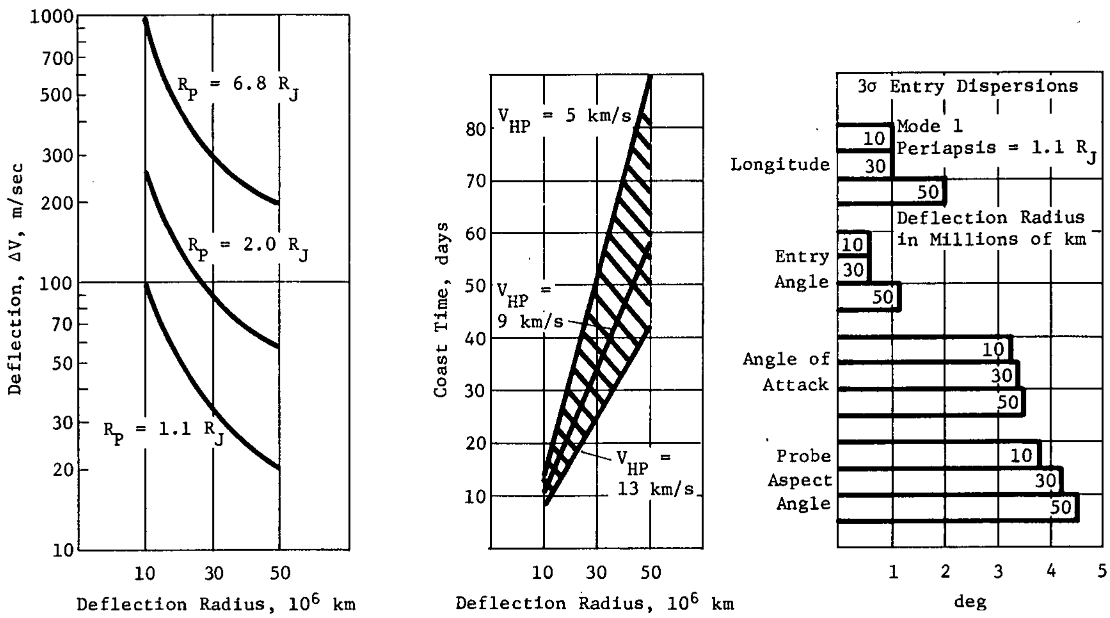

Fig. IV-27 Deflection Radius Selection

Conversely, the navigation process immediately preceding the deflection maneuver is enhanced as deflection radius is decreased. This is because tracking performance is improved as the spacecraft trajectory experiences greater and greater accelerative effects from Jupiter's gravitational force. Thus, the last midcourse maneuver is more effective, and the spacecraft position at deflection is more accurately known for missions with deflections close to Jupiter. A second factor supporting smaller deflection radii is that they lead to shorter coast times, resulting in less time for dispersions to grow from deflection to entry. These effects are indicated in Fig. IV-27.

Thus, selection of deflection radius depends on a careful assessment of resulting ΔV requirements and entry dispersions. It appears that the range of 10 to 50M km will generally be adequate for the deflection radius of turbopause missions.

E. PROBE CONFIGURATION

Both blunt and sharp configurations were considered for the entry probe. These shapes are shown in Fig. IV-28, in which the blunt shape is represented by the hemisphere/cylinder and the sharp configuration by the cone.

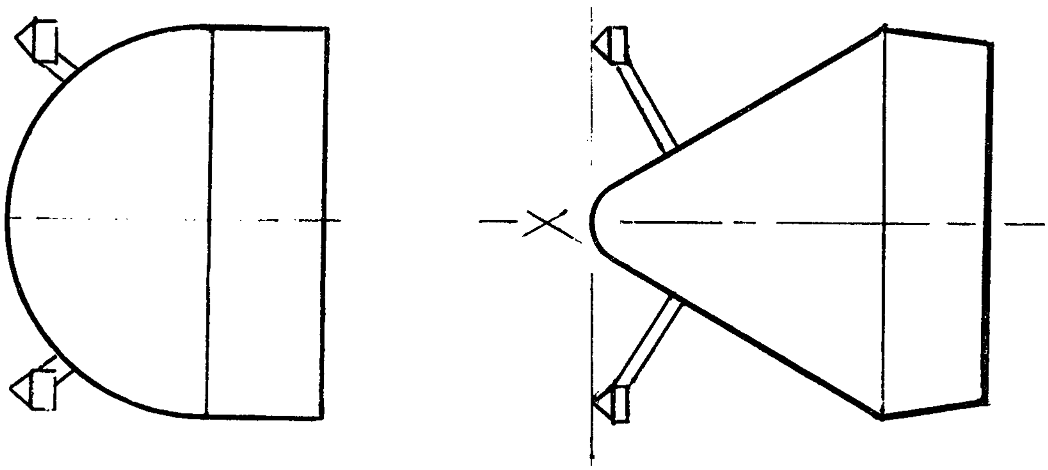

a. Hemisphere/ Cylinder Configuration

b. Cone Configuration

Fig. IV-28 Hemisphere/Cylinder and Cone Configurations

There are four basic criteria for comparison of these classes of configurations for the turbopause probe mission:

1) Location of science instruments relative to the probe surface for minimum measurement interference;
2) Sufficient roll inertia relative to pitch and yaw to maintain spin stability;
3) The effect of shape on the number of electrons generated in the wake, and thus, the blackout condition;
4) Local aerodynamic heating.

1. Science Instrument Interference

From the standpoint of instrument interference, no particular advantage could be found with one configuration compared to the other. The mass spectrometer is located with its inlet at the stagnation point in both cases in which minimum interference is experienced. The IRPA and NRPA instruments are best placed forward on booms even with the stagnation point and outboard, as shown. This requires longer booms for the cone shape; however, no particular problem is involved. The ETP and photometers can be mounted in equivalent locations.

2. Roll Inertia

Because the probe depends on spin stabilization over a long period, roll moment of inertia must be at least 1.1 times more than the inertia of the transverse axes, and preferably 1.2 times larger. Integration layouts of identical probe systems were prepared with hemisphere/cylinder and conical bodies. Despite the fact that the diameter of the conical design was increased by 5 cm (2.0 in.), the spin to transverse mass moment of inertia was only 1.07 compared to 1.20 for the hemisphere/cylinder. An additional factor to consider is that it is difficult to use the cone volume efficiently for packaging equipment. Therefore, installation of equipment to provide proper inertia ratios for spin stabilization definitely favors the blunt hemisphere/cylinder configuration.

From a structural and mechanical viewpoint, no characteristics were found that favor one configuration.

3. Electron Density in the Wake

Communications blackout is a direct function of electron density in the wake. The blunt shape develops an extensive normal shock region that generates extremely high shock temperatures and associated electrons that carry into the wake. A highly complex series of aerophysics computer programs were run to evaluate this condition, and the results are reported in Subsection B1. Because of its relatively sharp nose, the cone shape will develop a small normal shock region, and therefore, a smaller number of electrons will be generated about the stagnation area in this region. However, there are reasons to believe that there may be compensating flow-field actions as the flow is carried around the body into the wake (Vol II Chap X), and the resulting wake electron density for the sharp cone may remain nearly as high as that for the blunt hemisphere. Complete evaluation of the cone flow field was beyond the scope of this study. However, an evaluation similar to that for the hemisphere will be required to resolve this question.

4. Aerodynamic Heating

Initial aerodynamic heating is primarily convective heat transfer. Because convective heating is a direct function of $1/\sqrt{\text{nose radius}}$, the sharp cone will experience considerably higher stagnation-point heating than the hemisphere. However, most of the significant heating occurs after communications blackout, and therefore, is not a primary design factor. Local heating at the mass spectrometer inlet (stagnation point) should be checked to see that no contamination or melting of the inlet occurs before the end of the mission. Preliminary analyses indicate that this will not be a problem.

In summary, based on analyses completed within the scope of the study, the hemisphere/cylinder configuration has the clear advantage in the area of spin stabilization and equipment packaging. Additional aerophysics analysis is warranted for evaluation of electron density in the wake because the cone may show an advantage there. No particular advantage for either shape is seen in the areas of instrument interference, structural/mechanical design, and aeroheating.

V. DESIGN MISSIONS

A series of eight mission options were studied with launch opportunities from 1977 through 1980, and detailed mission and systems definitions were done for each mission that was feasible from an engineering standpoint. Three of these missions are summarized in Table V-1 and Sections A, B, and C so that a comparison can be made between the most favorable turbopause probe design, the Probe Optimized/Science Optimized Mission (1A), and the other two missions that are each constrained in some way.

The Radiation-Compatible Spacecraft Mission (2A) is similar to Mission 1A in most respects, except that the spacecraft flyby radius is constrained to 4.0 R_J to protect the spacecraft from possible severe radiation damage. Although the large radius results in some variations in encounter and entry parameters, the probe design is essentially identical to that of 1A, 59 kg (130 lb). The major effects are greater penalties in spacecraft modifications and support functions, which increased from 32 kg (70 lb) to 50 kg (110 lb). The weight penalty results from the increased deflection propellant required to achieve the 4 R_J flyby radius and addition of a despun probe tracking antenna on the spacecraft.

The Jupiter-Saturn 1977 (JS 77) Mission (7) has some major differences. A MOPS is required to conduct the post-Jupiter segment of the mission to Saturn, and a more complex probe is required, one incorporating attitude-control and deflection subsystems. This more complex probe weighs 81 kg (179 lb) compared to 59 kg (130 lb) for the less complex probes.

The remaining missions studied are identified in Section D.

Table V-1 Mission/System Design Parameters for Turbopause Probe Missions 1A, 2A, and 7

	Unit	1A Probe/Science Optimized	2A Radiation-Compatible Spacecraft	7 JS 77
Mission Parameters				
Launch Vehicle		Titan IIID/5-seg-Centaur-Burner II		
Spacecraft		Pioneer	Pioneer	MOPS
Launch Date		10/21/78	10/13/78	9/5/77
Arrival Date		11/19/80	7/29/80	3/1/79
Flight Time	Days	760	655	557
Deflection Mode		Spacecraft	Spacecraft	Probe
Deflection Radius	10^6 km	10	50	50
Deflection Velocity (ΔV)	m/sec	54.6	101	130.7
Entry Angle, γ_E	deg	-23.2	-29.0	-33.3
Periapsis Radius	R_J	1.1	4.0	4.85
Science Data Rate	bps	1300	914	914
Spacecraft Modification Weights				
Probe Adapter & Enclosure	kg (lb)	9.0 (20.0)	9.0 (20.0)	12.3 (27.2)
Antenna System	kg (lb)	1.4 (3.0)	13.5 (30.0)	3.7 (8.1)
Receiver System	kg (lb)	5.9 (13.0)	5.9 (13.0)	5.9 (13.0)
Data Handling System	kg (lb)	6.8 (15.0)	6.8 (15.0)	0
Propellant	kg (lb)	0	4.4 (9.7)	0
Other	kg (lb)	4.3 (9.4)	4.3 (9.4)	0
Contingency (15%)	kg (lb)	4.1 (9.0)	6.3 (14.5)	3.3 (7.3)
Total Modification	kg (lb)	31.5 (69.4)	50.2 (111.6)	25.2 (55.6)
Spacecraft Weight	kg (lb)	248.3 (547.0)	248.3 (547.6)	665.9 (1468.0)
Total Spacecraft + Modifications	kg (lb)	279.8 (616.4)	298.5 (658.6)	691.1 (1523.6)
Probe Systems Weights				
Science	kg (lb)	14.4 (31.7)	14.4 (31.7)	14.4 (31.7)
Structure & Heat Sink	kg (lb)	12.2 (26.9)	11.7 (25.9)	12.6 (27.7)
Communications & Data Handling	kg (lb)	10.7 (23.5)	10.7 (23.5)	10.7 (23.5)
Attitude Control	kg (lb)	1.2 (2.7)	1.2 (2.7)	7.8 (17.2)
Propulsion (incl propellant)	kg (lb)	0	0	6.9 (15.3)
Electrical	kg (lb)	7.0 (15.4)	7.0 (15.4)	9.9 (21.8)
Other	kg (lb)	6.5 (14.4)	6.5 (14.4)	8.9 (19.8)
Contingency (15%)	kg (lb)	7.8 (17.3)	7.8 (17.1)	10.1 (22.0)
Total	kg (lb)	59.8 (131.9)	59.4 (130.7)	81.2 (179.0)
Total LV Payload Weight (Probe, Spacecraft & Spacecraft mods)	kg (lb)	339.6 (748.3)	357.9 (789.3)	772.3 (1702.6)

A. PROBE OPTIMIZED/SCIENCE OPTIMIZED MISSION 1A

This mission has the most favorable probe design and science return. The probe is carried on a Pioneer spacecraft, launched in October 1978 with a Titan IIID/5-segment-Centaur-Burner II, on a Jupiter-dedicated mission.

Spacecraft and probe are targeted to the entry point and the spacecraft orients and releases the probe at an attitude that results in zero angle of attack at entry. The spacecraft then applies deflection ΔV to establish the correct trajectory for 1.1 R_J flyby and the desired communications geometry with the probe. This geometry minimizes probe-to-spacecraft aspect angle, communications losses, and probe/spacecraft geometry dispersions. The launch/arrival dates have been adjusted so that both the probe and spacecraft spin axes are lined up with Earth and each other at entry. This geometry allows a fixed tracking antenna to be used on the Pioneer. Thus, no despin and off-axis pointing is required of the probe tracking antenna.

The science payload, as on all missions, consists of the mass spectrometer (NMS), electron temperature probe (ETP), ion-retarding potential analyzer (IRPA), neutral-particle retarding potential analyzer (NRPA), and an optical spectrometer or photometer. Basic science bit rate of 914 bps has been increased to 1300 bps to enhance data return by providing an increased number of measurements and additional interpretive information.

Probe systems required for support of science instruments, data processing, and transmission to the spacecraft are activated at entry and have a total power requirement of 75.5 W-h, including a 20-W X-band RF transmitter.

Mission 1A trajectory design is shown in Fig. V-1, the probe configuration in Fig. V-2 and V-3, and the probe Pioneer spacecraft interface configuration in Fig. V-4. Probe weight, spacecraft modification weights, and other significant mission/systems design parameters are in Table V-1

B. RADIATION-COMPATIBLE SPACECRAFT MISSION 2A

This mission targets the spacecraft for a 4 R_J flyby radius to protect it from the more severe radiation damage of closer flyby radii. The probe is on a Pioneer launched in October 1978, with a Titan IIID/5-segment-Centaur-Burner II on a Jupiter-dedicated mission.

As in the Probe-Optimized Mission (1A), spacecraft and probe are targeted to the entry point and the spacecraft orients and releases the probe at an attitude that results in zero angle of attack at entry. The spacecraft then applies deflection ΔV to establish the correct trajectory for 4 R_J flyby and the desired communications geometry with the probe. This geometry minimizes the probe-to-spacecraft aspect angle, communications losses, and probe/spacecraft geometry dispersions. The trajectory constraints for this mission require a despun antenna on the Pioneer for probe tracking. The probe tracking antenna must look off the spacecraft spin axis about 25° and be capable of angular tracking of about 8° along the probe down-range dispersion direction.

Launch/arrival dates have been chosen to reduce the flight time from 760 days to 655 days compared to the Probe-Optimized Mission (1A); this results in a longer launch period and lower required launch energy (C_3).

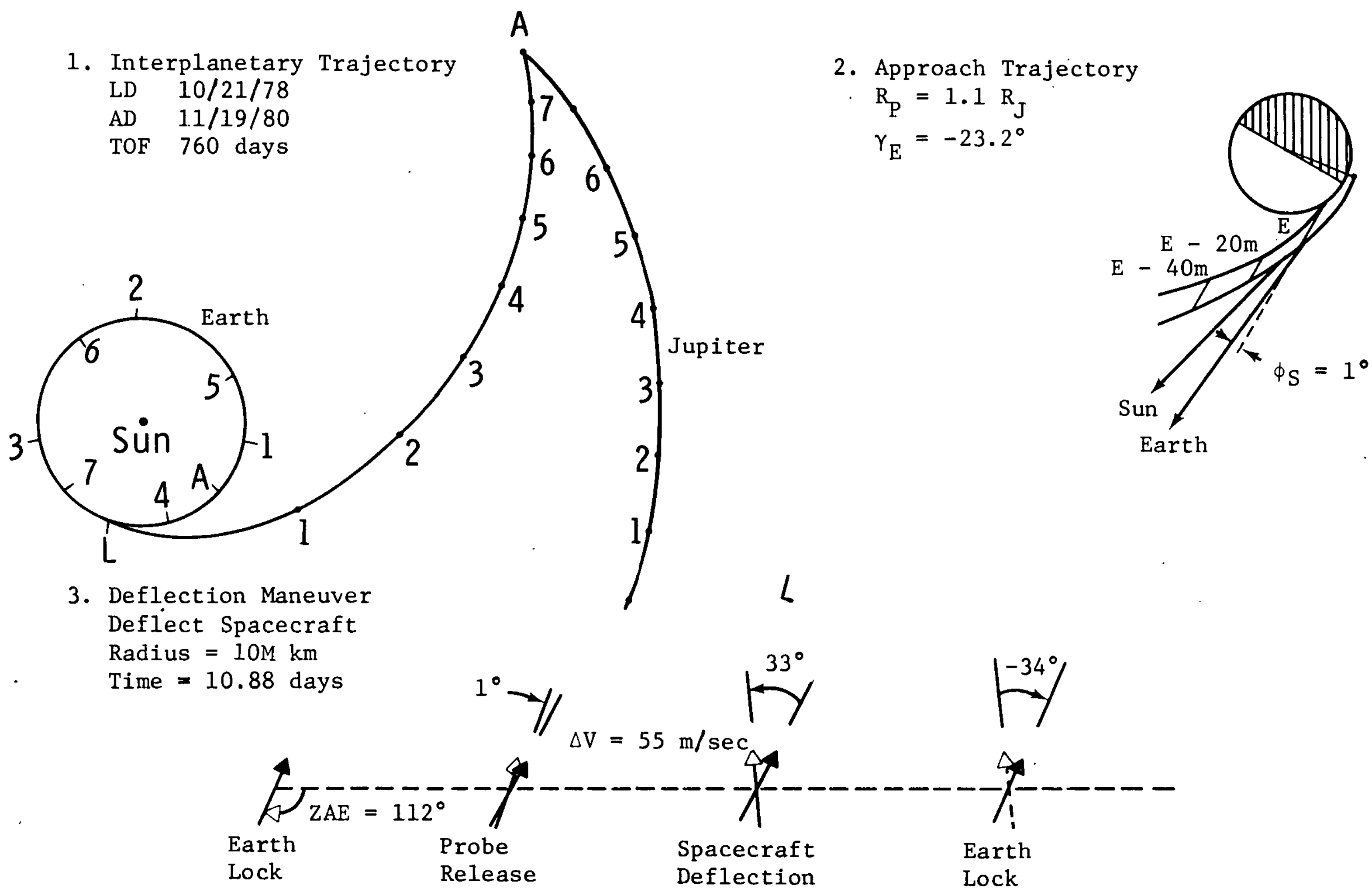

Fig. V-1 Probe Optimized/Science Optimized Mission 1A Trajectories

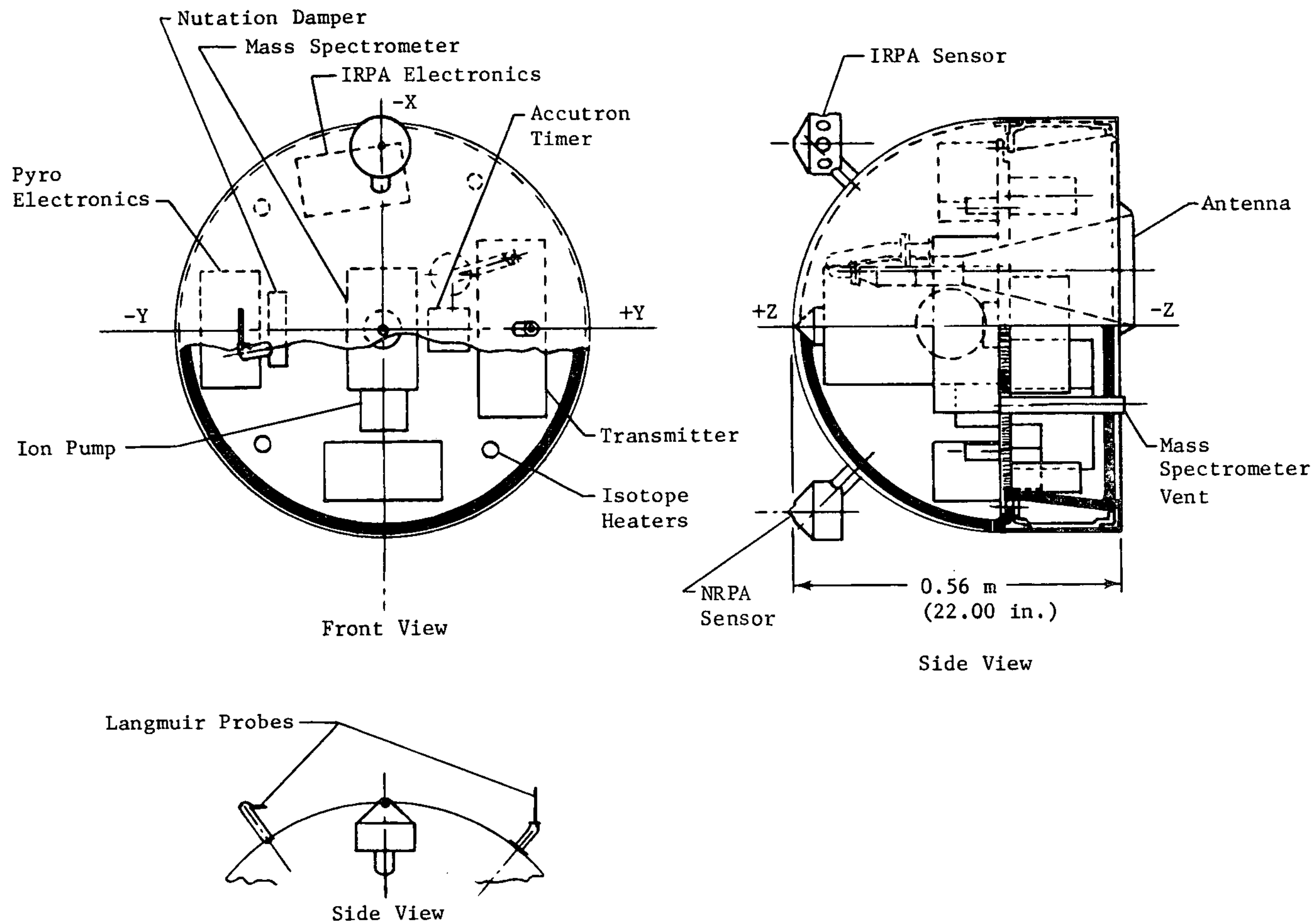

Fig. V-2 Mission 1A and 2A Probe Configuration Front and Side

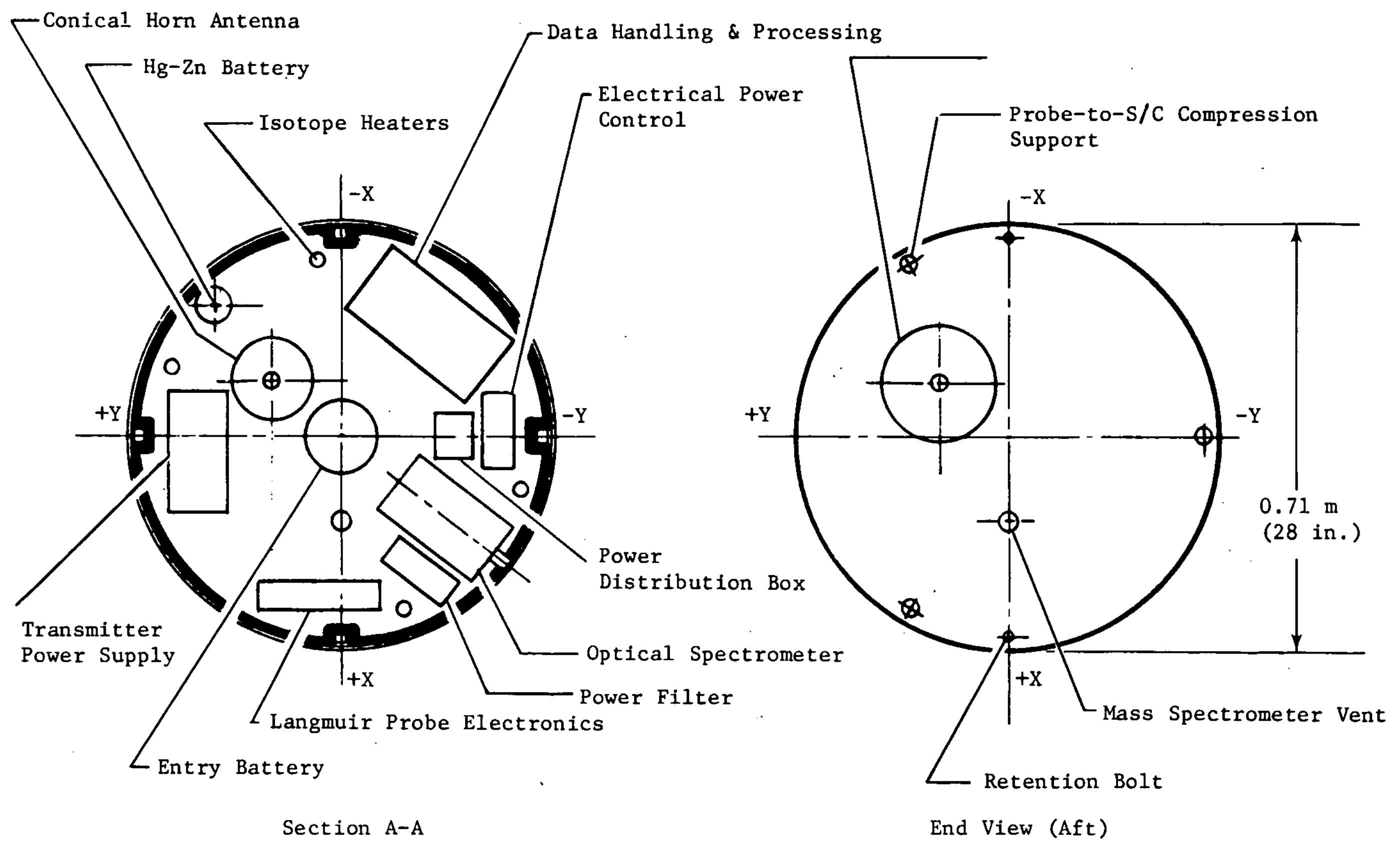

Fig. V-3 Mission 1A & 2A Probe Configuration End and Section

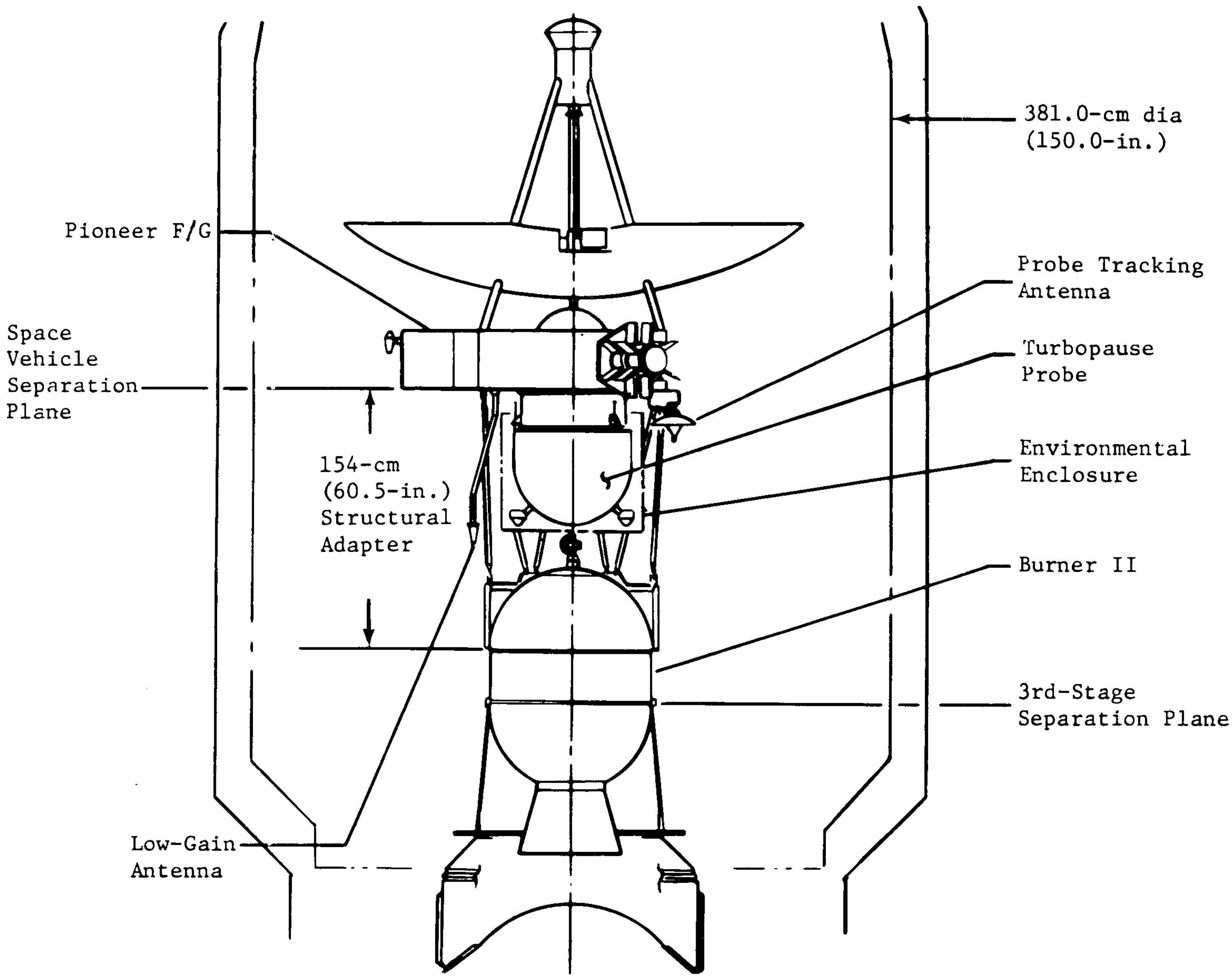

Fig. V-4 Probe-Spacecraft Interface for Mission 1A and 2A

The probe carries the nominal science payload, the bit rate is nominal, 914 bps. Mission design for this probe was built around the radiation avoidance constraint, which resulted in the requirement for a periapsis radius of 4 R_J. This radius was based on consideration of the nominal radiation environment from the 1971 Radiation Workshop Data* (Ref Vol II, Chapter III, Environmental Models), spacecraft (Pioneer) shielding of 0.5 gm/cm^2, and an assessment of the damage thresholds of the spacecraft's science instruments and components. These radiation levels and damage thresholds are summarized in Chapter IV, Subsection B3.

Probe systems required to support the science instruments, data processing, and transmission to the spacecraft are similar to those for Mission 1A, and are activated at entry with a total power requirement of 75.2 W-h, including a 20-W X-band RF transmitter.

The probe system configuration for Mission 2A (Fig. V-2 and V-3) is the same as that for Mission 1A (simplified, probe optimized). However, the increased periapsis radius does not allow the enhanced science data return and requires additional spacecraft modifications. The most significant of these cause weight penalties greater than the modifications required for Mission 1A:

1) Increased communications geometry range and dispersions, requiring a despun tracking antenna, increasing the weight by approximately 10.9 kg (24 lb).
2) Increased deflection velocity (101 m/sec compared to 55 m/sec for Mission 1A) requiring a propellant load approximately 4.5 kg (10 lb) greater than the present spacecraft tank capacity.

---

*D. M. Hunten: Letter to J. Bunting and W. Rumpel concerning model ionosphere, May 13, 1971.

The probe/spacecraft interface is nearly identical to that for Mission 1A, shown in Fig. V-4.

Figure V-5 shows the interplanetary and approach trajectories and deflection maneuver details for Mission 2A. Table V-1 summarizes the mission and system details.

C. JUPITER-SATURN 1977 MISSION 7

This mission uses the 1977 launch opportunity for a Jupiter-Saturn encounter and flyby. The multiplanet mission objective requires a MOPS-type vehicle with a trajectory designed to give the lowest Jupiter flyby radius (periapsis) practical without compromising the postencounter objective. The launch vehicle is a Titan IIID-5-segment Centaur-Burner II.

To avoid disturbing the spacecraft trajectory, a probe deflection maneuver is required. Spacecraft and probe are targeted for a 4.85 R_J flyby radius, and the spacecraft releases the probe in the attitude for the deflection maneuver. The probe then spins up and performs the deflection maneuver, then partially despins and precesses to the attitude required for zero angle of attack at entry. Additional probe systems required for this sequence include an attitude-control system and a solid rocket deflection system. This more complex probe design weighs 81 kg (179 lb) compared to 59 kg (130 lb) for the less complex probes.

As with Mission 2A, the large flyby radius of 4.85 R_J results in increased communications range and geometry dispersions, and the MOPS requires a search antenna for probe acquisition and tracking.

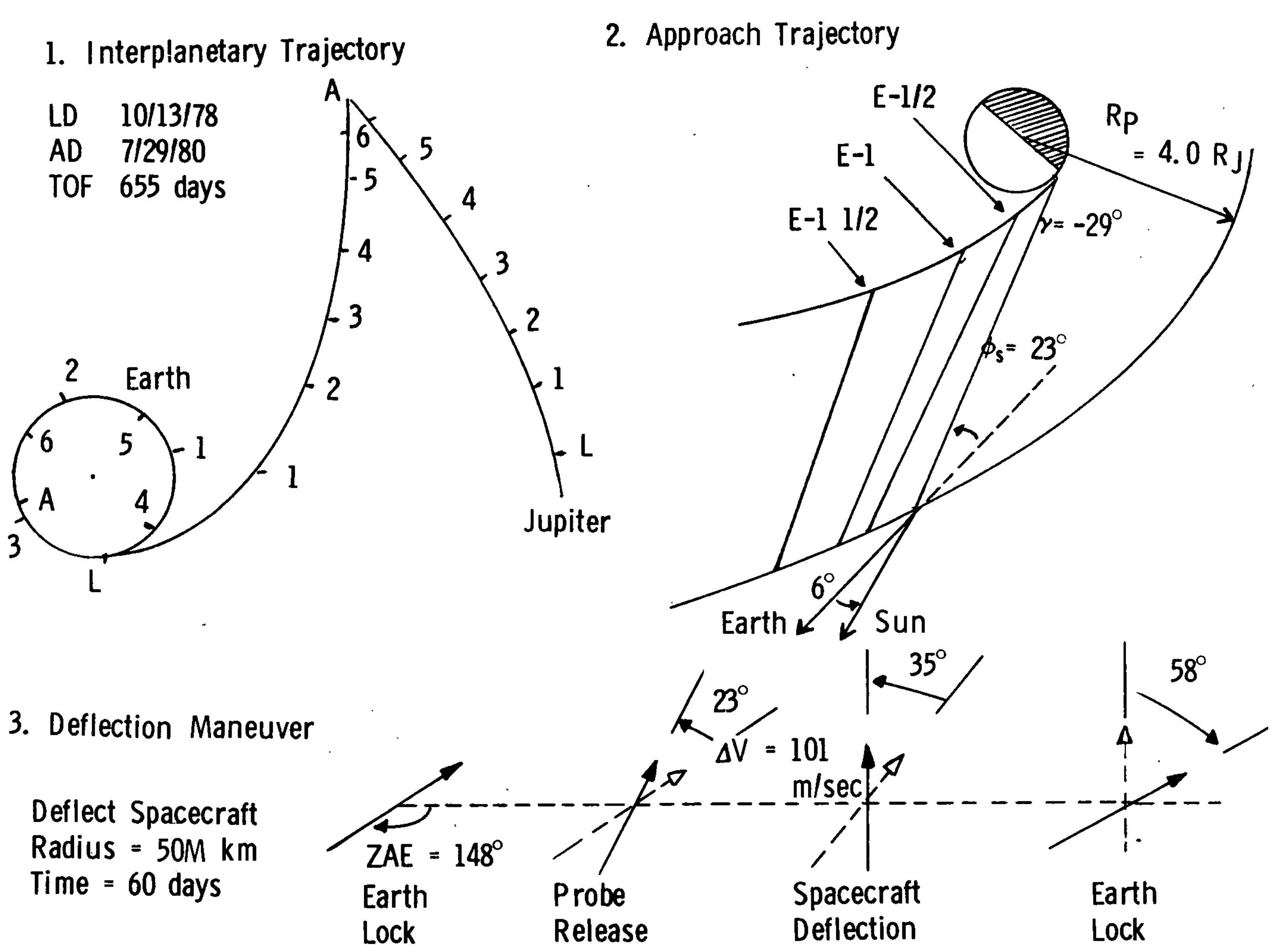

Fig. V-5 Radiation-Compatible Spacecraft Mission 2A Trajectories

Probe systems required at separation for spin-up, deflection propulsion, and precession are activated at separation and require a total of 51.4 W-h. At entry, the probe systems required for despin, science-instrument support, data handling, and transmission are activated. The total requirement at entry is 104.6 W-h, including a 20-W X-band RF transmitter.

Mission 7 trajectory design is shown in Fig. V-6, probe configuration in Fig. V-7 and V-8, and the probe/spacecraft interface configuration in Fig. V-9. Probe weight, spacecraft modification weights, and other significant mission/system design parameters are in Table V-1.

D. ADDITIONAL MISSION OPTIONS STUDIED

Table V-2 identifies the other mission options studied. Pertinent mission and system design data are tabulated for comparison and identification of the depth of study for each mission. Where applicable, the most significant limiting factors are noted.

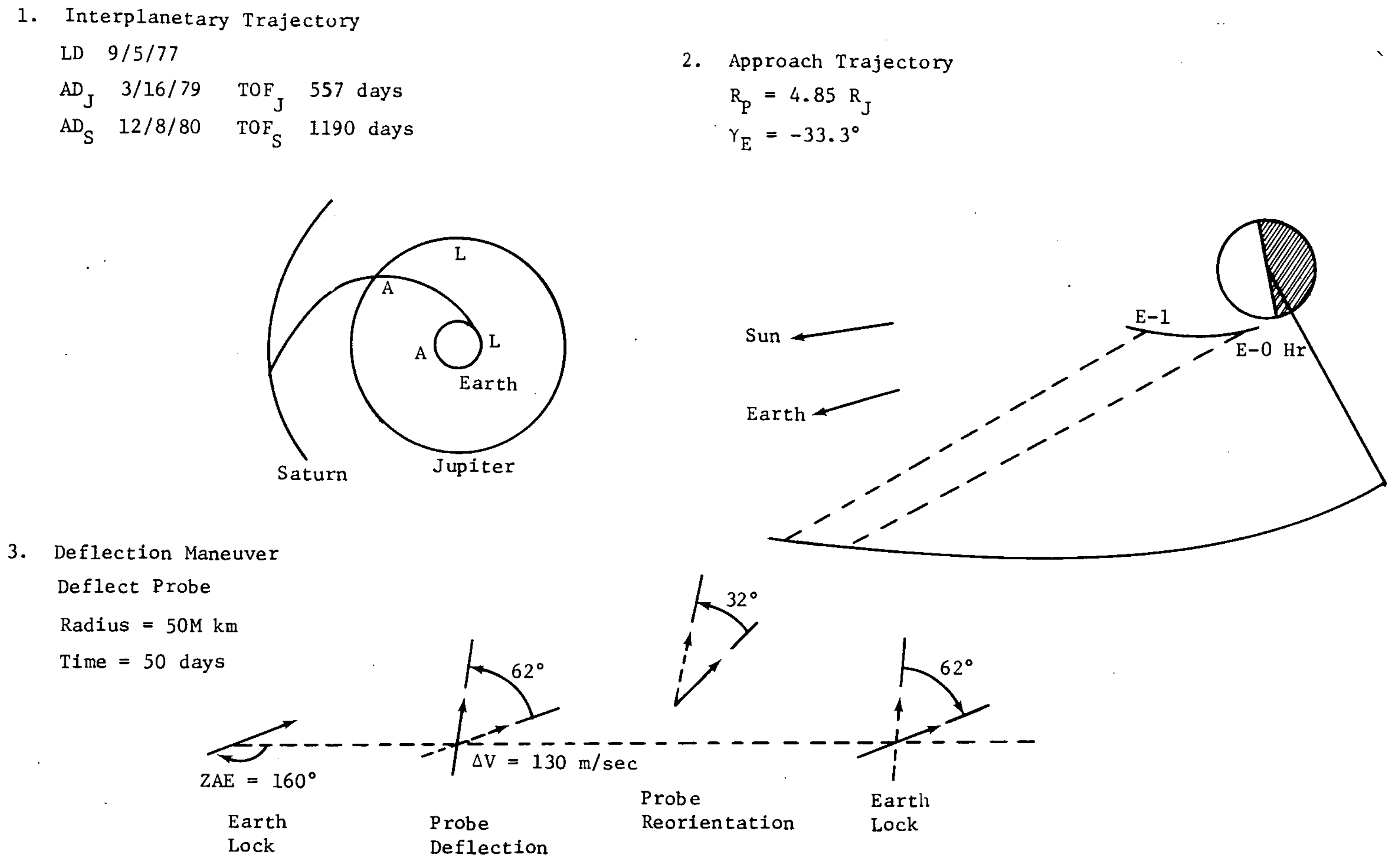

Fig. V-6 Jupiter-Saturn 1977 Mission 7 Trajectories

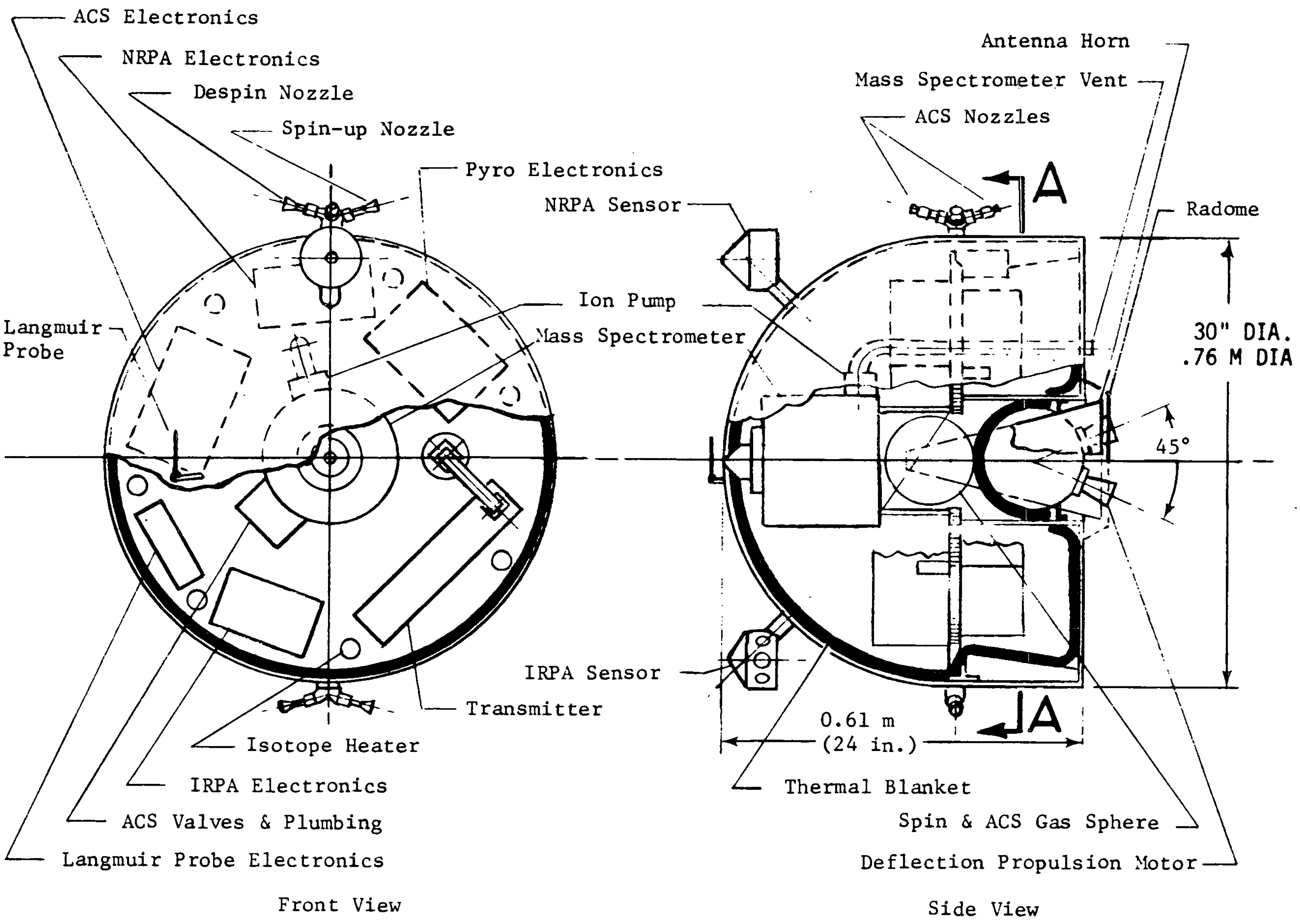

Fig. V-7 Mission 7 Probe Configuration Front and Side

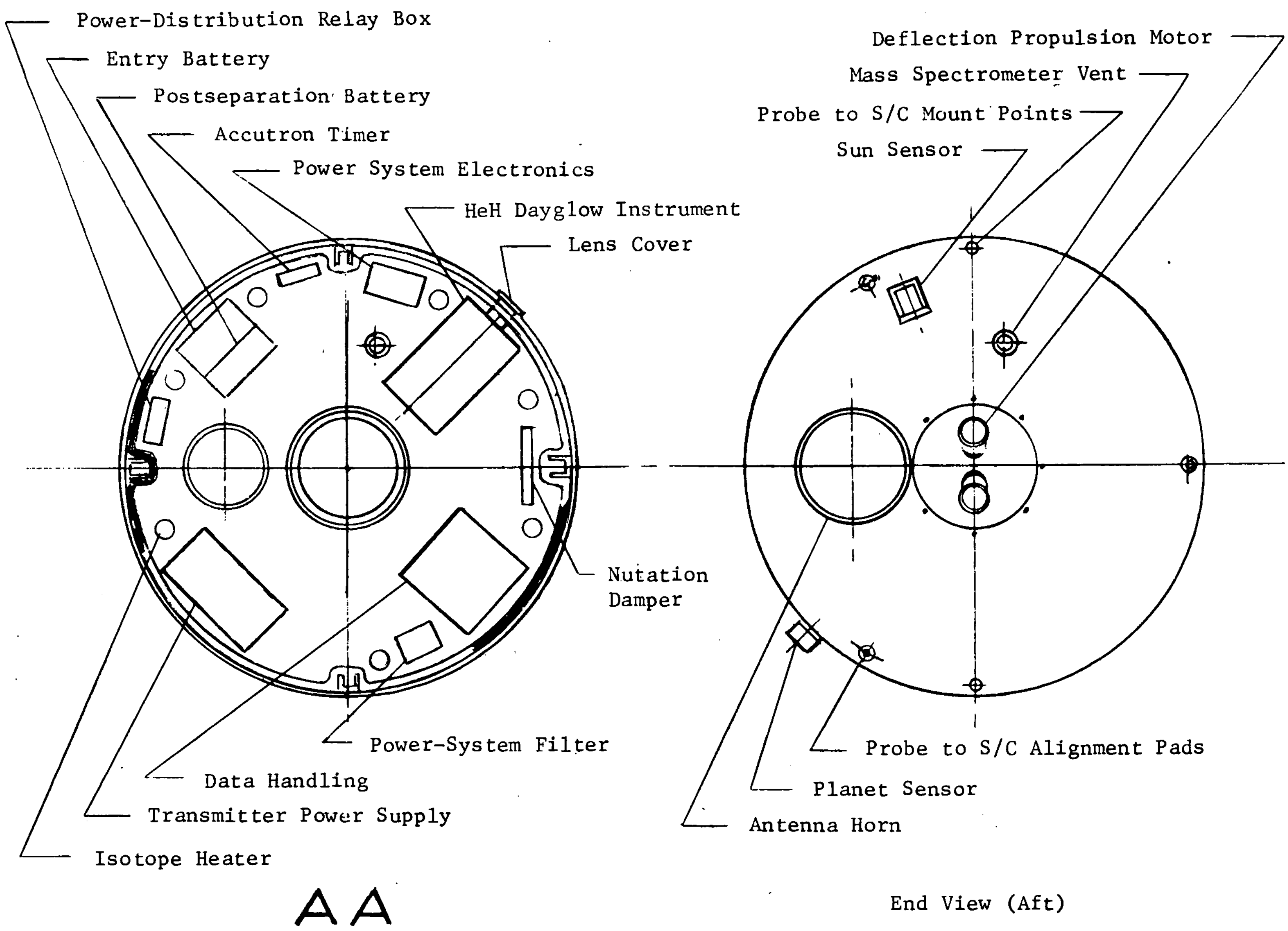

Fig. V-8 Mission 7 Probe Configuration End and Section

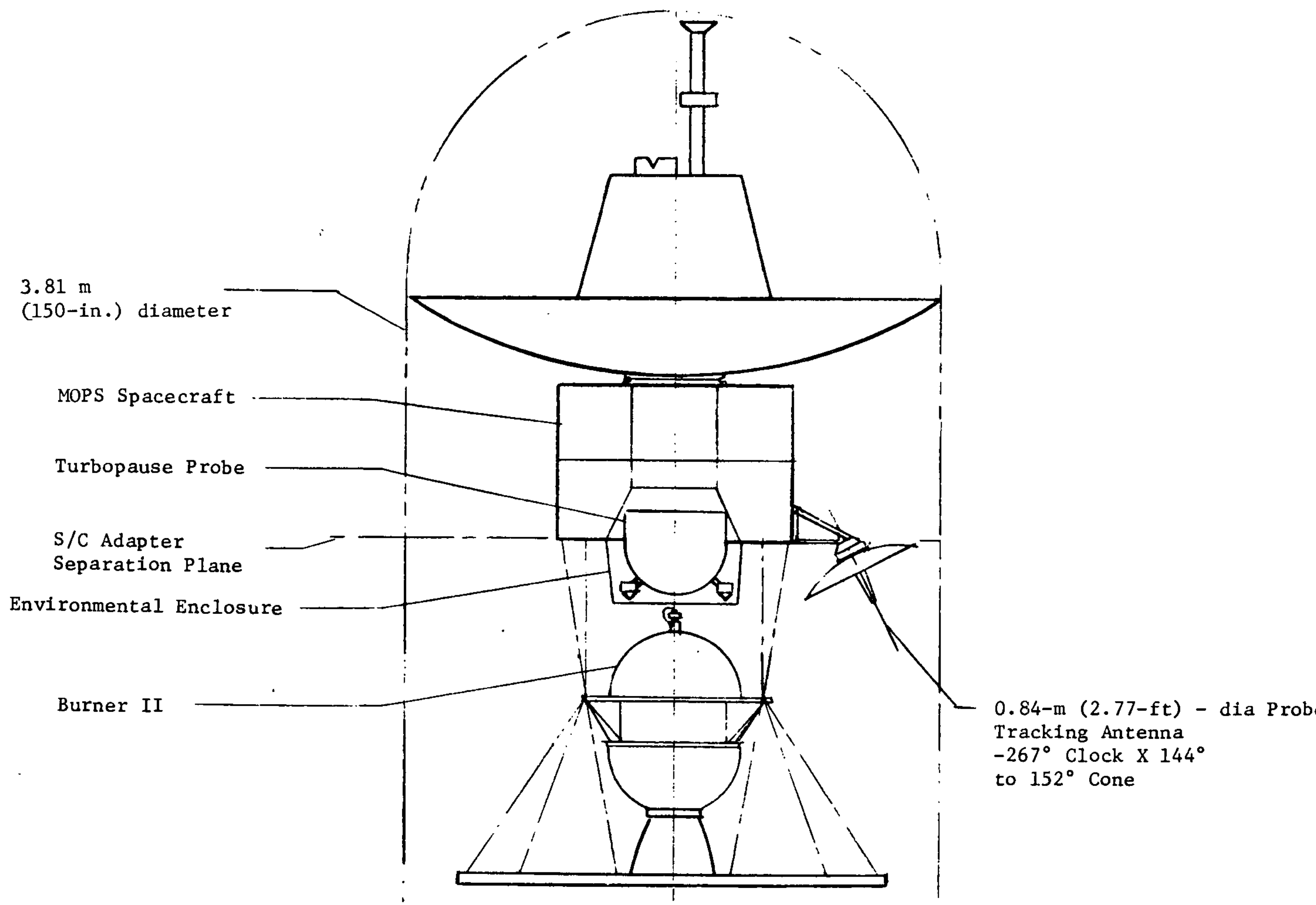

Fig. V-9 Probe-Spacecraft Interface for Mission 7

Table V-2 Mission Options Studied

Mission	Launch Vehicle	Spacecraft	Launch Date	Arrival Date	TOF, days	Deflection			R_P, R_J	Entry Angle, γ_E, deg	Science Data Rate, bps	Depth of Study	Remarks
						Mode	Radius, 10^6 km	Velocity, m/sec					
1 Probe Optimized	Titan IIID/ 5-seg/Centaur/ Burner II	Pioneer	10/21/78	12/26/80	797	S/C	30	16	1.1	-21	934	Complete system description	
1A Probe Optimized/ Science Optimized			10/21/78	11/19/80	760	S/C	10	54.6	1.1	-23.2	1300		Refinement of 1; reduced transmitter power rqmt used to increase data rate
2 Radiation-Compatible Spacecraft			10/13/78	7/29/80	655	S/C	50	101	4.0	-29.0	914		
2A Radiation-Compatible Spacecraft			10/13/78	7/29/80	655	S/C	50	101	4.0	-29.0	914		Refinement of 2; X-band transmitter reduces total power reqd
3 Grand Tour JUN 78	Titan IIID/ 7-seg/Centaur (w/wo Burner II)	TOPS	10/3/78	5/1/80	576	Probe	30	82	1.94	-33.0	958		
4 Grand Tour JUN 79			11/5/79	6/8/81	581	Probe	50	243	9.85	-33.0	958	Mission analysis & communications	Transmitter power rqmt high; large battery load; large ΔV required
			11/11/79	5/2/81	538	Probe	50	180	6.6	-34.0	958		
5 Solar Apex 78	Titan IIID/ 5-seg/Centaur (w/wo Burner II)	Pioneer	10/9/78	4/1/80	540	Probe	30	75	1.77	-34.0	958	Complete system description	
6 JU 80	--	TOPS	--	--	--	--	50	400	>15	--	--	Mission analysis	Transmitter power prohibitive; ΔV rqmt also prohibitive
7 JS 77	Titan IIID/ 5-seg/Centaur (w/wo Burner II)	MOPS	9/5/77	3/1/79	557	Probe	50	130.7	4.85	-33.3	914	Complete system description	
8 JS 80	--		10/5/78	7/31/80	543	Probe	50	402.1	15.7	-34.0	--	Mission analysis	Transmitter power prohibitive; ΔV rqmt also prohibitive

VI. PROBE HARDWARE STATUS

Probe hardware status is discussed in two categories--science instruments and probe engineering subsystems. In general, both science and engineering systems appear feasible, the design and hardware technology is state of the art today for all subsystems except two science instruments (NMS and NRPA), and the remotely activated battery. However, these three items appear within the 1975 state of the art. Early in the study, a K-band communications link was evaluated and found to be within the 1975 state of the art at powers up to 25 W. However, later in the study, it was found that a common X-band system would easily meet communications link requirements.

A. SCIENCE INSTRUMENT HARDWARE STATUS

Both the NRPA and the mass spectrometer will require some research and development. The NRPA has never been flown, but it is an offshoot of the IRPA, and no serious problems are anticipated in its development. It is essentially an IRPA with additional grids to repel all positive and negative charged particles. Only neutral particles are allowed to enter, and these are then ionized by an electron beam. It then functions as an IRPA.

The mass spectrometer consists of a sampling system and a measuring system. Its only unproven part is the inlet sampling system. The quadrupole measurement part of the system is state of the art and has been flown many times. However, the conventional sampling system, which employs a plug-type molecular leak, is not acceptable for this application. The turbopause probe mission requires rapid sampling (0.4 sec/sample) at very low pressure

(10^{-7} atm), and the conventional plug will not allow sufficient flow at this pressure. The alternative concept, which requires testing, is called the molecular-beam sampling system. This system essentially consists of two tandem orifices that collimate the incoming particles but allow some particles direct entrance into the quadrupole measuring section. This allows rapid continuous measurement. Theoretical analyses show the system to be adequate for the mission. However, hardware testing is necessary for development and proof.

The Langmuir probe is essentially fully developed, having been flown on over 10 satellites in the past 9 years. Inflight data processing has been demonstrated successfully on the ISIS-II version of this instrument.

All science instruments and their electronics must be tested in a radiation environment to determine threshold damage levels because shielding may be required for both protection from damage and reduction of background noise. Table VI-1 is a summary of hardware status of each science instrument.

B. PROBE ENGINEERING SUBSYSTEMS

Table VI-2 is a summary of equipment for the turbopause probe structure, mechanisms, thermal, and propulsion subsystems. No feasibility problems are foreseen, but some developmental work will be necessary.

The beryllium heat-sink analytical technique involves certain simplifications that should be further evaluated to better understand the effect of bilinear representation of modulus of elasticity change with temperature change. At present, there appear to be very little biaxial material property data on beryllium, and it will be necessary to acquire these data at the temperatures in-

Table VI-1 Science Hardware Status

Item	System	Probe Mission	Status/Technology Requirement	Remarks
Langmuir Probe	Science	All	State of art	Similar model flown on Explorers, ISIS A and B Advanced models being developed for AE-C, D, E
Ion RPA	Science	All	State of art	Similar model flown on ISIS B, OGO 1 thru 6, DMEA, etc Changes required in grid voltage & data handling
Dayglow Photometers (H, He)	Science	All	State of art	Experiments flown on early Mariner & rockets
Optical Spectrometer	Science	All	State of art	Mariner Venus/Mercury Flyby - 1973
Neutral Particle RPA	Science	All	New development	Extention of Ion RPA
Neutral Mass Spectrometer				
Analyzer Section	Science	All	State of art	Similar model flown on PAET Advanced model to be flown on AE Electronics may be adapted to turbopause probe
Inlet Section	Science	All	New Development	Inlet system (molecular beam type) will require development and test
Ion Pump	Science Support	All	Development required for pumping rate & low weight	

Table VI-2 Probe Hardware/Equipment List - Structural/Thermal/Propulsion

Item	System	Probe Mission	Status/Technology Requirement	Remarks
Structural/Mechanical				
Beryllium Heat Sink	Structure	All	Development required	Thermal stress analysis techniques Biaxial property data Test facility Platinum or rhodium plating development required
Fasteners	Structure	All	State of the art	Testing necessary
Pyro Mechanisms	Mechanical	All	State of the art	Routine development required Radiation sensitivity testing
Springs	Mechanical	All	State of the art	Routine development required
Bearings	Mechanical	All	State of the art	Routine development required
Thermal				
Radioisotope Heater	Thermal control	All	1-W & 15-W units available off the shelf; no change in state of art expected for 1975-1980	Both units have about the same specific power 0.057 kg/W (1/8 lb/W)
Multilayer Insulation Blanket	Thermal control	All	Many metallized film & separator materials available & in space use	Each blanket custom designed for given application
Propulsion				
Solid Rocket Motor (dual nozzle)	Deflection propulsion	3,5,7	State of the art	Analytical design parameters available; build & test required
Gaseous Nitrogen System	Spin & ACS (despin)	3,5 7	State of the art	Analytical design parameters available; build & test required

volved. Heat-sink testing will require scaling techniques because available test facilities will apply full-scale heating rate to only a 6 cm^2 model. Manufacturing the aeroshell is considered to be state of the art. Plating with rhodium or platinum will require some design development tests, but no technology development.

All other components are either off the shelf or normal development.

Table VI-3 presents the hardware status for the telecommunications/electrical and power systems, including the attitude-control system. Telecommunications hardware for the nominal designs uses X-band (10 GHz), and much equipment is available off the shelf with routine modifications for integration into the probe and spacecraft systems. Many similar X-band RF systems have been developed and flown. K-band (20 GHz) telecommunications equipment was also investigated and listed here because future designs might incorporate this frequency if atmospheric penetration depths greater than the designs of this study are required. A vendor survey showed that, for the projected 1975 state of the art, transmitter powers up to 25 W K-band should be available. Technology for the traveling-wave-tube power source is available today.

Data handling, antennas, and antenna despin mechanisms are state of the art. However, specific designs must be developed for the mission. Remotely activated battery technology is being developed today for fairly short-life batteries. Additional research and development is required for longer-life batteries, although this development should easily be state of the art by 1975.

The attitude-control subsystems and logic are state of the art. However, the cost will be a function of the accuracy required. For this study, a probe pointing accuracy of 1.5° (3σ) proved adequate for all missions.

Table VI-3 Probe Hardware/Equipment List - Telecommunication/Electrical/Power

Item	System	Status	Remarks
Probe Transmitter & Power Supply	Telecommunications	X-band (10 GHz) State of the art	Modified off-the-shelf equipment
		K-band (20 GHz) Development required	Projected 1975 state of the art up to 25 W
Data Handling	Telecommunications	State of the art	Normal engineering development for mission
Probe Antenna	Telecommunications	State of the art	Minimum cost, off-the-shelf design
S/C Antenna	Telecommunications	State of the art	Dish, off-the-shelf design
S/C Antenna Despin Mechanism	Telecommunications	State of the art	Design/development required; similar systems flown on Earth-orbit satellites
Battery	Power	Technology state of the art for remotely activated	Design/development required
Attitude Control	ACS	State of the art	Propulsion/electronics required routine design for mission; cost will be function of accuracy
Planet/Sun Sensors	ACS	Sun sensor, state of the art; planet sensor not now available but technology is state of the art	Planet sensor will be modified Sun sensor with optics; design for environment, light level

VII. CONCLUSIONS AND RECOMMENDATIONS

A. CONCLUSIONS

1. General

A nonsurvivable turbopause probe mission to Jupiter, with adequate data return to meet the science objectives, is feasible and practical within the 1975 state of the art. Except for the mass spectrometer, neutral-particle retarding potential analyzer, and remotely activated batteries, all science and engineering system technology is current state of the art. The major uncertainty that affects mission survival is the Jovian radiation belt model, which may significantly constrain mission design. However, current estimates of radiation intensity can be designed for by normal component hardening techniques and careful materials selection.

Many mission options for launch opportunities between 1977 and 1980 are adaptable to the nonsurvivable turbopause probe concept. A Jupiter-dedicated mission with probe can be flown in all years, and probes to Jupiter on spacecraft multiple-planet flyby missions are practical from 1977 to 1979. The primary restriction on the probe mission is a limit of spacecraft flyby radius to within about 7 R_J, because of communications-link losses. The Jupiter/Saturn-1977 mission with a flyby radius of 4.8 R_J provides a viable probe mission, as does the Jupiter/Uranus/Neptune 1978 mission. The JUN 1979 mission can be designed with a flyby radius of 6.6 R_J, which results in a feasible though marginal communications-link design. In the probe-optimized Jupiter-dedicated 1978 mission, appropriate selection of launch and arrival dates allowed alignment of the probe, spacecraft, and Earth so that a fixed spacecraft-probe tracking antenna is possible.

All missions using either the Pioneer or MOPS spacecraft can be launched with the 5-segment solids version of the Titan IIID-Centaur-Burner II. Missions designed for the cancelled TOPS spacecraft require the 7-segment solids on the launch vehicle.

Probe designs can all be grouped into either simple probes weighing 59 kg (130 lb) or complex probes at 81 kg (179 lb). Complex probes have the addition of a deflection propulsion solid rocket and an attitude-control system to handle the probe deflection targeting mode. Simple probes are used when the spacecraft provides the deflection maneuver.

2. Science

All science measurement criteria can be met or exceeded by the five instruments carried on the nonsurvivable turbopause probe for entry angles up to -26°. For entry angles as high as -34°, the highest angle required in any mission, all measurement criteria were met except the requirement of 1.0 measurement per scale height for neutral helium. A value of 0.9 measurements per scale height was obtained at -34° γ_E. But further analysis of the expected variation of neutral helium shows this measurement rate to be acceptable for meeting science objectives.

Critical measurements obtained by the mass spectrometer exceed by a factor of two the minimum criteria of two measurements below the turbopause. For entry angles from -20° to -34° the complete mass spectrometer sweeps below the turbopause vary from 7.3 to 4.6, respectively. The study also considered that location of the turbopause might be in error as much as one order of magnitude in density, resulting in lowering the altitude of the turbopause by 40 km. For this condition, the criteria can still be satisfied for entry angles up to -25°. Lower entry angles are desirable because they increase the time available for measurement. However, a lower limit on entry angle is imposed on each mission by a 20° light-side mask constraint required for the optical experiments and specific mission trajectory constraints.

Although the data taken above the turbopause are very important on their own, only 3 sec of data are obtained below the turbopause. Stated in terms of distance, the mission survives for 60 km, or 37 miles. Stated in terms of measurements, the mass spectrometer can make 5.5 measurements below the turbopause (for an entry angle of -25°), which is 5.5 sweeps through its 11 prime constituents. If even one measurement could be made, more sweeps would be redundant because the major constituents are generally constant below the turbopause, and further measurements would yield the same results. Thus, the 3 sec of data are wholly satisfactory.

3. Mission Survival

The most critical factors in mission survival are the communications blackout, probe heat protection, and radiation hazard. Communications blackout altitude estimates must be based on nonequilibrium flow-field analysis for the conditions encountered at Jupiter entry. At the extremely high entry velocities of about 50 km/sec, nonequilibrium thermochemical analysis of the hypersonic flow field shows electron densities considerably lower than those calculated by less exact equilibrium methods. Based on the nonequilibrium analysis, probe communications blackout altitude varies between 63 and 73 km below the turbopause for RF frequencies between X-band (10 GHz) and K-band (20 GHz). These depths provide more than twice the time required to obtain the necessary science measurements for all missions at frequencies from 8 to 20 GHz.

The probe entry heat-protection system consists of a beryllium heat sink, plated with either platinum or rhodium, backed by an insulation layer. The heat-sink concept with a high-atomic-weight plating material effectively protects the science instruments from contamination from surface sputtering. The heat protection system designed to provide probe survival to 80 km below the turbopause is about 8.5% of the total probe weight. This provides a margin of survival below the end-of-mission blackout point of more than 0.5 sec or 15 to 20 km for entry angles down to -20°. Because heating, blackout, and location of the turbopause are directly related to atmospheric density, burnup will always follow blackout altitude, even though atmospheric uncertainties may shift the actual locations of these occurrences.

The radiation belt results in direct radiation damage, residual reradiation, and background noise in the science data readings. Direct radiation intensity is expected to peak and then drop off before the probe reaches the actual entry measurement phase. Appropriate materials selection, component design, and local shielding will provide sufficient probe hardening for survival within the upper-limit radiation belt model. Residual reradiation may degrade the data somewhat, but designing to acceptable levels appears to be feasible.

4. Data Return

For all viable missions studied, sufficient data return at 900 to 1300 bps could be provided at an RF power of 20 W and X-band (10 GHz) to meet science objectives.

The most critical function in the data return sequence is acquisition of the probe RF signal by the spacecraft probe tracking antenna and receiver system. A practical acquisition system consists of a multiple-position tracking antenna capable of a 4- to 5-position search of the probe position uncertainty region and a frequency search and lockon system in the spacecraft receiver. This sequence requires about 2 min. Probe position uncertainty results from the coast time uncertainties caused by execution errors and spacecraft uncertainties at deflection.

The RF data link from the probe to the spacecraft is designed to use phase shift keying (PSK) to phase modulate (PM) the carrier with data that have been pulse code modulated (PCM). To conserve the amount of RF power required, a coherent link was chosen. Since both X-band and K-band frequencies allow enough atmospheric penetration to meet all science objectives, X-band was chosen because of availability of hardware within the current state of the art.

If future probe missions should require greater atmospheric penetration, a K-band transmitter of 25 W is predicted to be available within the 1975 state of the art.

5. Targeting Modes

Targeting modes considered were probe deflection, shared deflection, and spacecraft deflection. The spacecraft deflection mode is the most effective when minimum probe complexity and cost are desired. If the spacecraft trajectory cannot be modified for the probe mission, then the probe deflection mode is required, resulting in addition of a solid rocket motor and an attitude-control system on the probe. This mode has the lowest deflection propellant weight penalty.

The shared deflection mode requires more total propulsion system weight and introduces greater trajectory dispersions than the other concepts; however, it does not require probe reorientation after deflection.

6. Probe Configuration

Both blunt and sharp configurations were considered for the entry probe. The blunt hemisphere/cylinder configuration has a clear advantage over the sharp cone in the area of spin stabilization because of the relative ease of location of equipment to provide the roll to transverse moment of inertia ratio of 1.20. The cone can be expected to show some reduction in the wake electron density, therefore, an advantage in increased penetration of the atmosphere before blackout. However, compensating flow-field effects are expected to make this advantage small. Additional aerophysics analysis is required to accurately evaluate this effect.

No particular advantage is shown by either configuration in the areas of instrument interference, structural/mechanical design, and aeroheating.

7. Design Missions

Although a number of design mission options were investigated, two representative missions are discussed here.

The Probe Optimized/Science Optimized design is a Jupiter-dedicated mission. It represents the most favorable probe design and science return using a 1978 launch opportunity. The system is the least complex possible at a probe weight of 59.6 kg (131.6 lb). The Pioneer spacecraft has a fixed probe tracking antenna with a total spacecraft modification weight of 31.5 kg (69.4 lb) and a total probe/spacecraft system weight of 339.4 kg (748.0 lb). This is well within the capability of the Titan IIID-5-segment Centaur-Burner II launch vehicle.

The Jupiter-Saturn 1977 mission requires a MOPS spacecraft with a trajectory designed to give the lowest Jupiter flyby radius (periapsis) practical without compromising the postencounter objective. A complex probe that incorporates a deflection motor and attitude control is required, at a probe weight of 81.2 kg (179.0 lb), a spacecraft modification weight of 25.2 kg (55.6 lb), and a total probe/spacecraft weight of 772.3 kg (1702.6 lb). This is within the payload capability of the 5-segment solid Titan IIID-Centaur-Burner II.

8. Hardware Status

The Langmuir probe, ion-retarding potential anlyzer (IRPA), and optical instruments are current state of the art. The neutral-particle retarding potential analyzer (NRPA) and neutral mass spectrometer require some research and development. The NRPA has never been flown but is an adaptation of the tested IRPA, and no serious problems are anticipated in its development.

The mass spectrometer inlet sampling system, a molecular beam type, requires development and testing, and its development appears to be within the 1975 state of the art.

Engineering subsystem designs, except for remotely activated batteries, are current state of the art. Remotely activated battery technology is well within the 1975 state of the art because designs are now under development.

9. Spacecraft Support

The Pioneer spacecraft can adequately support a probe mission to Jupiter in 1977 to 1980. Required spacecraft modifications and additions include probe adapter and enclosure, probe tracking antenna, receiver, data handling, and propellant, with total modifications weighing 50 kg (110 lb). Most missions require a tracking antenna despin and pointing mechanism. For the probe-optimized mission, a fixed spacecraft probe tracking antenna is possible, as well as reduced deflection propellant, with a total modification weight of 32 kg (70 lb).

B. RECOMMENDATIONS

During this study, various analytical and technological areas have been identified in which additional work should be conducted as part of the planning for a Jupiter nonsurvivable probe mission.

1. Science Analysis and Technology Development

Science areas requiring additional work include:

1) Development and test of the mass spectrometer molecular beam inlet sampling system;

2) Development of the neutral particle retarding potential analyzer;

3) Evaluation of the magnetic and radiation field effects on science instrument performance and measurement bias.

2. Engineering Analysis and Technology Development

Engineering areas requiring additional work include:

1) Forebody and wake nonequilibrium flow analysis and the resulting wake electron density and RF attenuation;

2) Upgrade thermal stress analysis techniques for the beryllium heat sink evaluation;

3) Development of 30-day wet stand remotely activated battery;

4) Evaluation and selection of radiation-insensitive components.

Additional development and analyses will be required during the program, but these are not considered time-critical nor unusually difficult. Furthermore, results of studies of the Jovian environment appear directly applicable to other outer-planet atmospheric investigations. Therefore, it is recommended that follow-on studies be conducted to investigate the applicability of the Jovian turbopause probe concept to other outer planets.

APPENDIX

STUDY GROUND RULES AND CONSTRAINTS

1. Mission Accomplishment Shall be During the 1978 to 1980 Launch Opportunity (Specified by GSFC)

Baseline mission studies used the 1978 to 1980 launch opportunities. However, based on redirection during the latter part of the study, a 1977 launch opportunity was evaluated for a Jupiter-Saturn mission.

2. System State of the Art Will Be as of July 1975 (GSFC-furnished constraint)

3. Science Payload (GSFC-furnished baseline)

Science payload is based on a GSFC-suggested set of candidate instruments that meet the scientific objectives, types of measurements required, and desired quantities to be measured. These instruments are:

1) Quadrupole mass spectrometer
2) Ion retarding potential analyzer
3) Neutral particle retarding potential analyzer
4) Electron temperature and density probe (Langmuir probe)
5) Hydrogen and helium dayglow instruments

4. Launch-Vehicle Performance (GSFC-furnished constraint)

Launch energy requirements shall be based on use of the Titan IIID/Centaur with possible additional staging in accordance with JPL Section Document 131-09, *Titan III/Centaur Family Launch Vehicle Definition for a Jupiter Entry Mission Study*, January 30, 1970. In addition, based on GSFC redirection during the latter portion of the study, an updated version of the Titan IIID/5-segment Centaur-Burner II launch vehicle was included in the study of the

1977 Jupiter-Saturn mission. This vehicle has a payload capability about equal to the 7-segment Titan Centaur without Burner II. Figure 1 summarizes the payload capability of the various launch vehicles as a function of *vis viva* energy, C_3.

5. Astronomical Constants (GSFC-Furnished Constraint)

Astronomical constants, as specified by GSFC, were obtained from JPL TR-32-1306, *Constants and Related Information for Astrodynamic Calculations 1968*, July 15, 1968. These data are summarized in Table 1.

6. Transfer Trajectory Data

Transfer trajectory data, including launch and arrival date combinations and *vis viva* energy, C_3, requirements were generated as part of the study for the 1977 to 1980 mission opportunities.

7. DSN Capability (GSFC-Furnished Baseline)

As specified in JPL Section Document 131-11, *Summary of DSN Capabilities for Jupiter Atmospheric Probe Mission (1978 Launch Opportunity)*, January 30, 1970.

8. Spacecraft Candidates

GSFC specified that the TOPS program and Pioneer F and G spacecraft concepts be used as examples of realistic spacecraft constraints. For this study, both spacecraft descriptions were specified in JPL Section Document 131-08, *Outer Planet Spacecraft System Descriptions*, December 31, 1969 and other supplementary data. During the latter part of the study, based on GSFC redirection, the Modified Outer Planets Spacecraft (MOPS) was included in the study to be incorporated in a 1977 Jupiter-Saturn mission. This spacecraft design is based on Mariner technology. Because the MOPS design is not yet well defined, a Martin Marietta version

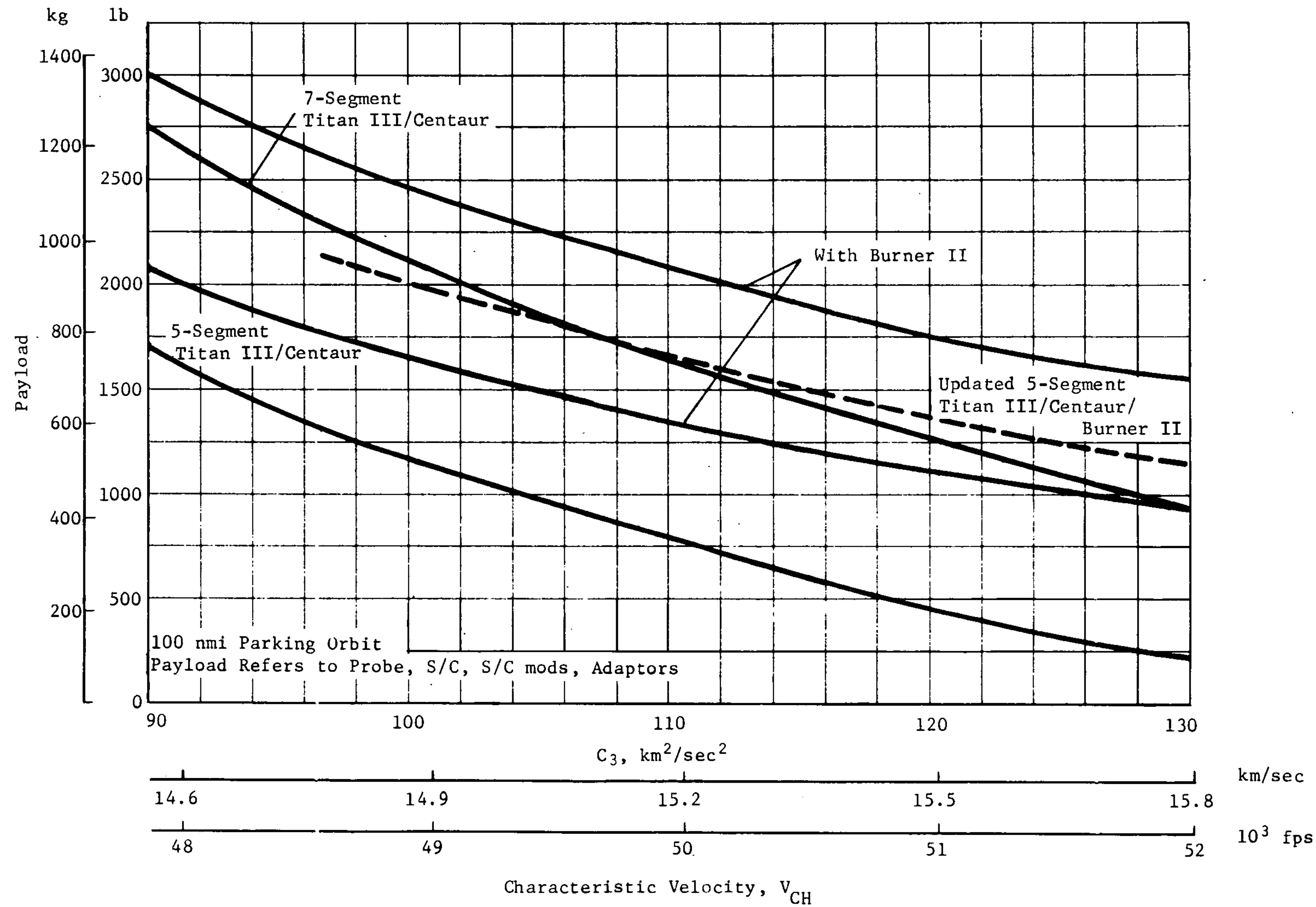

Fig. 1 Titan III/Centaur Performance Data

Table 1 Astronomical Constants

The constants used to define the ephemerides of the planets Jupiter and Earth were obtained from JPL TR 32-1306, *Constants and Related Information for Astrodynamic Calculations, 1968.* The mean ecliptic elements that define the ephemerides of the planets are shown below.

	Jupiter	Earth
a = semimajor axis ∿ A.U.	5.202803	1.00000023
i = inclination of orbit to ecliptic	$1^\circ\ 18'\ 31''.3 - 20''.0 * T$	0.0
Ω = longitude of ascending node of orbit on ecliptic	$99^\circ\ 26'\ 16''.3 + 3639''.5 * T$	0.0
ω = longitude of perihelion	$12^\circ\ 42'\ 41''.12 + 5800''.79 * T$	$101^\circ\ 13'\ 15''.0 + 6189''.03 * T + 1''.63 * T^2 + 0''.012 * T^3$
e = eccentricity	$0.0483376 + 0.00016302 * T$	$0.01675104 - .418 \times 10^{-4} * T - .126 \times 10^{-6} * T^2$
M = mean anomaly	$225^\circ\ 13'\ 17''.7 + 229''.123557 * d$	$358^\circ\ 28'\ 33''.04 + 1295\ 96579''.1 * T - 0''.54 * T^2 - 0''.012 * T^3$

d is the number of days from the epoch of 1900 January 0.5 ET and T is the number of Julian centuries of 365.25 days from the same epoch.

The orientation of Jupiter's rotational axis, with respect to the mean earth equator and equinox of date, is defined by

α = right ascension of pole = $268^\circ.0035 + 0.00103\ (t - 1910.0)$

δ = declination of pole = $64^\circ.5596 - 0.00017\ (t - 1910.0)$

Other pertinent constants for Jupiter include

μ = gravitation constant = $1.267077188 \times 10^8\ km^3/sec^2$

$= .44746367 \times 10^{19}\ ft^3/sec^2$

P = rotational period = 9.841667 hr

ω = rotational rate = 1.7734881×10^{-4} rad/sec was used in the mission study, described in Volume II, Chapter IX, and in a letter to GSFC, dated January 1972, "Modified Outer Planets Spacecraft System Description."

A Martin Marietta-imposed study ground rule for spacecraft/probe mission integration was that, for spacecraft missions with post-encounter objectives (i.e., multiple planet flybys), the spacecraft trajectory would not be modified for probe delivery. This requires the probe to provide the required deflection maneuver for entry. However, for missions only to Jupiter, other deflection modes are possible, including spacecraft deflection or combinations of probe and spacecraft deflection.

9. Atmosphere Model -
10. Ionosphere Model -
11. Trapped Radiation Model -
12. Micrometeoroid Model -
13. Magnetic Field Model -

See Vol. II. Chapter II

14. Planetary Quarantine

GSFC specified that planetary quarantine should not be considered in this study.